QUALITATIVE PERFORMANCE ANALYSIS FOR LARGE-SCALE SCIENTIFIC WORKFLOWS

by

Emilia S. Buneci

Department of Computer Science
Duke University

Date: _____

Approved:

_____
Daniel A. Reed, Supervisor

_____
Jeffrey S. Chase

_____
Carla S. Ellis

_____
Vincent W. Freeh

Dissertation submitted in partial fulfillment of the
requirements for the degree of Doctor of Philosophy
in the Department of Computer Science
in the Graduate School of
Duke University

2008

ABSTRACT

QUALITATIVE PERFORMANCE ANALYSIS FOR LARGE-SCALE SCIENTIFIC WORKFLOWS

by

Emilia S. Buneci

Department of Computer Science
Duke University

Date: _____

Approved:

_____
Daniel A. Reed, Supervisor

_____
Jeffrey S. Chase

_____
Carla S. Ellis

_____
Vincent W. Freeh

An abstract of a dissertation submitted in partial fulfillment of the requirements for the degree of Doctor of Philosophy in the Department of Computer Science in the Graduate School of Duke University

2008

Abstract

Today, large-scale scientific applications are both data driven and distributed. To support the scale and inherent distribution of these applications, significant heterogeneous and geographically distributed resources are required over long periods of time to ensure adequate performance. Furthermore, the behavior of these applications depends on a large number of factors related to the application, the system software, the underlying hardware, and other running applications, as well as potential interactions among these factors.

Most Grid application users are primarily concerned with obtaining the result of the application as fast as possible, without worrying about the details involved in monitoring and understanding factors affecting application performance. In this work, we aim to provide the application users with a simple and intuitive performance evaluation mechanism during the execution time of their long-running Grid applications or workflows. Our performance evaluation mechanism provides a qualitative and periodic assessment of the application's behavior by informing the user whether the application's performance is expected or unexpected. Furthermore, it can help improve overall application performance by informing and guiding fault-tolerance services when the application exhibits persistent unexpected performance behaviors.

This thesis addresses the hypotheses that in order to qualitatively assess application behavioral states in long-running scientific Grid applications: (1) it is necessary to extract temporal information in performance time series data, and that (2) it is sufficient to extract variance and pattern as specific examples of temporal information. Evidence supporting these hypotheses can lead to the ability to qualitatively assess the overall behavior of the application and, if needed, to offer a most likely

diagnostic of the underlying problem.

To test the stated hypotheses, we develop and evaluate a general *qualitative performance analysis* framework that incorporates (a) techniques from time series analysis and machine learning to extract and learn from data, structural and temporal features associated with application performance in order to reach a qualitative interpretation of the application's behavior, and (b) mechanisms and policies to reason over time and across the distributed resource space about the behavior of the application.

Experiments with two scientific applications from meteorology and astronomy comparing signatures generated from instantaneous values of performance data versus those generated from temporal characteristics support the former hypothesis that temporal information is necessary to extract from performance time series data to be able to accurately interpret the behavior of these applications. Furthermore, temporal signatures incorporating variance and pattern information generated for these applications reveal signatures that have distinct characteristics during well-performing versus poor-performing executions. This leads to the framework's accurate classification of instances of similar behaviors, which represents supporting evidence for the latter hypothesis. The proposed framework's ability to generate a qualitative assessment of performance behavior for scientific applications using temporal information present in performance time series data represents a step towards simplifying and improving the quality of service for Grid applications.

Acknowledgements

There are many people who have contributed to this work and have supported me throughout this journey. First, I would like to thank my advisor, Dan Reed, for his guidance and encouragement throughout my graduate career. He consistently challenged me to see the "bigger picture" and helped me focus on the important aspects of this work. I would like to thank my committee members –Jeff Chase, Carla Ellis and Vince Freeh – for their time and patience in guiding me through the process. I would particularly like to acknowledge and thank Jeff Chase for his time towards the end of the journey, for his consistent questioning and guidance that have helped improve this work significantly.

This work has benefited from the input of many people throughout various stages, including Lavanya Ramakrishnan, Aydan Yumerefendi, Piyush Shivam, Anirban Mandal, Gopi Kandaswamy, Sarat Kocherlakota, Shivnath Babu, Ilinca Stănciulescu, Diane Pozefsky, Alan Porterfield, Rob Fowler, Xiaobai Sun, Rachael Brady, John Good, Todd Gamblin, Tingting Jiang, and Seda Vural. Thank you all for your time.

On a more personal level, I am indebted to my family for their support through the year: my mom, for her constant encouragement, my sister Dana, for making me laugh and helping me see life from a different angle. And finally, I will be eternally indebted to the one person who suffered most throughout this research: Saul, thank you for your love, friendship and support.

Contents

Abstract **iv**

Acknowledgements **vi**

List of Figures **xii**

List of Tables **xvi**

1 Introduction **1**

1.1 Challenge: User-Centric, Qualitative Performance Analysis 4

1.2 Research Questions 6

1.3 Contributions 7

2 Background **9**

2.1 The Computational Grid Environment 9

2.2 Large-Scale Scientific Applications 10

2.2.1 Distributed Scientific Workflows 12

2.2.2 Workflow Performance Analysis On Grid Resources 17

2.3 Summary 18

3 Methodologies for Data Analysis and Visualization **19**

3.1 Time Series 19

3.1.1 Stationary Time Series 21

3.1.2 The Auto-correlation Function and Its Properties 23

3.2 Temporal Signatures 30

3.2.1 Feature Selection and Extraction 30

3.2.2 Building Temporal Signatures 42

3.3 Supervised Learning 43
3.3.1 Training 44
3.3.2 Classification 44
3.3.3 General Issues Affecting Classifiers 48
3.4 Methodologies for Data Visualization 50
3.4.1 Performance Time Series Data Visualizations 50
3.4.2 Temporal Signatures Visualizations 52
3.5 Summary 60

4 Qualitative Performance Analysis Framework 61

4.1 Architecture 61
4.2 Characteristics 65
4.3 Temporal Signature Component 67
4.3.1 Performance Time Series Selection 68
4.3.2 Features Selection and Extraction 69
4.3.3 Temporal Signature Definition 69
4.3.4 Temporal Signature Generation 70
4.4 Supervised Learning Component 71
4.4.1 Training: Learning Expected and Unexpected Signatures . . . 71
4.4.2 Classification: Performance Validation and Diagnosis 73
4.5 Qualitative Reasoning Component 74
4.6 Summary 76

5 Framework Evaluation 77

5.1 Execution Environment 78
5.1.1 Computational Resources 78

5.1.2 Performance Time Series Data Collection 81
5.2 Scientific Workflows 81
5.2.1 Montage 82
5.2.2 LEAD 83
5.3 Labeling Application Performance Expectation 89
5.4 Temporal Signatures of Expected Application Executions 92
5.4.1 Temporal Signature for a Task Within an Experiment 92
5.4.2 Temporal Signatures for a Group of Tasks in an Experiment . 94
5.4.3 Temporal Signatures Across Experiments 94
5.4.4 Summary 100
5.5 Temporal Signatures for Unexpected Application Executions 100
5.5.1 Case 1: Diagnosed Data-Intensive Application Running on Slow Network 101
5.5.2 Case 2: Diagnosed Corrupted Monitoring Data File Binary . . 105
5.5.3 Case 3: Undiagnosed Consistently Different Resource Characteristics Across Experiments 105
5.5.4 Summary 107
5.6 Qualitative Performance Validation and Diagnosis 108
5.6.1 Task-Level 108
5.6.2 Workflow-Level 109
5.7 Framework Evaluation 113
5.7.1 Comparison of Classification Accuracy Between Instantaneous Values Signatures and Temporal Signatures 113
5.7.2 Classification Accuracy Using Temporal Signatures 117
5.8 Performance Impact of Framework 121

5.9 Limitations . . . 123
5.9.1 Limitations of the Current Evaluation . . . 123
5.9.2 Limitations of the Approach . . . 126
5.10 Summary . . . 128
6 Related Work **130**
6.1 Temporal Signatures . . . 130
6.1.1 Time Series Analysis . . . 131
6.1.2 Dimensionality Reduction for Time Series Data . . . 133
6.1.3 Application and System Signatures . . . 138
6.2 Learning Techniques for Problem Diagnosis . . . 141
6.2.1 Classification Techniques . . . 141
6.2.2 Clustering Techniques . . . 142
6.3 Context: Performance Analysis of Scientific Workflows . . . 142
6.3.1 Performance Monitoring . . . 143
6.3.2 Workflow Optimizations . . . 144
6.3.3 Comprehensive Workflow Performance Analysis . . . 147
6.3.4 Performance Analysis and Visualization . . . 148
6.3.5 Discussion . . . 149
6.4 Summary . . . 152
7 Conclusion and Future Directions **154**
7.1 Conclusions . . . 154
7.2 Future Directions . . . 154
7.2.1 Variable and Feature Selection for Performance Data . . . 155
7.2.2 Learning Techniques . . . 156

7.2.3 Reasoning with Qualitative Information 157

7.2.4 Problem Diagnosis: Correlation and Causation 157

A Upper Bound Calculation for Sample Variance **159**

Bibliography **161**

Biography **171**

List of Figures

2.1 Example of static workflow in astronomy. 13

2.2 Simplified LEAD workflow. 15

2.3 Detailed LEAD workflow. 16

3.1 Performance time series data example. 21

3.2 Random time series and its auto-correlation function. 25

3.3 Flat time series and its auto-correlation function. 27

3.4 Periodic time series and its auto-correlation function. 28

3.5 Ramp time series and their auto-correlation function. 29

3.6 Auto-correlation function for a random time series. 35

3.7 Computed confidence bands values for k $\geqslant 1$ 35

3.8 Auto-correlation function for a periodic time series. 37

3.9 Auto-correlation function for a ramp time series. 38

3.10 Auto-correlation function for an almost periodic time series. 40

3.11 Auto-correlation function of a ramp time series with added noise. . . 41

3.12 Auto-correlation function for time series with periodic and ramp behaviors. 42

3.13 Example of k-nearest neighbor classifier for $k = 1$ and $k = 5$. From [32]. 46

3.14 Semi-log y-axis visualization of multiple mime series. 51

3.15 Performance time series visualized as a set of stacked individual plots. 52

3.16 Temporal signature visualization as a set of two bar charts. 53

3.17 Temporal signature visualization as color vector. 54

3.18 Example of the projection of a data point P in 8 dimensions. From [55]. 55

3.19 $P_1 - P_6$ using two different software implementations of Star-Coordinates. 57

3.20 $P_1 - P_6$ visualized on a Kiviat diagram. 58

3.21 Visualization of groups of temporal signatures using our novel color matrix visualization. 59

4.1 `Teresa`: high-level process overview. 62

4.2 `Teresa`: framework components. 62

4.3 `Teresa`: detailed framework architecture. 64

4.4 `Teresa` as Grid service. 65

4.5 `Teresa`: Temporal signature design component. 67

4.6 `Teresa`: Supervised learning component. 72

4.7 `Teresa`: Qualitative reasoning component. 74

4.8 Global workflow performance ratio, R for different values of N. 76

5.1 Architecture overview: Dante cluster. 79

5.2 Architecture overview: NCSA TeraGrid Mercury Cluster. 80

5.3 Example Montage workflow. 82

5.4 Example LEAD workflow. 86

5.5 Execution times for all experiments with `mProjExec`. 91

5.6 Performance time series and temporal signature for one task from `mProjExec` Experiment #5. 93

5.7 Temporal signatures for `mProjExec` Experiment # 5. 95

5.8 Temporal signatures across experiments: `mProjExec` experiments # 5, 6, 7. 96

5.9 Temporal signatures across experiments: `mProjExec` experiments # 12, 13, 14. 97

5.10 Temporal signatures across experiments: `mProjExec` experiments # 20, 21, 22. 98

5.11 Temporal signatures across experiments: `WRF` experiments # 35, 36, 37. 99

5.12 Performance time series and temporal signature for one task from unexpected `mProjExec` experiment #23. 102

5.13 Unexpected temporal signatures for `mProjExec` Experiments # 23, 24, 25. 103

5.14 Temporal signatures across `slowio` cluster for unexpected `mProjExec` application executions. 104

5.15 Unexpected temporal signatures on specific nodes during `WRF` experiments # 51, 52, 53. 106

5.16 Time series data from `WRF` Experiment #51 for the compute node `tg-c256` exhibiting the abnormal behavior. 107

5.17 Periodic evaluation of application behavior using temporal signatures. 109

5.18 Scenario 1: Workflow instance with expected qualitative behavior. . . 111

5.19 Scenario 2: Workflow instance with unexpected qualitative behavior. 112

5.20 Examples of instantaneous signatures extracted from both expected and unexpected performance data. 115

5.21 Balanced accuracy results for classification with instantaneous signatures and with temporal signatures. 117

5.22 Impact of smoothing on the variance feature calculation and the direct impact on framework accuracy. 121

6.1 Related areas and problem context 131

6.2 Time series from the electrocardiogram diagnosis of a healthy and unhealthy patient. 136

6.3 Kiviat-graphs, visual system signatures. 139

6.4 Application signature using poly-lines. 139

6.5 Example of two time profiles of identical processes. 140

6.6 Example of two temporal signatures of system-calls used for intrusion detection. 140

7.1 Other contexts where `Teresa` can be applied. 156

List of Tables

3.1 Summarized properties of the ACF given specific patterns in time series. 24

3.2 Encoding the pattern into a discrete value within $\{1, 2, 3, 4, 5\}$. 32

3.3 Accuracy results for identifying random patterns in time series of different lengths, N and with varying amplitudes. 39

3.4 Numerical values for six vectors in 8D, comprising two different categories. 56

4.1 Example of input performance time series metrics. 69

5.1 Architectural characteristics of computing resource sites. 78

5.2 Set of system-level performance time series analyzed. 81

5.3 `mProjExec` with data set `M101` on all clusters. 84

5.4 `mProjExec` with data set `M57` on all four clusters. 85

5.5 `WRF2.2` and `WRF2.0`* with `mesoscale` data set on all four clusters. . . 88

5.6 WRF2.2 with `non-mesoscale` data set on all clusters except* `slowio`. 89

5.7 Framework efficacy evaluation. 119

5.8 Considerate use of smoothing: impact of unfit application of smoothing for calculation of variance feature. 120

5.9 Performance impact of temporal signatures and their subsequent classification. 122

Chapter 1

Introduction

Grids are systems that coordinate distributed resources using standard, general-purpose protocols and interfaces to deliver desired qualities of service [38]. They represent one of the solutions offering a computational infrastructure enabling progress and new modes of research and collaboration in both science and industry. Grids enable organizations to tackle problems previously infeasible to solve due to computing and data-integration constraints. They also reduce costs through automation and improved IT resource utilization.

Scientists use Grids to solve grand challenge problems like weather modeling [29], earthquake simulation [104, 113], high-energy physics simulations [58], or help understand the mechanisms behind protein folding [83]. For example, thousands of physicists from universities and laboratories around the world have joined forces to design, create, operate, and analyze the products of a major particle accelerator, and are pooling their computing, storage, and networking resources to analyze petabytes of data [39, 88, 45].

Companies use Grids and service oriented infrastructures to automate business transactions and enable cross-industry collaborations to increase profit and competitiveness [79]. Consider an industrial consortium commissioning the study of the feasibility of a next-generation supersonic aircraft by multidisciplinary simulation of the entire aircraft. Generating this type of simulation involves integrating proprietary software and coordinating resource sharing for a prearranged set of resources (i.e., design databases, data, or computing resources) [39]. More recently, companies have started to offer cloud or utility computing [65, 68], a web-scale virtual comput-

ing environment offering on-demand access to storage [6], computing [5], and other services on a pay-per-use basis. Science or research "clouds" are under development; they will function as huge virtual laboratories, where authorized users will be able to analyze data, build new tools and share this data with other researchers [10].

These examples from both the academic and business world differ in many respects: the number and type of participants, the resources being shared, the duration of the interaction, and the type of activity. However, in each case, interested participants want to share resources to perform some task that each could not perform independently. Sharing implies providing access to a multitude of resources: software, computers, data, sensors, and other resources. Grids and, more recently, computing clouds, offer technologies to coordinate resource sharing and problem solving.

Grids are complex and highly dynamic systems and their ease of management and utilization are key to their success. As part of the effort to make Grids easier to use within the scientific application domain, it is important to understand the characteristics of the factors affecting application performance, and to support scientific users with intuitive tools to evaluate and interpret application behavior during execution.

Previous efforts in performance diagnosis and optimizations include quantitative mechanisms that assess, based on performance metric thresholds, whether an application's performance expectations are being met at a given point [93, 96, 109, 106, 37]. Threshold-based techniques are a form of service level agreements (SLAs) for scientific Grid applications. Such approaches are definitely useful to a user who knows (1) the key metrics to monitor, and (2) the best value of the threshold that would capture the most important performance problems without triggering too many false alarms. The major weakness of threshold-based approaches that rely on static, non-adaptive thresholds is the assumption that these meaningful threshold values are known in advance. This is seldom true in practice. In a complex and dynamic environment such

as a Grid, on which different applications with varied characteristics execute, finding meaningful performance metric thresholds may be very difficult. Furthermore, from a usability perspective, threshold-level approaches work well if there are relatively few metrics specified and monitored, and if the impact of these metrics on the application performance, both individually and as a set, is simple and easy to understand and predict.

In this thesis, we propose an alternative and novel performance analysis methodology which addresses the disadvantages of static threshold-based approaches by learning differences between characteristics of performance time series data during good and degraded application performance states. Our approach redefines and expands the concept of an SLA in terms of the qualitative notion of performance as perceived by the scientific application user. Instead of depending on a user to specify a set of numerical thresholds within an SLA (i.e., the application's memory utilization should be $\leqslant 1$ GB, and the available network bandwidth should be in the range of [100 Mb/s−300 Mb/s]), our framework relies on the user to express his or her level of satisfaction with various executions of the application by labeling these executions as having a desirable or undesirable performance[1]. From these sets of historical expected and unexpected behaviors, our framework provides the workflow user with periodic qualitative assessments of application behavior during on-line execution.

Because our target applications are long-running scientific applications (i.e., execution times can take days, weeks or even months), persistent changes in performance behaviors are of interest and not transient or localized ones. Therefore, to qualitatively assess application behavior in this class of applications, we investigate the hypotheses that: (1) it is necessary to analyze and extract temporal/historical information in performance time series data, and that (2) it is sufficient to use vari-

[1]Additionally, we may refer throughout the thesis to these binary states of performance as *good* and *poor* or as *expected* and *unexpected*.

ance and pattern as representative features of temporal information for a reasonably accurate characterization of behaviors.

1.1 Challenge: User-Centric, Qualitative Performance Analysis

In a dynamic environment such as the Grid, extrinsic forces can affect application performance, which leads to significant difficulties in obtaining accurate models of application performance. We are interested in exploring a qualitative approach to performance analysis, which draws on human experience [59] in creating and using qualitative descriptions of mechanisms. We want to provide a *qualitative* evaluation of application performance because simple to use and understand descriptions of application behaviors are easier for workflow users to reason with than complex performance models, and because they can reduce the complexity of the scheduling policies by supporting categorical resource control in Grid environments.

In the context of scientific Grid applications, we seek to define and extract characteristics of monitored performance data that correlate well with important high-level application states (i.e., well-performing, poor-performing). For example, consider a case where the user is unsatisfied with the recent executions of his or her application, as the average run times may be twice as long as previous runs. There could be different and multiple causes of degraded application performance such as more competition for network bandwidth, changes of configuration in the computational environment or application source code changes, to name a few of the possibilities. Our framework's goal is twofold: to automatically detect (1) the existence of a possible problem, and (2) the type of problem affecting application performance during executions.

We define *qualitative performance analysis* as the qualitative performance validation and diagnosis of applications. Qualitative performance validation assesses

whether an observed behavior is expected or unexpected. Qualitative performance diagnosis searches and offers the application user possible causes of unexpected behavior (e.g., low network bandwidth). These simple, intuitive and qualitative answers to the possible problems affecting large-scale scientific workflows can be used to build and deploy rescheduling policies for a simplified resource control in complex distributed environments, similarly to the qualitative preference specifications used to exercise effective control over quantitative trust-based resource allocations proposed in [27].

Below, we summarize the main challenge we address and the problem specification, together with the assumptions and requirements.

Challenge

To bound the performance variability of scientific Grid applications.

Problem Specification

Input: Continuous performance time series collected from Grid computing resources where applications execute.

Output: Qualitative performance analysis of the application.

Assumptions: The following assumptions apply: (1) workloads of interest are long-running component workflow scientific applications, and (2) performance time series metrics are selected by an expert[2], and reflect the temporal performance of the workloads over time.

Requirements: The following requirements apply:

1. On-line re-evaluation of behavior is necessary at larger time scales (i.e., tens of minutes) rather than smaller time scales (i.e., minutes or seconds), because target applications have significant resource requirements[3], resulting in a high

[2]Either human or software-based.

[3]See Section 2.2.1 for LEAD workflow resource requirements [29, 100].

cost for application migration, restart or over-provisioning.

2. Performance metrics of interest are easy to collect and are provided by existing distributed monitoring software.

3. Answers to the output questions are accurate to a specified level and useful most of the time.

4. Approach is scalable to thousands of Grid computing resources.

1.2 Research Questions

This thesis answers the following questions:

1. **What does it mean to assess the performance of an application *qualitatively*?** We investigate the user-centric definition of well-performing and poor-performing application states in the context of large-scale scientific applications executing on distributed resources. Furthermore, we study how periodically sampled performance data can be correlated with the qualitative behavior of the application.

2. **What characteristics present in the performance time series data are necessary and sufficient to correlate with the high-level behavior of these long-running applications?** We test the hypothesis that temporal information present in performance data is necessary to analyze in order to characterize more accurately the application's behavior. Moreover, we investigate if specific examples of temporal features in performance data, such as relative variance and pattern are sufficient to characterize expected and unexpected application behaviors.

3. **How can we gather samples of application behavior effectively and accurately?** We investigate the cost of gathering samples of performance data

correlated with qualitative application behavior and propose methodologies for gathering samples of behaviors as effectively and accurately as possible.

4. **How can we use samples of application behavior for qualitative performance analysis (i.e., validation and diagnosis)?** We use the sample knowledge base acquired to show how it can be utilized for on-line qualitative performance validation and diagnosis for large-scale scientific workflows, within a specified accuracy.

1.3 Contributions

This thesis proposes a novel, *qualitative* performance analysis framework that supports workflow users in (a) understanding via intuitive behavioral characterizations the performance of their applications, and (b) supporting fault-tolerance and rescheduling services by simplifying and categorizing the space of scheduling policies options. Moreover, the framework investigates what performance data features are necessary and sufficient to characterize the higher-level behavior of applications. To support these goals, our framework:

1. Defines a general process to extract useful features from multi-variate performance time series data, and to generate a compact signature of this data. We present the mathematical details of generating a signature from performance data in Chapter 3, and detail the high-level process of using signatures for performance validation and diagnosis in Chapter 4.

2. Demonstrates how to use generated performance signatures to automatically learn characteristics associated with both well-performing and poor-performing application behavioral states. We describe the learning process in Chapter 4, and we detail specific examples of learning in the evaluation chapter, Chapter 5.

3. Develops techniques and policies for reasoning about observed application behavior temporally and spatially. We evaluate the techniques proposed on two large-scale scientific workflows and we present results in Chapter 5.

Chapter 2

Background

This chapter describes the context in which the proposed framework works, including characteristics of the computational Grid environment, and those of the target scientific Grid applications.

2.1 The Computational Grid Environment

The computing environments where distributed scientific applications execute are often *heterogeneous*. They include a variety of computing resources such as supercomputers, homogeneous commodity clusters, servers or ensembles of workstations, all with a variety of architectural characteristics (processor speeds, memory, network interconnects). Similarly, there is heterogeneity in the software available on computing resources, with different operating systems, scientific applications, libraries or other software applications of interest. Grids often have a highly heterogeneous and unbalanced communication network, comprising a mix of different inter-machine networks and a variety of Internet connections whose bandwidth and latency vary greatly in time and space.

The reason for the heterogeneity of Grids is at least three-fold: (1) organizations participating with computing resources often have different hardware configurations, network speeds, storage systems and software stacks on their computing resources, (2) failed or misbehaving components or computational resources are usually replaced with different (more powerful) ones, as cost per performance ratios keep falling, and (3) any necessary increases in performance or capacity due to expected increases in load are usually obtained with better performing components.

Another important characteristic of the computational Grid environment is the

availability of resources. Computational Grid resources can be dedicated, shared, or on-demand. Their availability can vary significantly, not only because of unavoidable system failures, but also because the owners of the resources can decide when and under what circumstances their resources will be shared (i.e., dedicated supercomputer becomes unavailable).

The dynamic resource fluctuation and the resource sharing can dramatically impact the performance of the system or application of interest. Therefore, automatic mechanisms, which monitor and detect persistent behavior anomalies of applications are critical to the creation of a robust computational framework.

2.2 Large-Scale Scientific Applications

The computational Grid environment provides the necessary infrastructure for scientists to solve problems that were previously infeasible due to computing and data-integration constraints.

For example, the Linked Environments for Atmospheric Discovery (LEAD) multidisciplinary effort addresses the fundamental IT research challenges to accommodate the real-time, on-demand, and dynamically-adaptive needs of *mesoscale weather research*[1] [29]. The LEAD project utilizes the Grid to achieve its scientific research goals. This effort is a major shift away from a 50 year paradigm, in which weather sensing and prediction, and computing infrastructures operated in fixed modes independent of weather conditions [28].

Scientific fields have developed over long periods of time large-scale software codes to assist them in their research. These large-scale scientific applications have traditionally been computationally focused. They have been mostly implemented as parallel codes designed to be executed on supercomputers, clusters and/or symmetric

[1]Mesoscale weather - floods, tornadoes, hail, strong wind, lightning and winter storms - causes hundreds of deaths, routinely disrupts transportation and commerce and results in significant economic losses.

multiprocessors (SMPs). Two emerging trends have been changing these scientific applications.

First, many scientific fields such as biology, astronomy, physics, meteorology have recently seen an exponential increase in scientific data following significant technological breakthroughs in scientific instruments. The improved instruments can generate large amounts of data, which typically require complex and computationally-intensive analysis and multi-level modeling [11]. In astronomy, breakthroughs in telescope, detector and computer technologies have resulted in astronomical sky surveys producing petabytes (PB) of data in the form of sky images and sky object catalogs [114]. Sky survey databases such as DPOSS (Palomar Digital Sky Survey) [26], and the 2MASS (Two Micron All Sky Survey) [2] are three and ten TB respectively. In high-energy physics, the prime experimental data from the CERN CMS detector will be over one petabyte (PB) a year [78]. In the future, CMS and other experiments now being built to run at CERN's Large Hadron Collider will accumulate data on the order of 100 PB within the next decade.

Second, recent improvements in the computing infrastructure (e.g., computers, networks, storage systems, sensors) have enabled collaboration, data sharing and other new modes of interaction which involve distributed resources. The result is an emphasis on coupling the existing distributed infrastructure via easy to use tools with standard interfaces.

The unifying theme is that traditionally, computationally focused large-scale scientific applications have been changing due to the exponential increase in scientific data and due to the improved coupling infrastructure. The emerging large-scale scientific applications are data driven and distributed: they analyze distributed data sources, use distributed computing resources and software tools which enable scientists in their pursuance of answering fundamental scientific questions.

2.2.1 Distributed Scientific Workflows

The new large-scale scientific Grid applications are no longer monolithic codes; rather, they are represented by various components or tasks which perform data collection, pre-processing, transformations, analysis and visualizations as part of a workflow.

A workflow is a systematic way of specifying application logic and coordination. Scientists can simply specify what tasks/components need to be accomplished and in what order, and can specify the data inputs and flow among the components. Once a workflow is specified, various mechanisms, such as those in Pegasus [25], automatically map it on available computing resources meeting desired requirements.

Workflows can be static or dynamic. A static workflow executes all the components in the order specified and outputs results of various stages. A dynamic workflow can change the execution flow of one or more components adaptively, depending on current system conditions or results of components of interest.

Two examples of scientific workflows are detailed in the following section. We present a static workflow from astronomy and a dynamic workflow from meteorology.

Static Workflows

The National Virtual Observatory (NVO) [114] is contributing to a new mode of performing astrophysics research. The NVO was designed to support the federation of astronomical sky surveys because there are probably many undiscovered phenomena in the data that have not yet been discovered due to the tremendous amount of data requiring analysis. Therefore, it provides the tools to explore within and extract relevant information from these massive, multi-frequency surveys. This type of unprecedented access enabled astronomers to: (1) perform detailed correlation within the data, (2) understand the basis of the physical processes that result in the correlations, and (3) potentially identify new classes of astrophysical phenomena.

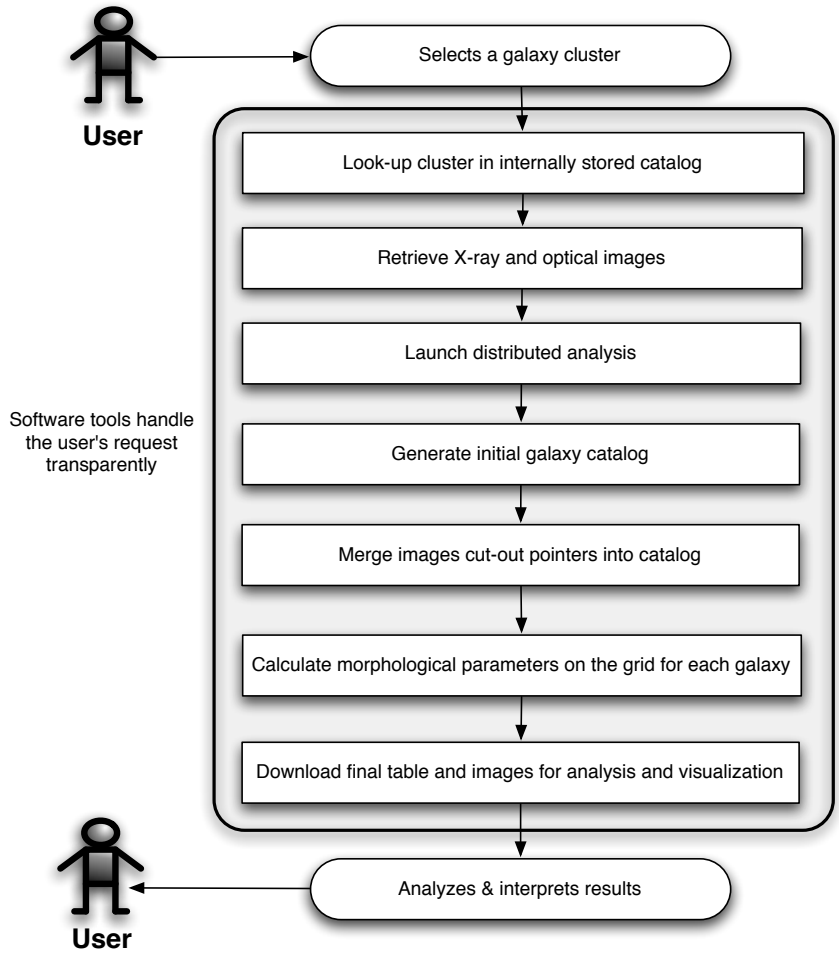

Figure 2.1: Static scientific workflow in astronomy. Adapted from [92].

Figure 2.1 shows a static scientific workflow used in the NVO project. Initially, the user selects a galaxy cluster of interest, which is then looked up in the internally stored catalog. Multi-frequency images of the cluster are retrieved from sky survey databases, then a distributed analysis is launched on Grid computing resources. An initial galaxy catalog is generated, within which image cutout pointers are merged. Various morphological parameters are calculated on the Grid for each galaxy. Finally, the user downloads tables and images for analysis and visualization.

These workflows, which perform multi-frequency image and/or database analysis, constitute an example of federation of information: bringing data from different

sources into the same frame of reference. This type of data federation is very important in astronomy because it enables discoveries of new sky objects and phenomena (i.e., brown dwarf stars can be found by a search spanning infrared image catalogs) [114].

Dynamic Workflows

In the meteorology science context, traditional weather forecasts are static, linear workflows with no adaptive response to weather. Consider the simplified dynamic LEAD workflow shown in Figure 2.2. Meteorological data sets and streams generated by radars, satellites, weather balloons and other weather instruments are transported via shared networks to distributed and shared computing resources for processing. The different data types are integrated and transformed such that numerical weather forecast codes can be initiated. The results of the forecasting are visualized.

Automated data-mining algorithms analyzing forecast output can dynamically request new real-time data from data-collecting instruments in case severe weather patterns are detected. The entire or part of the workflow process is repeated following the arrival of new real-time data. Figure 2.3 shows the actual LEAD workflow of Figure 2.2 with its components.

Dynamic workflows are different from static workflows in that the totality or parts of the workflow can be repeated as needed based on run-time criteria. Dynamic workflows result in more uncertainty regarding what applications will run and what resources will be used. For LEAD dynamic workflows, uncertainty is introduced by two meteorological needs: (1) more accurate, and (2) immediate forecast of weather, given the detection of severe weather. To obtain more accurate forecasts, meteorologists typically run ensemble forecasts[2]. The more computational resources

[2]Multiple predictions from a group or ensemble of slightly different initial conditions and/or various versions of models. The objective is to improve the accuracy of the forecast through averaging many forecasts, which reduces the number of non-predictable components, and to provide reliable information on forecast uncertainties from the diversity among ensemble members [42].

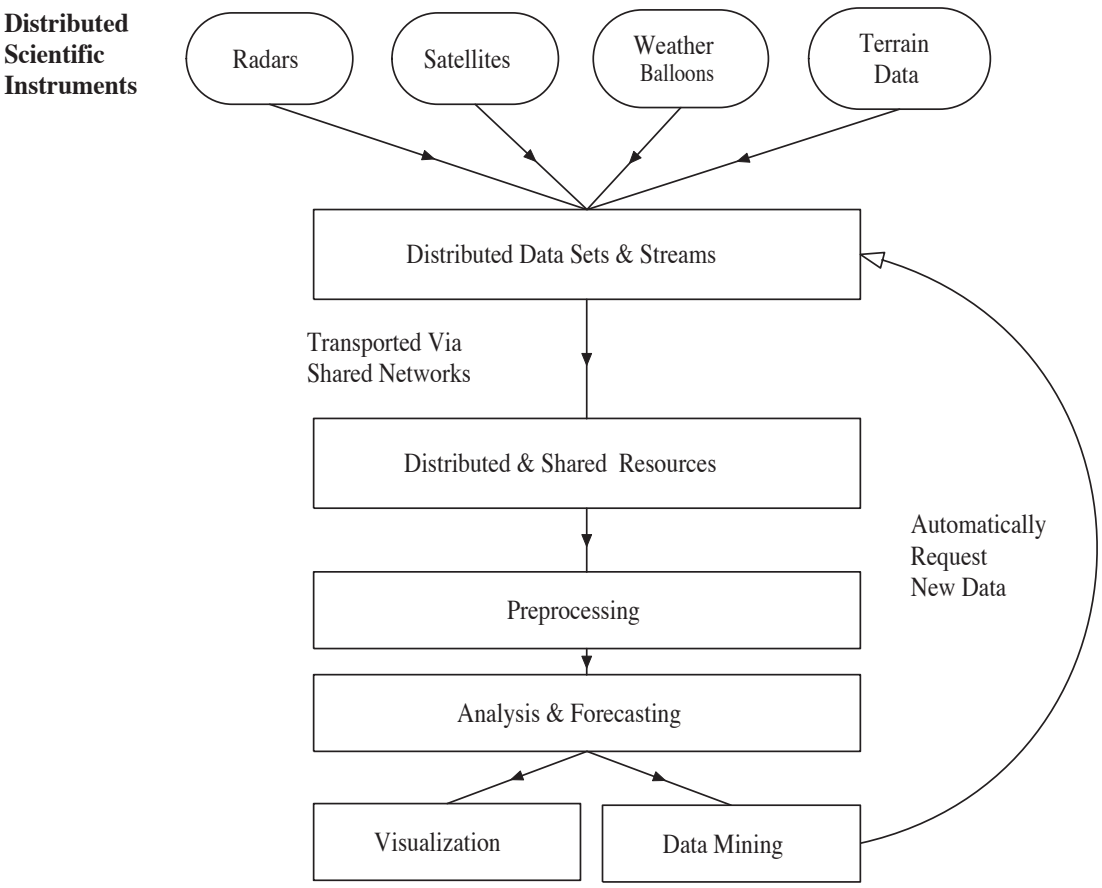

Figure 2.2: Simplified LEAD workflow.

available, the more accurate the forecast. Immediate forecast of weather means that computing resources need to be available *now*, because a delayed prediction of severe weather conditions is not useful.

Many of the distributed scientific workflows require great storage and computational capacity. For example, in the LEAD workflow various types of high-volume data sets and streams (i.e., terrain input, satellite or radar data) are collected at remote, geographically distributed sites, and transferred via shared networks to other distributed computing centers for further processing and analysis. Currently, each NEXRAD (Next Generation Radar) Level II can output 4.3 GB/day [80]. In case of severe weather, the application may demand streaming of data from many NEXRADs

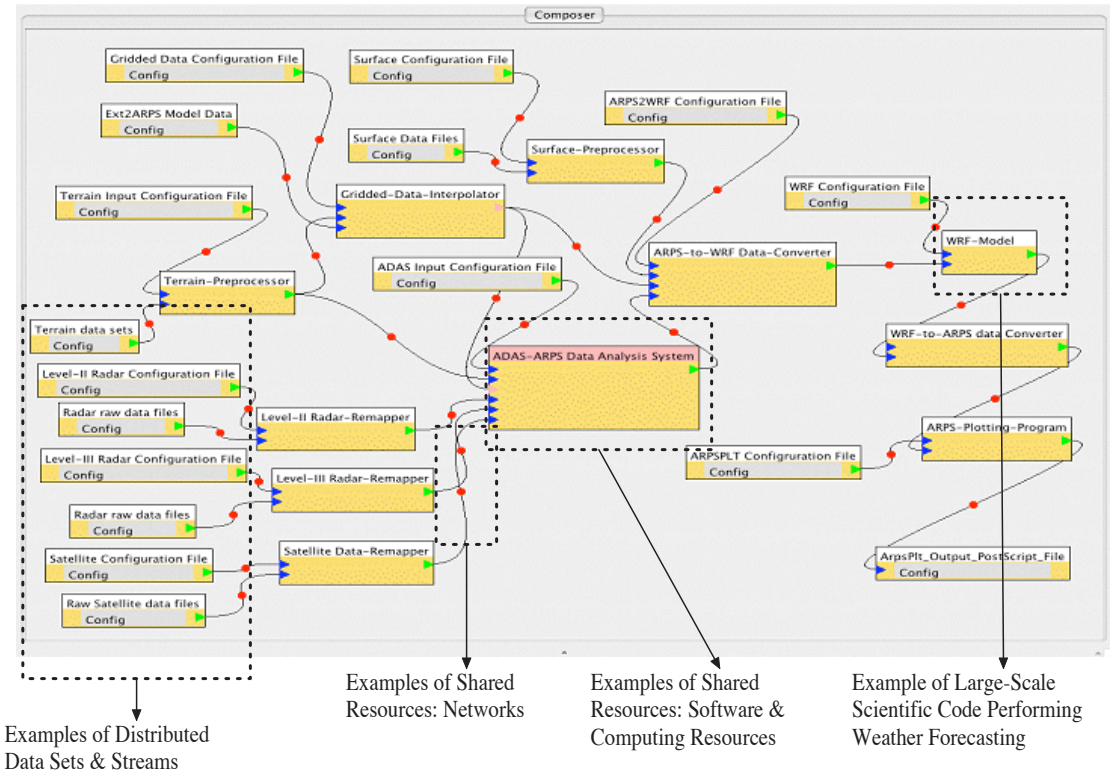

Figure 2.3: LEAD workflow for data ingestion, analysis and weather forecast. Adapted from [29].

as well as other meteorological instruments for more accurate weather predictions.

The computational demands of numerical forecast models such as the Weather Research and Forecasting (WRF) code [72] and its data-assimilation systems [16] are significant [29]. A recent experiment [100] conducted by the Center for Analysis and Prediction of Storms (CAPS) and the Pittsburgh Supercomputing Center (PSC) generated the highest-resolution numerical weather forecasts yet attempted. The forecasts had twice the horizontal resolution and nearly 50 percent greater vertical resolution, with a spacing between grid points of two kilometers. This increased spacial resolution was five times finer than the one used in the National Weather Service's most advanced model. As a result, the experiment demanded approximately 300 times more raw computing power. The higher resolution offered meteorologists

improved storm forecast capability, such as the ability to capture individual thunderstorms together with their rotation information.

CAPS used the numerical forecast model WRF executing on 307 Alphaserver ES45 nodes (four 1 GHz processors with 4 GB RAM per node) to produce the daily forecast from mid-April through early June during 2005 for over two-thirds of the continental United States. The forecasts executed approximately two months on these high-performing computational resources.

2.2.2 Workflow Performance Analysis On Grid Resources

For the astronomy application example, the Grid implications are that these massive astronomical data collections are made available without worries about differences in storage systems, security environment or access mechanisms. These static workflows execute a series of workflow components, sequentially or in parallel, following a directed acyclic graph flow. The workflows may have real-time constraints on the total execution time. Thus, workflow performance analysis tools must detect timely if components are not performing as expected. Both quantitative and qualitative performance analysis approaches offer methods to enforce soft or hard performance guarantees.

For the meteorology application example, generating *accurate* and *immediate* severe weather forecasts requires significant computational and data demands. The data and computational resources utilized are distributed and are integrated via coupling tools such as Grids and web services. However, in an integrated, distributed computing environment there are a variety of challenges to overcome, such as resource contention, software and hardware failures, data dependencies and optimal resource allocations. Resource contention and sharing in this environment cause the performance of applications to vary widely and unexpectedly. Therefore, creating mechanisms that enable soft real-time performance guarantees by characterizing re-

source behavior to ensure timely completion of tasks is especially critical in real-time environments.

2.3 Summary

We presented the context in which we apply our qualitative performance analysis framework: large-scale scientific Grid applications executing in a distributed computing environment. The complexity and dynamism of these new scientific applications makes monitoring and understanding application resource behavior both critical and challenging. This work complements existing quantitative Grid performance analysis approaches with qualitative ones, which together will offer a more robust computational environment during the execution of scientific workflows.

Chapter 3

Methodologies for Data Analysis and Visualization

This chapter describes methodologies for performance data analysis and visualization which we employ to extract temporal information from time series data and to characterize qualitatively the behavior of long-running scientific applications. We introduce concepts from time series analysis and pattern recognition in time series and show how to build temporal signatures from time series data. We also introduce fundamental concepts from supervised learning and show how we use it on temporal signatures to differentiate between desired and undesired application performance states. Lastly, we describe supporting techniques from multi-variate data visualization which help with the analysis and interpretation of results from our performance data.

3.1 Time Series

A time series T is a set of observations, denoted by z_0, z_1,$\cdots$, z_k,$\cdots$,z_N generated sequentially at time points τ_0, τ_1, $\cdots$, τ_k,$\cdots$, τ_N. Successive time points can be collected at a fixed interval of time, h, or at different intervals of time. In this thesis, we are concerned with equidistant series.

Time series analysis uses statistical methods to analyze dependencies in a chronological sequence of observations. When applied to performance metric time series, the observations can be any quantitative data gathered from any metric of interest (i.e., CPU utilization, amount of free memory, or number of I/O read requests). Figure 3.1 depicts a performance data time series, number of disk transactions per second $z_0, \cdots, z_k, \cdots, z_{2000}$, collected every $\tau_k = 100$ seconds during the execution of

an application on a computing system.

Our objective is to characterize *temporally* the behavior of the underlying process generating the series. This characterization is achieved by exploiting correlations among observations to identify a qualitative temporal structure for the performance data processes.

When collecting performance metrics, the value of τ_0 corresponds to starting an application's execution on a computing system, and h corresponds to the frequency of sampling of performance data. The value of N corresponds to the completion of the execution of the application on the computing resource.

Two characteristics of time series are essential to the type of analysis that can be applied: *stationary* and *non-stationary*. In a *stationary series*, the underlying process remains in statistical equilibrium, with observations fluctuating around a constant mean with constant variance. In contrast, a *non-stationary series* has unfixed moments (i.e., mean or variance) which tend to increase or decrease over time.

Although many empirical time series are non-stationary, we assume that most snapshots of the time series analyzed will at least meet the *weak stationarity* condition, that is only the first two moments (i.e., mean and variance) do not vary with respect to time. If most time series analyzed in the experimental setting will not meet this condition, then estimation formulas for mean, variance and auto-correlation commonly utilized under the stationary and weakly-stationary conditions, will result in biased estimates. The use of such formulas and therefore of our specific temporal information extraction techniques under non-stationarity will result in a decreased efficacy for our framework, as the extracted features will not be accurately describing temporal behaviors. However, other methodologies from pattern recognition and analysis of time series such as those proposed in [64, 87, 95] can be employed to achieve the same goal of compact temporal characterization of behavior from performance

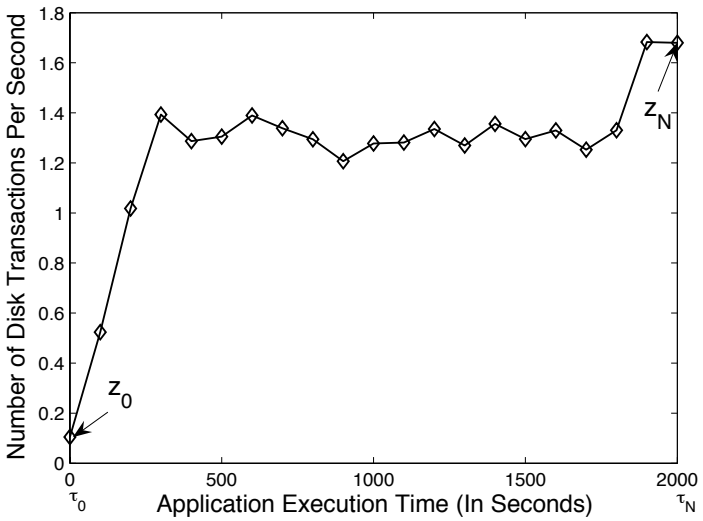

Figure 3.1: Performance data time series collected during the execution of an application.

time series that are non-stationary.

3.1.1 Stationary Time Series

When a time series is stationary, certain statistics such as *mean*, *variance*, *auto-covariance*, or *auto-correlation* can be calculated using closed form mathematical formulas. These measures are important because they help characterize important features from a time series such as amount of variability and patterns.

The mean of a stationary process, μ, can be estimated by the mean

$$m = \frac{1}{N}\sum_{t=1}^{N} z_t \tag{3.1}$$

of the time series, and the variance σ^2, of the stationary process, can be estimated by the variance

$$s^2 = \frac{1}{N}\sum_{t=1}^{N}(z_t - m)^2 \tag{3.2}$$

of the time series. Similarly, the covariance between z_t and its value z_{t+k} separated by k intervals of time is called the *auto-covariance* at lag k and can be estimated by

$$c_k = \frac{1}{N} \sum_{t=1}^{N-k} (z_t - m)(z_{t+k} - m), k = 0, 1, 2, \cdots, K. \tag{3.3}$$

From Equation 3.3 it follows that the *auto-correlation* of a time series at lag k can be estimated by

$$r_k = \frac{c_k}{c_0}. \tag{3.4}$$

We are interested in characterizing temporal features of the performance time series, such as a relative description of the variance in the data (e.g., higher variance or lower variance), and the type of pattern observed (e.g., oscillatory, random, flat, ramp). We chose to extract these specific patterns in the performance time series for three reasons:

1. We have experimentally observed from initial studies of scientific applications that these patterns are common in the performance time series data analyzed,

2. These patterns have also been documented in several studies [89, 76, 110] as being commonly observed during scientific application executions, and

3. In engineering and science domains where time series are ubiquitous, some of these patterns are considered primitives [87, 40] and are fundamental to the analysis and modeling of behaviors.

Although variance characterization can be derived from a normalization of the variance equation, Equation 3.2, a description of the pattern in a time series involves analyzing temporal correlations within the series, which can be achieved by applying the auto-correlation function (ACF) to the series. The following section defines the ACF, and describes its mathematical properties which help in pattern identification.

3.1.2 The Auto-correlation Function and Its Properties

As shown in Equation 3.4, the auto-correlation coefficient at lag k measures the covariance between two values z_t and z_{t+k}, a distance k apart, normalized by the value of the covariance at $k = 0$. The set of all the auto-correlation coefficients of a time series T constitute the auto-correlation function, ACF of the series T

$$\text{ACF (T)} = \{r_0, r_1, \cdots, r_k, \cdots, r_N\}, \tag{3.5}$$

$$\text{ACF (T)} = \left\{\frac{c_0}{c_0}, \frac{c_1}{c_0}, \cdots, \frac{c_k}{c_0}, \cdots, \frac{c_N}{c_0}\right\}. \tag{3.6}$$

Notice that for a constant, zero-mean time series T, $c_0 = 0$ and therefore the ACF is undefined

$$\text{ACF (T}(m = 0,\ s^2 = 0\ )\ ) = \text{Undefined, since } c_0 = 0. \tag{3.7}$$

Intuitively, the ACF is the cross-correlation of a time series with a time-shifted version of itself. Note that the auto-correlation function is dimensionless; it is independent of the measurement scale in a series. In practice, the auto-correlation function is used for the following two purposes: (1) to detect non-randomness in the data, and (2) to identify an appropriate time series model if the data is not random [14].

When the auto-correlation is used to detect non-randomness, usually only the first, r_1 auto-correlation is of interest. When the auto-correlation is used to identify an appropriate time series model, the auto-correlations are usually plotted for many lags. The ACF plots are then inspected for certain characteristics and a time series model is selected. The time series model is then used to predict values that may be observed in the future (e.g., stock forecasting, amount of future CO_2 in the atmosphere, predicted number of IO read requests to a disk, and so on).

In this work, our interest lies in finding a compact yet useful representation of a

time series and not in finding a time series model in order to forecast future values. In essence, we want to extract –similarly with [3]– possible features of interest in the time series that may help differentiate between good and degraded performance application states.

One of the features of interest is the pattern present in the time series. The goal is to develop an algorithm capable of identifying patterns of interest only from analyzing the properties of the ACF, shown in Table 3.1.

Series Pattern	**ACF Property**
Random	ACF is effectively zero, for $k \geqslant 1$.
Flat	ACF is effectively zero, beyond $k \geqslant 1$.
Periodic	ACF is periodic and has positive values at k's matching peaks and negative values at ks matching peak-valley regions.
Ramp	ACF is monotonically decreasing toward 0.

Table 3.1: Summarized properties of the auto-correlation function for a time series with specified pattern.

The following examples show random, flat, periodic, and ramp series; we show how the auto-correlation coefficients are calculated, and how the coefficients' values can be used to distinguish different patterns in time series data.

Example of a Random Series and Its ACF

The auto-correlation of a white noise or random series has the maximum value at $r_0 = 1$ by definition, while the remaining r_k are very close to zero for $k \geqslant 1$. This shows that a sampled instance of a white noise series is not statistically correlated to a sample instance of the same white noise series at another time.

Figures 3.2(a) and 3.2(b) show a white-noise time series of zero-mean and its ACF. Consider the synthetic random series with 75 time measurements of 3.2(a) with mean

$\mu \approx 0$ and sample variance $s^2 = 1.33$:

Index	1	2	3	4	5	6	7	8	9	10
+0	0.40	0.74	−1.19	0.63	−0.33	−0.44	1.42	1.45	−0.26	1.52
+10	−1.38	−0.06	−2.45	−1.49	−1.22	−1.39	−0.61	−0.37	−0.46	−1.24
+20	−1.59	−0.33	2.01	0.32	−0.64	0.17	0.70	−0.51	0.41	−0.63
+30	1.33	−0.74	−1.58	−0.99	−0.28	−0.20	2.90	−1.54	0.67	0.84
+40	1.27	−0.17	1.10	0.74	−0.25	−0.25	−1.32	1.19	−0.45	−0.05
+50	1.96	0.97	−1.59	0.94	−0.15	−0.50	0.68	−0.22	1.15	1.14
+60	−0.52	2.22	0.95	−0.77	0.01	−0.29	0.36	0.32	0.70	−1.54
+70	1.72	0.31	2.97	−1.09	−2.30	–	–	–	–	–

Initially, the auto-covariance coefficient at lag zero is estimated in order to calculate the normalized auto-correlation coefficients:

$$c_0 \quad = \quad \frac{1}{75}\sum_{t=1}^{75} z_t^2 = \frac{98.20}{75}.$$

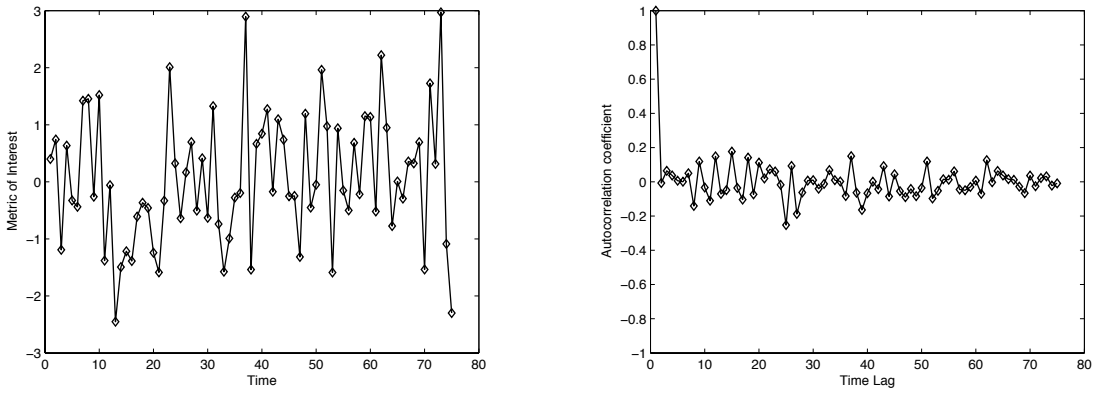

(a) White noise time series, T_{random}

(b) ACF for T_{random}.

Figure 3.2: Example of a random time series and its auto-correlation function.

The auto-correlation at lag one computes the average variation of observations

that are one time step apart:

$$\begin{aligned} r_1 &= \frac{c_1}{c_0} \\ r_1 &= \frac{75}{98.20} \cdot \Big[\frac{1}{75} \sum_{t=1}^{74} (z_t \cdot z_{t+1}) \Big] \\ r_1 &= \frac{1}{98.20} \cdot (z_1 \cdot z_2 + z_2 \cdot z_3 + \cdots + z_{74} \cdot z_{75}) = -0.007. \end{aligned}$$

Similarly, the auto-correlation at lag 37 computes the average variation of observations that are 37 time steps apart:

$$\begin{aligned} r_{37} &= \frac{c_{37}}{c_0} \\ r_{37} &= \frac{75}{98.20} \cdot \Big[\frac{1}{75} \sum_{t=1}^{38} (z_t \cdot z_{t+37}) \Big] \\ r_{37} &= \frac{1}{98.20} \cdot (z_1 \cdot z_{38} + z_2 \cdot z_{39} + \cdots + z_{38} \cdot z_{75}) = 0.15. \end{aligned}$$

Example of a Flat Series and Its ACF

When the time series is flat and has small variance, e.g., 3.3(a), its ACF transformation, 3.3(b), looks similar to the ACF of a random series, though a significant number of r_i coefficients are actually 0 (assuming some degree of variance surrounding the constant time series). Consider the synthetic flat series with 75 time measurements of 3.3(a) with mean $\mu \approx 0$ and sample variance $s^2 = 0.19$

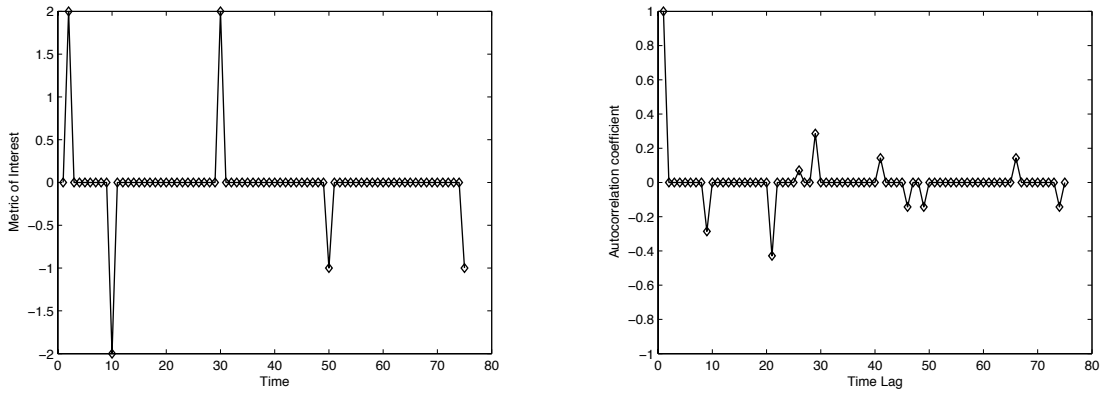

(a) Flat time series, T_{flat}, with some variance.

(b) ACF for T_{flat}.

Figure 3.3: Example of a flat time series and its auto-correlation function.

Index	1	2	3	4	5	6	7	8	9	10
+0	0.00	2.00	0.00	0.00	0.00	0.00	0.00	0.00	0.00	−2.00
+10	0.00	0.00	0.00	0.00	0.00	0.00	0.00	0.00	0.00	0.00
+20	0.00	0.00	0.00	0.00	0.00	0.00	0.00	0.00	0.00	2.00
+30	0.00	0.00	0.00	0.00	0.00	0.00	0.00	0.00	0.00	0.00
+40	0.00	0.00	0.00	0.00	0.00	0.00	0.00	0.00	0.00	−1.00
+50	0.00	0.00	0.00	0.00	0.00	0.00	0.00	0.00	0.00	0.00
+60	0.00	0.00	0.00	0.00	0.00	0.00	0.00	0.00	0.00	0.00
+70	0.00	0.00	0.00	0.00	−1.00	−	−	−	−	−

.

The auto-correlation at lag one is $r_1 = 0$, while the coefficient at lag 20 is $r_{20} = -0.4286$, reflecting that when one of the series measurements increases the other one, 20 lags apart, decreases or vice versa.

Example of a Periodic Series and Its ACF

When a series is periodic, the ACF transformation is also periodic. The intuition behind this property stems from the fact that as one compares two time-shifted versions of a periodic series, when the series' peaks overlap, the ACF coefficients are positive while when the series' peaks and valleys overlap, the ACF coefficients are

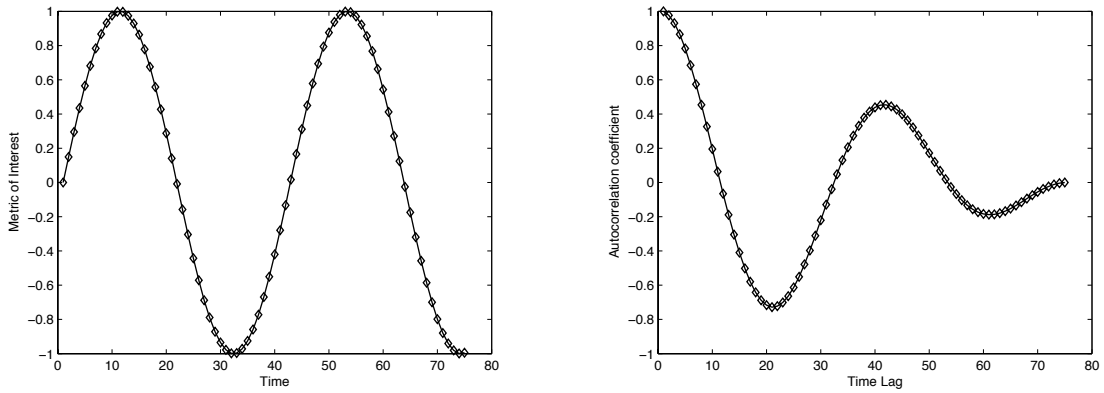

(a) Periodic time series, $T_{periodic}$, with some variance.

(b) ACF for $T_{periodic}$.

Figure 3.4: Example of a periodic time series and its auto-correlation function.

negative[1].

Figure 3.4(a) shows a periodic sinusoidal time series with its ACF illustrated in Figure 3.4(b). Consider the synthetic periodic series with 75 time measurements of Figure 3.4(a) with mean, $\mu \approx 0$ and sample variance, $s^2 = 0.51$

Index	1	2	3	4	5	6	7	8	9	10
+0	0.00	0.15	0.30	0.43	0.56	0.68	0.78	0.87	0.93	0.98
+10	1.00	1.00	0.97	0.93	0.86	0.78	0.68	0.56	0.43	0.29
+20	0.14	−0.01	−0.16	−0.30	−0.44	−0.57	−0.69	−0.79	−0.87	−0.94
+30	−0.98	−1.00	−1.00	−0.97	−0.93	−0.86	−0.77	−0.67	−0.55	−0.42
+40	−0.28	−0.13	0.02	0.17	0.31	0.45	0.58	0.69	0.79	0.88
+50	0.94	0.98	1.00	1.00	0.97	0.92	0.85	0.77	0.66	0.54
+60	0.41	0.27	0.12	−0.03	−0.17	−0.32	−0.46	−0.59	−0.70	−0.80
+70	−0.88	−0.94	−0.98	−1.00	−0.99	–	–	–	–	–

The auto-correlation coefficient at lag 40 is $r_{40} = 0.44$ reflecting that observations that are 40 time steps apart are increasing at the same time. The lag at 20 is negative, $r_{20} = -0.72$, and reflects that when one of the series measurements increases the other one, 20 lags apart, decreases or vice versa.

[1]All the time series analyzed are normalized to zero-mean.

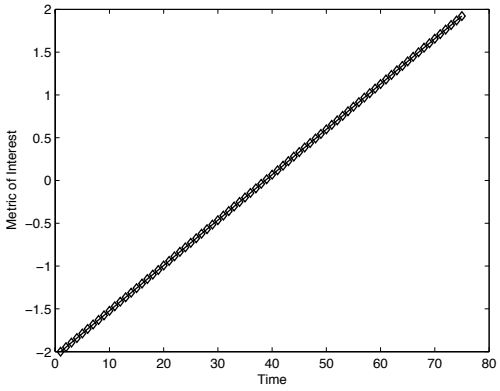

(a) Ramp-up time series, $T_{ramp-up}$.

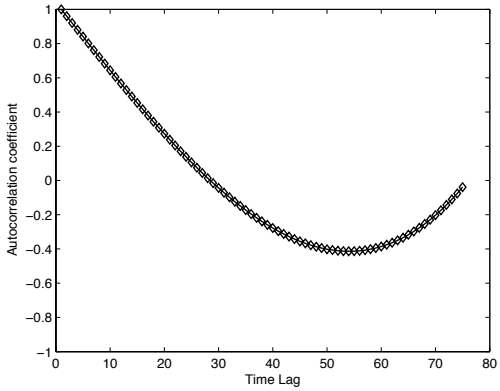

(b) ACF for $T_{ramp-up}$.

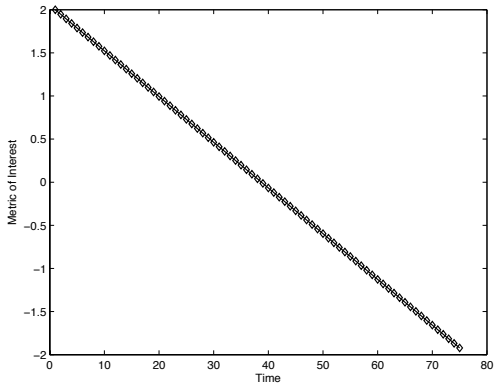

(c) Ramp-down time series, $T_{ramp-down}$.

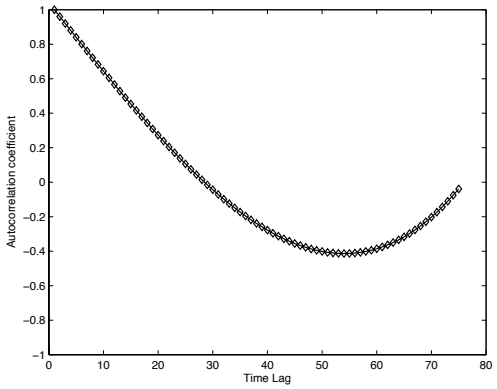

(d) ACF for $T_{ramp-down}$.

Figure 3.5: Example of ramp time series and their auto-correlation function.

Example of a Ramp Series and Its ACF

When a series resembles a ramp, the ACF transformation is monotonically decreasing for the majority of the length of the ACF. Figure 3.5(a) shows a time series resembling a ramp. Its ACF, illustrated in Figure 3.5(b), decreases as the lag increases up to a minimum after which it increases slowly toward zero. The reason why the ACF decreases up to the minimum is because latter values of the original series are not very correlated with earlier ones; also, the reason why there is an increase in the values of ACF after the minimum is an artifact of the numerical estimation of the lags at the end of the series, where there are fewer numerical values contributing

to a more negative value of the lag. Consider the synthetic ramp series with 75 time measurements of Figure 3.5(a) with mean $\mu \approx 0$ and sample variance $s^2 = 1.33$

Index	1	2	3	4	5	6	7	8	9	10
+0	−2.00	−1.95	−1.89	−1.84	−1.79	−1.73	−1.68	−1.63	−1.58	−1.52
+10	−1.47	−1.42	−1.36	−1.31	−1.26	−1.21	−1.15	−1.10	−1.05	−0.99
+20	−0.94	−0.89	−0.83	−0.78	−0.73	−0.68	−0.62	−0.57	−0.52	−0.46
+30	−0.41	−0.36	−0.30	−0.25	−0.20	−0.15	−0.09	−0.04	0.01	0.07
+40	0.12	0.17	0.23	0.28	0.33	0.38	0.44	0.49	0.54	0.60
+50	0.65	0.70	0.76	0.81	0.86	0.91	0.97	1.02	1.07	1.13
+60	1.18	1.23	1.29	1.34	1.39	1.44	1.50	1.55	1.60	1.66
+70	1.71	1.76	1.82	1.87	1.92	–	–	–	–	–

The auto-correlation coefficient at lag ten is $r_{10} = 0.64$, considerably smaller at lag 50, $r_{50} = -0.40$ where it is negative because earlier larger negative values from the beginning of the series are multiplied with later smaller positive values.

3.2 Temporal Signatures

We define a temporal signature to be the a vector containing features of interest for a group of performance time series data. We explain in the next sections what features are relevant for scientific applications; we show how those features are extracted, and how we build a temporal signature.

3.2.1 Feature Selection and Extraction

The process of *feature selection* refers to identifying a small set of features from data that can be useful in the characterization and classification of that data given some objective function. The process of *feature extraction* refers to the process by which a selected feature can be extracted from the data.

In our framework, we choose to study features of interest based on domain knowledge in order to classify performance time series data for application performance validation and diagnosis. If domain knowledge is not available for feature selection, automated feature selection schemes for time series data, such as those proposed in

[87], can be employed. The following sections motivate the choice of our features, and explain the process of extracting those features from the set of performance time series data.

Relative Variance

We extract the *amount of variability* present in time series because it is an indicator of fluctuation around the average resource utilization of applications. This data can be extracted using the sample variance s^2 defined in Equation 3.2. However, the sample variance depends on the scale of the measurement of a particular performance data time series. Therefore, we transform the s^2 values to a normalized $[0, 1]$ space, with 0 signifying the lowest variance seen in the particular metric and +1 signifying the highest variance observed. This data normalization must be performed because (1) the value of the feature extracted must be independent of the scale of the time series, and (2) future application of clustering and classification algorithms requires bounded and normalized values in order to produce unbiased results. The normalized variance is labeled as s_n^2. Furthermore, we discretize this normalized variance into three different categorical levels: (1) low, (2) moderate, and (3) high, corresponding to normalized variance ranges of [0-0.33], [0.34-0.66] and [0.67-1]. We call our measure of variability the *normalized, categorical* variance $s_{n,c}^2$, and it takes the categorical values of $\{1, 2, 3\}$ corresponding to the {low, moderate, high} variability in the data.

Pattern Identification

Another important feature to extract from a time series is the type of pattern present in the data. The pattern information supplements the information provided by the variance in the time series, because it further characterizes how the metric varies around an expected baseline. Consider there is a pattern identification mechanism that, given a time series of interest, can tell if the series is most likely from a

random distribution, whether it is oscillatory in nature, whether it is flat or whether it is similar to a ramp. Other patterns may occur, such as a self-similar pattern; however, currently we are interested in detecting among four different patterns: random, periodic, flat or ramp. Treating the pattern identification mechanism as a black box taking as input time series T and outputting one of the four patterns or an unknown pattern, we map the results into a numeric space in the discrete set $\{1, 2, 3, 4, 5\}$, such that pattern p takes the numeric ranges shown in Table 3.2. We further describe a

Series Pattern	**Value for** p
Unknown	$p = 1$
Ramp	$p = 2$
Periodic	$p = 3$
Random	$p = 4$
Flat	$p = 5$

Table 3.2: Encoding the pattern into a discrete value within $\{1, 2, 3, 4, 5\}$.

simple heuristic methodology that discriminates between time series with these four different patterns: random, periodic, ramp or flat. The methodology is based on the properties of the ACF. The enumerated patterns are important because they are commonly observed patterns in performance data time series of scientific applications. For example, long-running computationally intensive applications generate flat CPU time series patterns, while data-intensive applications request data through the memory hierarchy at periodic intervals, generating disk or network time series with periodic patterns. These characteristics of scientific applications have been noted in several papers [89, 76, 110].

We describe the pseudo code for the pattern identification mechanism in Algorithm 1, and summarize the methodologies for Test-Random(T), Test-Ramp(T), and Test-Periodic(T) in Algorithm 2.

```
IDENTIFY-PATTERN( TIME SERIES T )

Compute ACF( T ): r(1) ... r(N)

if ( ACF( T ) is defined ) then
    if ( TEST-RANDOM( T ) is TRUE ) then
        if ( Variance( T ) is LOW ) then
            T is FLAT, p=5
        else
            T is RANDOM, p=4
    elseif ( TEST-PERIODIC( T ) is TRUE ) then
        T is PERIODIC, p=3
    elseif ( TEST-RAMP( T ) is TRUE ) then
        T is RAMP, p=2
    else
        Pattern of T is UNKNOWN, p=1
else ( ACF( T ) is undefined )
     T is FLAT, p=5
```

Algorithm 1: Heuristic algorithm for pattern identification for a zero-mean time series, T.

```
MaxR = max( ACF( T )[2:N] )
MinR = min( ACF( T )[1:N] )
i1 = index( ACF( T ), MinR )
Max2R = max( ACF( T )[i1:N] )

TEST-RANDOM( T )
  if r(1,L) <= r(1) <= r(1,U)
    return TRUE

TEST-PERIODIC( T )
  if MaxR >= r(1,U) AND
     MinR <= r(1,L) AND Max2R >= r(1,U)
     return TRUE

TEST-RAMP( T )
% min. occurs towards tail of series
  if index( minR ) >= 70% N
     return TRUE
```

Algorithm 2: Heuristic methodologies for identification of random, ramp and periodic patterns.

Random Pattern Identification: TEST-RANDOM(T)

The function that tests for randomness in a time series T is based on a simple statistical test applied to the first auto-correlation coefficient, r_1. The first-order auto-correlation coefficient is tested against the null hypothesis that the corresponding population value $\rho_1 = 0$. The critical value of r_1 for a 95% confidence is based on the two-tailed test [8, 99], since the time series are of zero mean, the auto-correlation coefficients are both positive and negative:

$$r_k = \frac{-1 \pm 1.96\sqrt{N-k-1}}{N-k} \tag{3.8}$$

where N represents the length of the time series and k is lag. The test is only for $k = 1$. The confidence bands for r_1 are calculated using the formula:

$$r_1 = \frac{-1 \pm 1.96\sqrt{N-2}}{N-1} \tag{3.9}$$

The test for deciding with 95% confidence that the series is from a random distribution reduces to the simple comparison test to verify that the actual r_1 of the ACF of the time series is between the upper $r_{1,U} = \frac{-1+1.96\sqrt{N-2}}{N-1}$ and the lower $r_{1,L} = \frac{-1-1.96\sqrt{N-2}}{N-1}$ confidence bands:

$$\text{If } r_{1,L} \leqslant r_1 \leqslant r_{1,U}, \text{ Series T is RANDOM .}$$

Figure 3.6 illustrates the ACF of a random time series of length $N = 100$ and the upper and lower confidence bands at 95% for r_1. In this case, this series, although from a random distribution will be flagged as "unknown" because the value of the r_1 coefficient is outside the lower confidence band.

The confidence bands for $k = 1$ are the tightest possible. Values of $r_{k,U}$ and $r_{k,L}$ increase and decrease respectively as k approaches N. Figure 3.7 illustrates the

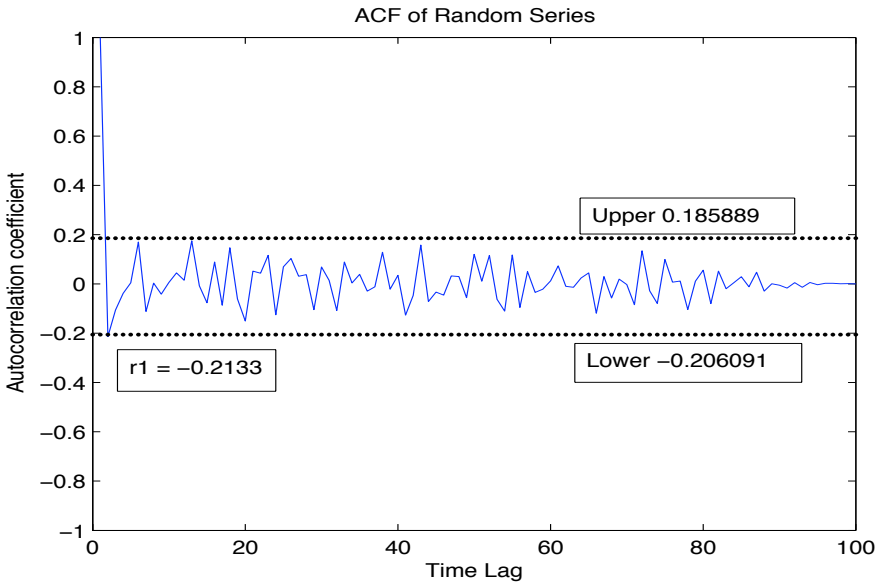

Figure 3.6: ACF of a random time series. Value of r_1 is slightly outside confidence bands; IDENTIFY-PATTERN(T) procedure identifies series as"unknown".

values of the upper $r_{k,U}$ and lower $r_{k,L}$ confidence bands for k ranging from 1 to 90, for a time series of length $N = 100$.

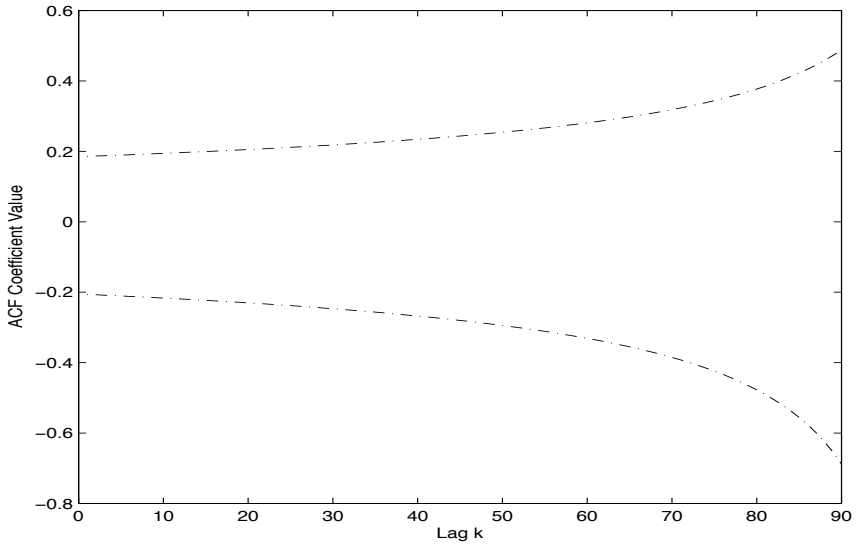

Figure 3.7: Computed confidence bands values for k $\geqslant 1$

Alternate methods could be employed to make this decision, such as calculating

the Q-statistic as in [63], which requires the stricter condition that all r_k beyond a given lag k are effectively zero.

Periodic Pattern Identification: TEST-PERIODIC(T)

A function $f(x)$ is periodic with period ϕ if $f(x) = f(x + n \cdot \phi)$. The constant function $f(x) = 0$ is also considered theoretically periodic with any period ϕ, but for the purposes of our analysis, we consider the constant function as a distinct pattern to identify in the given time series.

The auto-correlation function of a periodic time series has the important property that it is also periodic. Periods in the time series will be reflected at lags in the ACF where the values are positive and closer to one.

Since we are only trying to identify whether a series is periodic or not, the problem reduces to a simplified one, in comparison to the general problem of periodicity detection in time series. The heuristic for identifying periodicity in any time series is based on the properties of the ACF. A periodic series has a periodic ACF that gradually decays to zero as the lag k approaches N. The heuristic developed is illustrated in Figure 3.8 and is described below:

$$\begin{aligned} \text{If } \max_1 \text{ beyond lag } k = 1 \notin [r_{1,L}, r_{1,U}] \text{ AND} \\ \min_1 \text{ beyond lag } k(\max_1) \notin [r_{1,L}, r_{1,U}] \text{ AND} \\ \max_2 \text{ beyond lag } k(\min_1) \notin [r_{1,L}, r_{1,U}] \text{ THEN} \\ \text{Series T is PERIODIC .} \end{aligned}$$

An alternate method to check for existing periodic behavior may be based on spectral analysis as in [50]. However, since the auto-correlation function (ACF) and the spectral density function (SDF) of a series are mathematically equivalent, any pattern identification technique experimentally successful in one domain of analysis

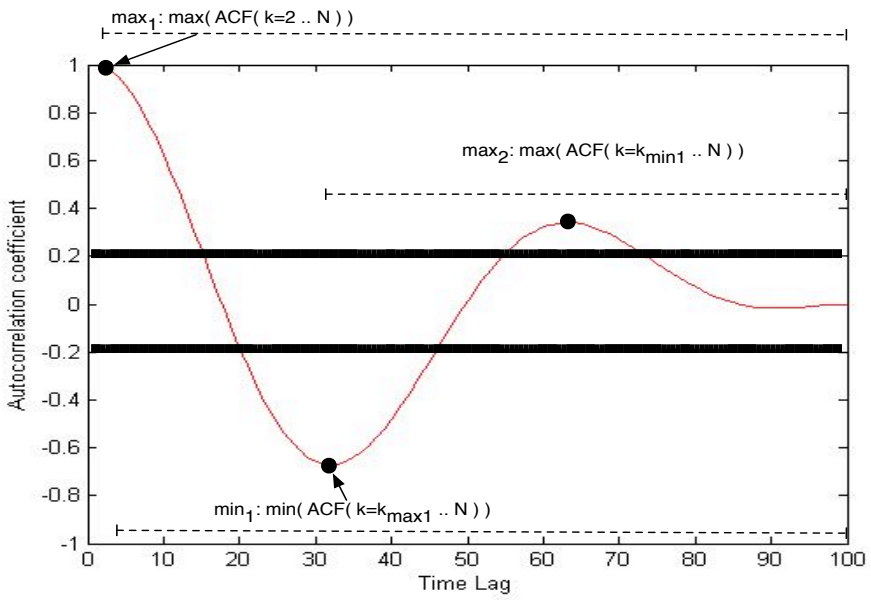

Figure 3.8: ACF of a periodic time series. Illustration of the heuristic for identifying whether the series is periodic.

is sufficient in the current context.

Ramp Pattern Identification: TEST-RAMP(T)

The auto-correlation function of a ramp-resembling series will slowly decay to zero in an approximately linear fashion. The intuition is that for a ramp-like series, initial values of the series are less correlated with later values of the series. Based on this observation, a simple heuristic for testing for a ramp time series is illustrated in Figure 3.9 and is described below:

$$\begin{aligned} &\text{If } \max_1 \text{ beyond lag } k = 1 \notin [r_{1,L}, r_{1,U}] \text{ AND} \\ &\min_1 \text{ beyond lag } k(\max_1) \notin [r_{1,L}, r_{1,U}] \text{ AND} \\ &\min_1 \text{ occurs toward tail of the ACF THEN} \\ &\qquad\qquad \text{Series T is RAMP .} \end{aligned}$$

During the course of various experiments with the ramp heuristic, checking that the first minimum occurs beyond any lag k which is greater than 70% of the length of N

yields good experimental identification results. Note that we only detect whether the series is a ramp (i.e., either up or down). In these experiments, we do not discriminate between the two cases, though that can be easily extended by checking a number of pairs of consecutive measurements from the original series and deciding whether the time series is most likely a ramp/slope-up or a ramp/slope-down.

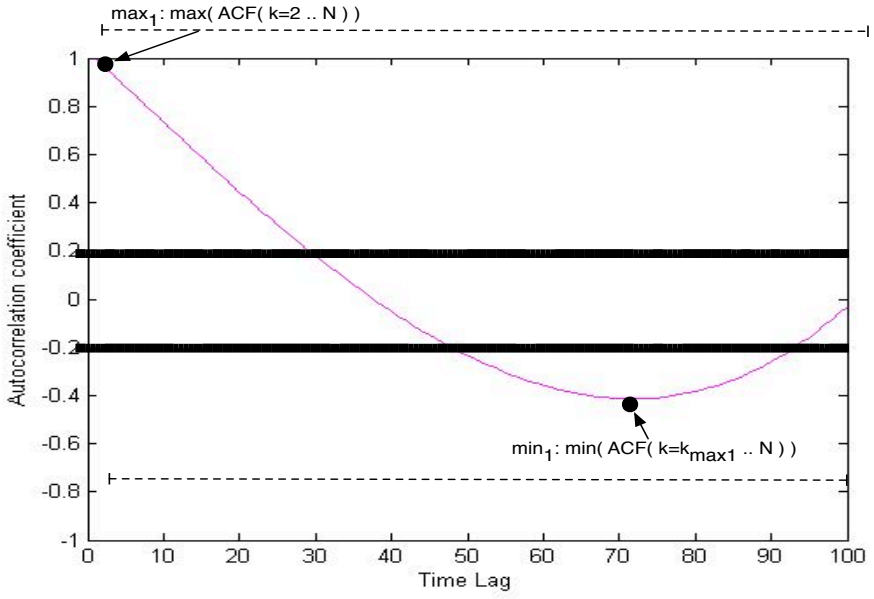

Figure 3.9: ACF of a ramp time series. Illustration of the heuristic for identifying whether the series is similar to a ramp.

Accuracy of Proposed Pattern Identification Mechanism

We simulated time series with different patterns, amplitudes, and lengths, and checked the accuracy of the pattern identification mechanism. For all simulated time series, we generated series with four different lengths, $N = \{100, 500, 1000, 10000\}$. We conducted five different identification tests, and for each test we have generated 100 different time series. Therefore, each test checks the pattern identification on $(N = 4) \times 100 = 400$ simulated time series.

Simulated Random Series

The statistical test applied to determine if a series is random or not yields an

N	**Test 1**	**Test 2**	**Test 3**	**Test 4**	**Test 5**	**Average Accuracy**
100	99	98	100	94	91	96.4
500	98	100	93	97	94	96.4
1000	94	95	95	96	95	95
10000	99	98	95	96	95	96.6
Overall						**96.1**

Table 3.3: Accuracy results for identifying random patterns in time series of different lengths, N and with varying amplitudes.

overall identification accuracy of 96.1%. The detailed results for the time series of different lengths, and for the different tests conducted are shown in Table 3.3. The statistical test on r_1 is rather simple and has very good experimental results; from all the 2000 random time series generated, approximately 1922 have been identified as random.

Simulated Flat Series

We have generated flat time series with and without added noise. For all the flat time series with no noise we obtained an accuracy of detection of 100%. For the tests where white noise is added, the accuracy of identification decreases with the amount of noise added to the flat series.

Simulated Periodic Series

We have generated a set of `sin()` and `cos()` functions of increasing frequency and different amplitudes. We conducted tests with and without added white noise.

The periodic heuristic test has performed very well in the case of generated periodic time series without added noise. For all the time series with at least one visibly identifiable period during the length of the time series, the heuristic has correctly identified all series, with an accuracy of 100%.

In the case of periodic time series with an almost clear visible period, the heuristic has failed to identify them as periodic, as expected. Figure 3.10 shows the ACF of such an "almost" periodic series. For experiments where noise is introduced, the

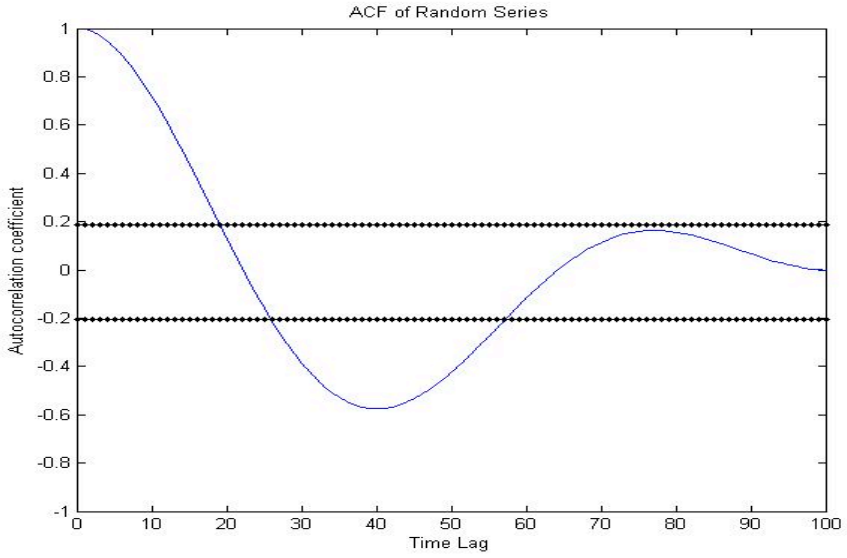

Figure 3.10: ACF of a periodic time series having almost a complete period. Heuristic fails to identify it as periodic since the $\max_2$ is within the confidence bands.

identification accuracy decreases as a function of the amount of noise present in the data. In general, if the periodic signal can be extracted by visual inspection of the series, then the heuristic algorithm can correctly identify it.

Experiments of time series with different phases of series with multiple periods show the heuristic identifying the presence of oscillatory behavior with 100% accuracy where there is no added noise, and with decreased accuracy with increased noise to signal ratio.

Simulated Ramp Series

We generate ramp time series with a increasing or decreasing slope angle. We conduct tests with and without added white noise. Experiments conducted with ramp time series of different slope angles, without added noise show the heuristic having an accuracy of detection of the actual pattern of 100%.

For experiments where noise is introduced, the identification accuracy decreases

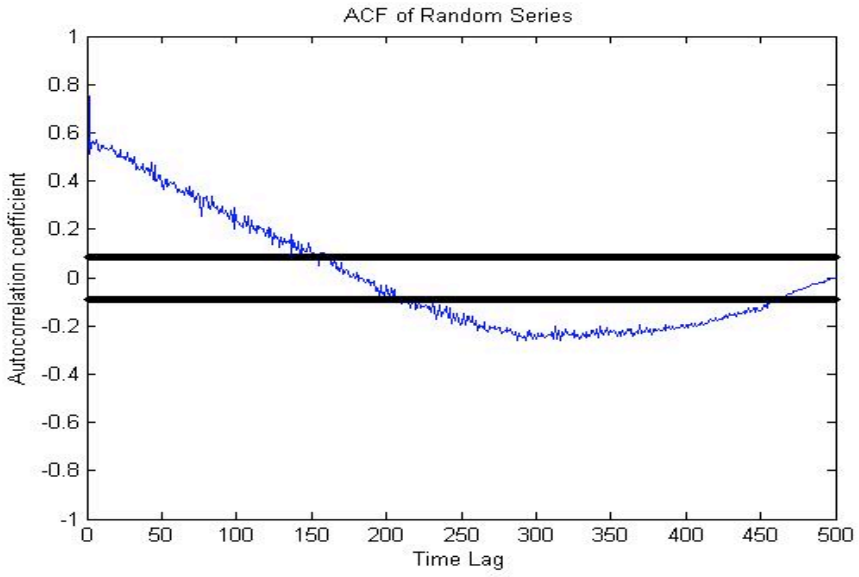

Figure 3.11: ACF of a ramp time series with added noise. Heuristic fails to identify it as ramp, due to amount of noise or possibly to the experimental choice of imposing the first minimum to be beyond 70% of N.

as a function of the amount of noise present in the data and the obscured noised ramp series are identified as *random* series, as expected. Figure 3.11 illustrates such an example.

Other Simulated Patterns

We have also generated a set of simulated time series that reflect both a periodic behavior and a ramp behavior. We conduct tests on such mixed pattern time series with and without added noise. We observe that in most of these combined pattern types the heuristic proposed fails. For example, Figure 3.12 shows the ACF of a periodic series that ramps down. The heuristic methodology identifies this series as *unknown*, because neither the periodic nor the ramp tests are true. Figure 3.12 show the ACF of such a series.

This is not considered troublesome, because most performance time series data observed from real systems do not contain frequently these types of complex series.

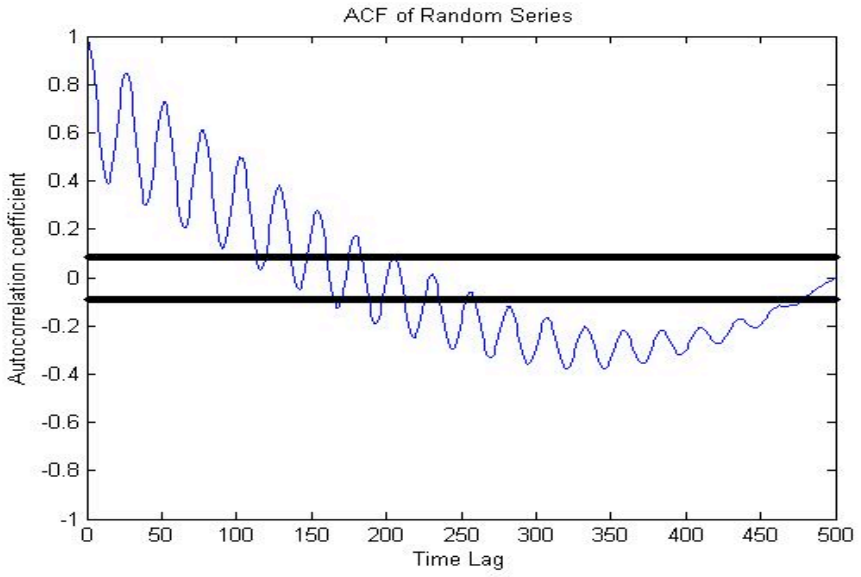

Figure 3.12: ACF of a periodic+ramp time series. Heuristic fails to identify any of the present pattern types.

However, if the most common patterns in performance data collected from computing systems changes, the current heuristics need to be modified to take any new type of relevant patterns into consideration.

3.2.2 Building Temporal Signatures

Given one performance time series T_i, we define the *temporal signature of a series* (s) to be a vector combining a set of m features of interest $F = \{f_1, \cdots, f_j, \cdots, f_m\}$:

$$s = [f_{1,T_i}, \cdots, f_{j,T_i}, \cdots, f_{m,T_i}]. \tag{3.10}$$

The *temporal signature of a set of time series* $\mathcal{S}$ can be generally defined as the concatenated vector of the temporal signatures for all series:

$$\mathcal{S} = \{f_{1,T_1} \cdots f_{1,T_M}, \cdots, f_{m,T_1} \cdots f_{m,T_M}\}. \tag{3.11}$$

Examples of features f_i that may be of interest to general time series can include

both *quantitative* or *statistical* features such as mean, variance, number of outliers, as well as *qualitative* features such as pattern, relative variance, sudden changes in trend, convexity, concavity and so on. We describe in Section 6.1.2 other examples of feature that can be extracted from time series from other domains.

Temporal Signatures for Scientific Applications

We define the temporal signature of a time series (s) as:

$$s \quad = \quad [\text{Relative Variance}(T_i), \text{Pattern}(T_i)] = [s^2_{n,c}(T_i), p(T_i)].$$

Given a set of M performance time series, (T_1 through T_M), having been selected a priori to be as independent as possible, we further define the *temporal signature of set of time series*, $\mathcal{S}$ as the concatenated vector of the temporal signatures of all series:

$$\mathcal{S} = \{s^2_{n,c}(T_1) \cdots s^2_{n,c}(T_M), p(T_1) \cdots p(T_M)\}. \tag{3.12}$$

The temporal signature captures features of interest for a set of performance time series; it represents a quantitative vector that carries compressed information about characteristics of the set of time series. We hypothesize that we can use temporal signatures to differentiate between well-performing and ill-performing application states executing on distributed computing resources.

3.3 Supervised Learning

Supervised learning is a machine learning technique for creating a function or mapping from a set of training data to a set of output values [32]. The training data consist of pairs of input objects (typically vectors), and desired outputs. In our framework's case, the training data is the set of feature vectors (temporal signatures - $\mathcal{S}$) of applications, while the outputs represent a qualitative label of application performance (e.g., *expected*, *unexpected - slow disk performance*, *unexpected - memory*

leak, and so on).

The object of the supervised learner is to predict the value of the function for any valid input data after being trained on a number of training samples (e.g., pairs of temporal signatures and target output - qualitative performance of application).

3.3.1 Training

When gathering a set of training data points, one must carefully design experimental conditions in order for the training set to be characteristic of the "real-world" use of the classifier function. In our framework, we gather a set of performance time series metrics during application execution, which are transformed in temporal signatures - that is, the input objects to the classification function. The corresponding outputs are also gathered from either (a) an automatic system defining application performance, or from (b) workflow application users.

The accuracy of the classifier will depend on how the input object is represented: that is, it will depend on the temporal signature definition. The temporal signature is a feature vector, which is descriptive of the original time series data. The number of features should not be too large, but should be large enough to accurately predict the output (see more about the issue of over-fitting in Section 3.3.3).

3.3.2 Classification

Classification is the act of distributing objects into classes or categories of the same type. Classes or categories are defined *a priori* either by an expert, or found with unsupervised learning techniques (i.e., clustering techniques). There exist a wide range of classification techniques available for data analysis. The most widely used classifiers include k-nearest neighbors, neural networks, fuzzy, Gaussian mixture model, Bayesian, decision trees and support vector machines [32]. Each of the classifiers have strengths and weaknesses. There is no single classifier that works best on

all given problems. Classifier performance depends greatly on the characteristics of the data to be classified.

In our data analysis, we use a classifier based on the k-nearest-neighbor (knn) rule. Given a set of n labeled feature vectors $\vec{x_j}$ with label D, $\{\vec{x_1}, \vec{x_2}, \ldots, \vec{x_n}\}$ belonging to label D, let $\vec{x_j} \in D$ be the training sample nearest to a new test point $\vec{x}$. Then, the *nearest-neighbor rule* ($k = 1$) for classifying $\vec{x}$ is to assign it the label associated with $\vec{x_j}$ [32]. Figure 3.13(a) illustrates the rule in a $2D$ space where two prototypes are labeled as lighter points and darker points. The nearest point is one from the dark-colored point class, and therefore the new point's label or class will also be the dark-colored class.

An extension to the nearest-neighbor rule is the k-nearest neighbor rule. This rule classifies $\vec{x}$ by assigning it the label most frequently represented among the k nearest samples. The process is illustrated in Figure 3.13(b). Out of the five nearest points, three are in the dark-colored class while two are in the light-colored class. Since the majority of the five points neighboring $\vec{x}$ are in the dark-colored class, the new point's class will also be the dark-colored class.

Depending on the data present in the feature vectors $\vec{x}$, various measures of similarity can be used, depending on context. Common choices of similarity definitions include the squared Euclidean distance, Pearson's correlation coefficient, the Mahalanobis (city-block) distance or the Hamming distance when the data is binary or categorical. For the specific instance of our current temporal signature $\mathcal{S}$, where the features have categorical values, we use as a measure of similarity the normalized Hamming distance. The Hamming distance is defined as the number n of features (or columns) that must be changed in a feature vector in order to transform one vector $\vec{x_A}$ into another one $\vec{x_B}$. The normalized Hamming distance divides n by the total number of features in the vector. To illustrate with an example, given

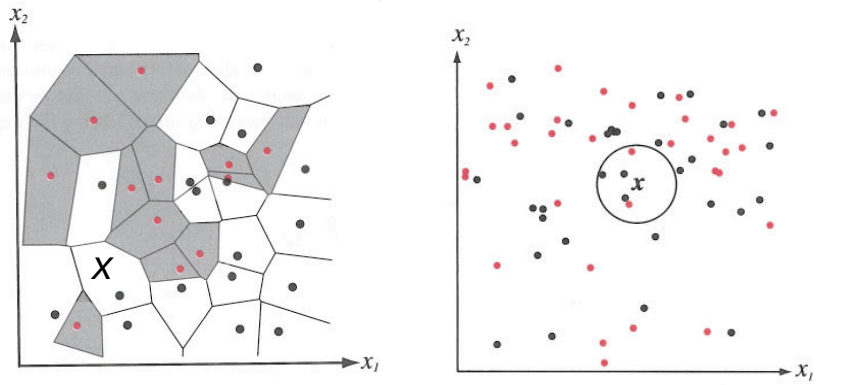

(a) Nearest neighbor process in 2D.The algorithm leads to a partitioning of the space into Voronoi cells.

(b) K-nearest neighbors process in 2D with $K = 5$.

Figure 3.13: Example of k-nearest neighbor classifier for $k = 1$ and $k = 5$. From [32].

$\vec{x_A} = \{1, 1, 1, 2, 3\}$ and $\vec{x_B} = \{1, 1, 1, 4, 3\}$, the Hamming distance between $\vec{x_A}$ and $\vec{x_B}$ is 1, because we must only change the element in the 4th column in either vector to obtain the other vector. The normalized Hamming distance is $\frac{1}{5}$. Specifically to our framework, $\vec{x}$ represents the temporal signature $\mathcal{S}$ for the execution of an application during an experimental condition, while $\vec{x'}$ represents another temporal signature $\mathcal{S}'$ for a execution of the application under another experimental condition.

Measuring Classifier Performance

We need a measure to assess how well the classifier identifies new temporal signatures. Ideally, the classification of a new temporal signature $\mathcal{S}$ with respect to the training data set should be both accurate and precise. With respect to *qualitative performance validation* of an application, our scope is to assess whether the observed performance data and its corresponding temporal signature $\mathcal{S}$ resembles previously learned signatures of *expected* application behavior versus *unexpected* application behavior. This translates to a binary classification problem, where one tries to label a temporal signature with one of the two labels. A classic measure of classifier perfor-

mance is the *classification accuracy* (A), which is a measure of how well the classifier correctly identifies or excludes a condition:

$$A = \frac{N_{TP} + N_{TN}}{N_{TP} + N_{FP} + N_{FN} + N_{TN}}, \tag{3.13}$$

that is, the proportion of true results in the population (where N_{TP} is the number of true positives, N_{TN} is the number of true negatives, N_{FP} is the number of false positives, and N_{FN} is the number of false negatives). However, in cases where target classes are rare (e.g., such as performance problems), using the above *classification accuracy* as a measure of classifier performance may be misleading, as the accuracy value (A) may be inflated due to a larger number of expected application performance states that can typically be gathered. For example, consider that we have collected $n = 100$ samples of application performance and have extracted corresponding temporal signatures. Consider we have $n_1 = 80$ of the cases representing *expected* application behavior and $n_2 = 20$ representing *unexpected* application behavior. Assume that the *knn* classifier identifies correctly all of the expected cases, resulting in $N_{TP} = 80$, and that it miss-classifies all of the unexpected cases, resulting in $N_{TN} = 0$. The accuracy of the classifier will be misleadingly high:

$$A = \frac{80 + 0}{100} = 0.8. \tag{3.14}$$

Our goal is to classify signatures from both *expected* and *unexpected* categories. Therefore, similarly to [21, 30], we additionally use as a measure of classifier performance the *balanced accuracy* (BA):

$$BA = \frac{(1 - R_{FP}) + (1 - R_{FN})}{2}, \tag{3.15}$$

where R_{FP} is the ratio of false positives (i.e., indicating there is a performance problem where there is none), and R_{FN} is the ratio of false negatives (i.e., failing to indicate there is an actual problem affecting application performance). In the example given above, the value of the *balanced accuracy* will be only 0.5., more indicative of a less accurate classification.

Furthermore, with respect to *qualitative performance diagnosis* of an application, our scope is to identify the most likely performance problem affecting the application. This translates to a multi-category classification problem, where the various categories are the examples of performance problems available in our training data. We assume in our experimental context that the number of samples of temporal signatures of performance problems is about the same across the different *unexpected* categories. Thus, within this context, using the classic measure of classifier performance A seems appropriate. However, it is still possible that within the categories of unexpected behaviors to have more samples for relatively frequently-occurring performance problems, and to have fewer samples for rarer events. If that is indeed the case, one can choose different metrics of accuracy that account for classes with fewer samples, such as those proposed in [53].

3.3.3 General Issues Affecting Classifiers

We briefly discuss some important issues affecting any supervised learner technique. These issues are significant because the different numbers of metrics analyzed, the different features, as well as the sample size of the training set will affect the accuracy of our framework.

Problems of Dimensionality

When designing a classifier, one must pay attention to how the accuracy of the classifier depends upon the dimensionality of the data (e.g., number of features in

the temporal signature), and on the amount of training data points (e.g., number of application experiments which are used for learning a knowledge base). Another issue of importance is how complex (in terms of time and space) the classifier chosen should be.

Inductive Bias

The inductive bias of a learning algorithm is a set of assumptions that the classifier function uses to predict outputs in case of novel input patterns. Below are two questions we address with respect to this issue.

What happens if the experimental data from which training is performed is actually incorrectly labeled (e.g., data is a false negative or false positive)? These types of data instances are usually treated as noise as they would typically be further away from the rest of the crowd from their actual class. It is usually accepted that the training data sets will not be perfect and therefore the focus is on making the classifier more robust.

What happens if a new signature to be tested is not like anything ever seen before in the training data set? Most conventional supervised learning techniques assume that the training and test data are drawn from the same distribution. Under this assumption, data from training and testing should be similar. The opposite case is called "sample selection bias," which means the training set is biased because of some experimental setup difference. When designing learning algorithms, it is the convention to assume similar data from train and test.

However, we may run in this issue in the cases of performance problems never encountered. In this case, the data will be incorrectly labeled and the accuracy of the classifier will decrease over time, as the classifier will be unable to correctly predict the new cases of performance problems. This issue can be addressed by extending our framework to include an adaptive learning classifier, that will self-correct over

time, and gradually include new samples of performance problems in applications.

Over-fitting

Over-fitting is an important area of research in statistical pattern recognition, as it is important to strike a balance between the complexity of the classifying function and the efficacy of classification. A classifier function should be "sufficiently" complex so that it can capture the differences between categories on training data, yet not too complex so that it performs poorly on new patterns [32].

3.4 Methodologies for Data Visualization

Our framework analyzes multi-variate time series data and extracts features from this data; therefore, we must employ the help of any available multi-variate visualization techniques to better understand the data and the efficacy of the techniques we propose. In the following sections, we describe a series of techniques to visualize multi-variate performance time series data, temporal signatures, as well as methods to visualize groups of temporal signatures in the corresponding high-dimensional variable and feature space.

3.4.1 Performance Time Series Data Visualizations

We consider the case of plotting a set of M time series, $T_1 \cdots T_M$, where each series T_i has a set of equidistant sampled values, $z_1, \cdots z_n$, that have values at potentially different scales (e.g., T_1 has samples revolving around 10 while T_5 has samples revolving around $10,000$). We have studied two different methods of visualizing these sets of time series data: (1) a semi-log on the y-axis visualization, and (2) a stacked-plots visualization. Each has advantages and disadvantages, which we further discuss.

Semi-log Y-Axis Visualization

We plot all time series on the same plot using a semi-log plot, where we compact the y-axis to display time series at various scales. Figure 3.14 shows an example of a set of seven time series metrics on the same plot. Notice that the single plot mostly preserves the visual information relating to the variance and pattern of each series. However, it may obscure certain features in the data occurring on the performance time series with scales closer to zero.

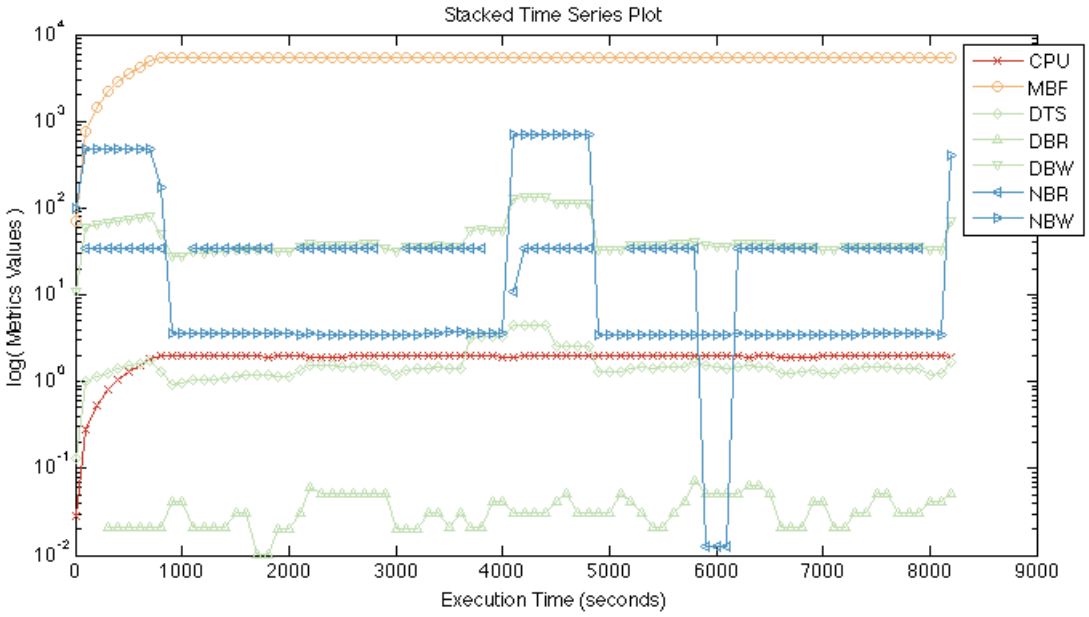

Figure 3.14: Semi-log y-axis visualization of seven time series.

Stacked-Plots Visualization

We also plot all the selected time series as a set of stacked plots, where each time series is plotted on its own independent axis, according to the scale recorded for each metric. We show such an example in Figure 3.15. The advantage of this plotting technique is that all the information in each time series is displayed in each individual axis. The disadvantage of this technique is that, as the number of time series increases, it becomes cumbersome to visualize and potentially scroll through a

long stack of performance time series plots.

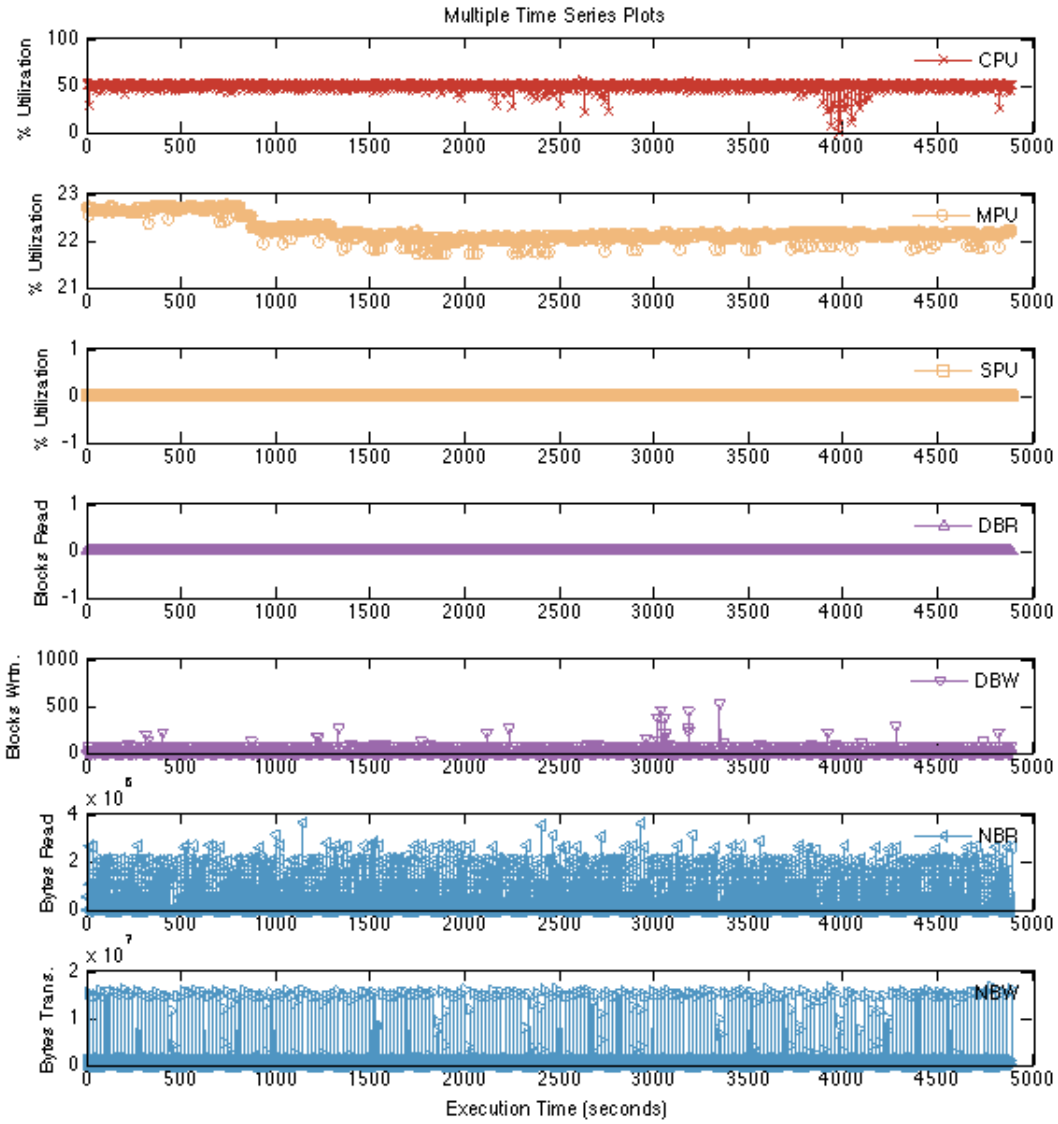

Figure 3.15: Performance time series visualized as a set of stacked individual plots.

3.4.2 Temporal Signatures Visualizations

We present methodologies for visualizing both an individual temporal signature $\mathcal{S}$ and a group of signatures $\{\mathcal{S}_1, \cdots, \mathcal{S}_n\}$ associated with the performance data collected during the execution of various applications.

Individual Signature Visualization

We have created two visualizations for our novel temporal signatures: (1) a bar chart, and (2) a color vector visualization. The temporal signature $\mathcal{S}$ for a set of seven performance time series as shown in Figure 3.15 is a vector of length 14, encoding the normalized, categorical variance and the pattern for each of the seven time series $\mathcal{S} = [1, 1, 1, 1, 1, 1, 2; 3, 1, 5, 5, 3, 3, 3]$. Two different visualizations of this signature are shown in Figures 3.16 and 3.17. The "bars" visualization separates the two categories of features –variance, pattern– and displays the values as bars.

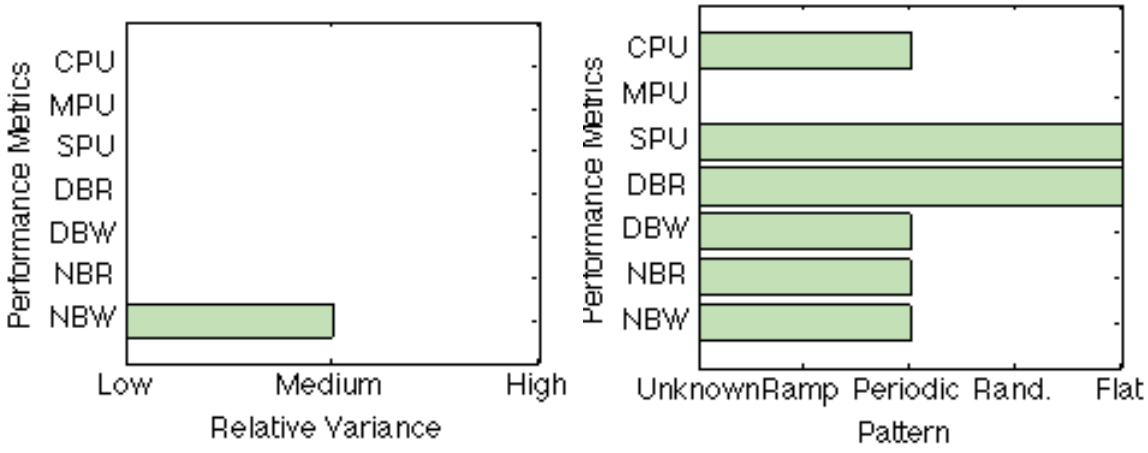

Figure 3.16: Visualization of $\mathcal{S} = [1, 1, 1, 1, 1, 1, 2; 3, 1, 5, 5, 3, 3, 3]$ as a set of two bar charts.

The second "color vector" visualization encodes the five different patterns as five different colors, and it encodes the variance as a bar of three different heights within each color box. As various people have different ways to perceive information, it is best to display the same data in forms that appeal to as many uses as possible.

Multiple Signatures Visualization

In our temporal signature methodology, we transform a set of time series into a compressed feature vector. The vector has length $M \times F_m$, because there are M

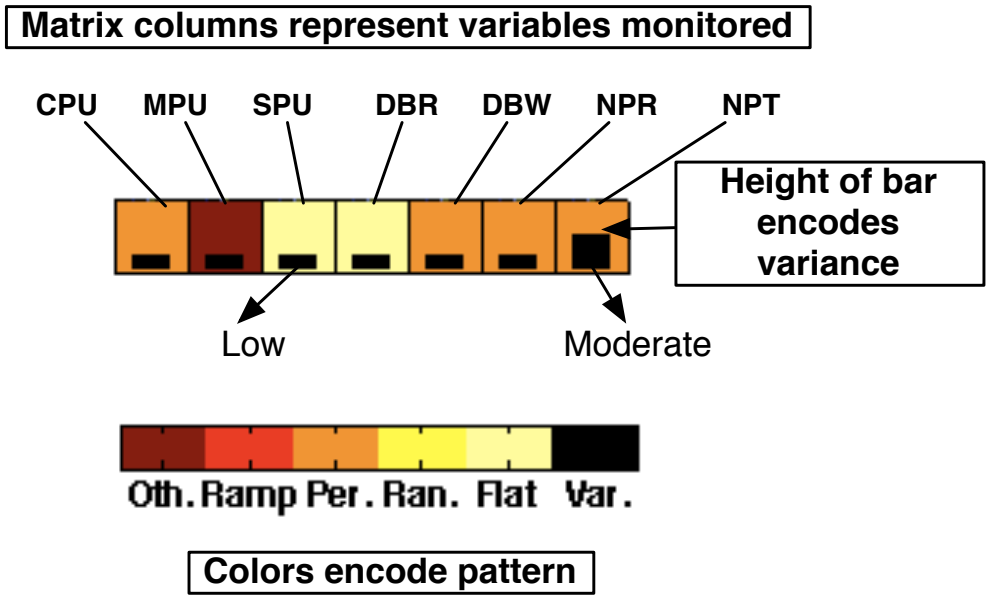

Figure 3.17: Visualization of $\mathcal{S} = [1, 1, 1, 1, 1, 1, 2; 3, 1, 5, 5, 3, 3, 3]$ as color vector.

time series with F_m different features extracted (in our case, $F_m = 2$). We have described in the previous subsection methods for visualizing one individual temporal signature, provided a set of time series data from a specified interval. However, in order to understand characteristics of many temporal signatures for applications across different configuration parameters (e.g., time intervals, computing environments, expected and diagnostic states), we need a technique such that we can visualize groups of signatures.

We have evaluated a set of multi-dimensional visualization techniques such as parallel coordinates, scatter plots, Andrews plots and Chernoff faces, described in [36] that are readily available in mathematical software packages such as Matlab [70].

We have found that two different visualizations for groups of temporal signatures work best for our data. The first method is a relatively new visualization technique called *Star-coordinates*, proposed by [55]. The second method is a novel method called *color matrix* signature visualization that we have developed based on the color vector representation proposed for an individual signature visualization.

Star-coordinates Visualization. We use a freely available visualization software called VISTA [19], which is an extended implementation of the original technique. The author of [55] has also provided us access to an implementation of the proposed technique, and we illustrate the technique as well.

$P = [d_{j1}, d_{j2}, d_{j3}, d_{j4}, d_{j5}, d_{j6}, d_{j7}, d_{j8}]$							
d_{j1}	d_{j2}	d_{j3}	d_{j4}	d_{j5}	d_{j6}	d_{j7}	d_{j8}
0.15	0.10	0.25	0.65	0.50	0.20	0.10	0.15

(a) Vector P of length 8.

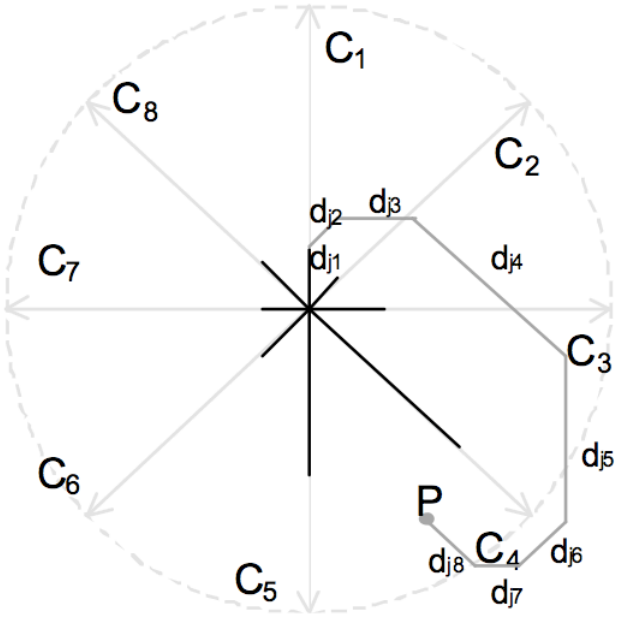

(b) Projection for P, from [55].

Figure 3.18: Example of the projection of a data point P in 8 dimensions. From [55].

Star-coordinates can be seen as an extension of the 2D scatter plot to dimensions higher than three. The technique arranges coordinates on a circle sharing the same origin at the center, and it uses points to represent the multi-dimensional data, treating each dimension uniformly [55]. Figure 3.19 illustrates the methodology for projecting a vector of length $n = 8$ (or equivalently, a point P in 8 dimensions). The

purpose of the technique is not numerical analysis but to gain insight of the data. It performs well and has been found to support users in detecting true clusters in high-dimensional data with dimensions $\leqslant 50$.

For temporal signatures, the star-coordinates method can help us visualize how temporal signatures look in expected versus diagnostic states or under different variations (i.e., across applications or execution environments). It is also important to note that the visualization introduces some ambiguity, as a single data point P may correspond to a number of data values. However, this drawback is remedied by the availability of interactive features in the software, allowing the user to apply different operations on the visualization (scaling, rotation, and so on) to help resolve these ambiguities.

P_i	[	d_1	d_2	d_3	d_4	d_5	d_6	d_7	d_8	]
P_1	[	0.1	0.0	0.2	0.1	1.0	0.9	0.8	1.0	]
P_2	[	0.0	0.2	0.3	0.0	0.7	0.9	1.0	1.0	]
P_3	[	0.1	0.0	0.2	0.1	0.9	0.9	0.9	1.0	]
P_4	[	1.0	0.9	0.8	1.0	0.1	0.0	0.2	0.0	]
P_5	[	0.7	0.9	1.0	1.0	0.2	0.2	0.1	0.2	]
P_6	[	0.9	0.9	0.8	1.0	0.3	0.0	0.1	0.2	]

Table 3.4: Values for six vectors in 8D, comprising two different categories.$P_1 - P_3$ have low values on $d_1 - d_4$ and high values on $d_5 - d_8$, while $P_4 - P6$ have high values on $d_1 - d_4$ and low values on $d_5 - d_8$.

Consider an example displaying a set of vectors in 8D shown in Table 3.4. The star-coordinates visualizations shown in Figures 3.19(a) and 3.19(b) display the six points in 8D, preserving characteristics of their data, and correctly suggesting that there are two groups of categories in this data.

Although the technique may seem similar to Kiviat diagrams[1], there are some important differences to note. The vector P is represented on a Kiviat diagram by the closed polygon marked by the values in the vector, as shown in Figure 3.20(a).

[1]Or star glyph plots.

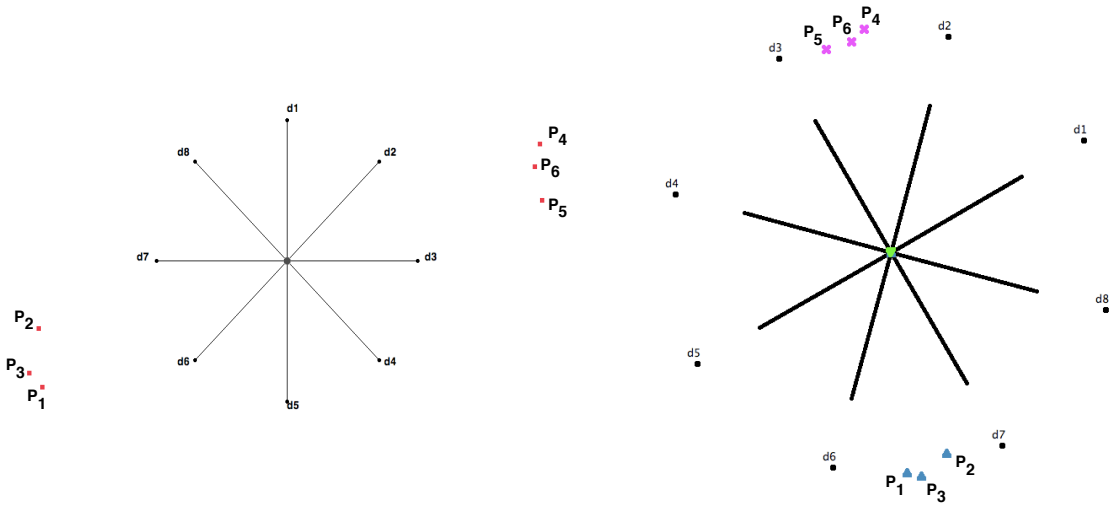

(a) StarDeck Software, by [55].

(b) VISTA Software, by [19].

Figure 3.19: $P_1 - P_6$ using two different software implementations of Star-Coordinates.

Similarly, the set of vectors P_1-P_6 are displayed in Figures 3.20(b) and 3.20(c). Notice that Kiviat diagrams work well only for visualizations of a small set of vectors (even tens of vectors, where each vector is plotted on its own set of radial graph axes). However, the Star-coordinates projection will scale better with an increase in the number of vectors to be displayed.

Color Matrix Visualization. While an individual temporal signature visualized as a color-vector may not have a great advantage over alternate representations, such as the "bars" visualization, groups of these color vectors displayed adjacently may be suggestive of differences in groups of signatures. We call a stacked set of color vectors a *color matrix* visualization. Consider a set of eight signatures, $\{\mathcal{S}_1, \mathcal{S}_2, \mathcal{S}_3, \mathcal{S}_4, \mathcal{S}_5, \mathcal{S}_6, \mathcal{S}_7, \mathcal{S}_8\}$ generated from sets of time series data. The data can be data generated for a set of eight different MPI tasks of a scientific applications for the same time interval, or it can represent a set of eight consecutive intervals of time for one single application. Our focus is to see what groups of signatures look like; Figures 3.21(a) and 3.21(b) display two different sets of eight temporal signatures.

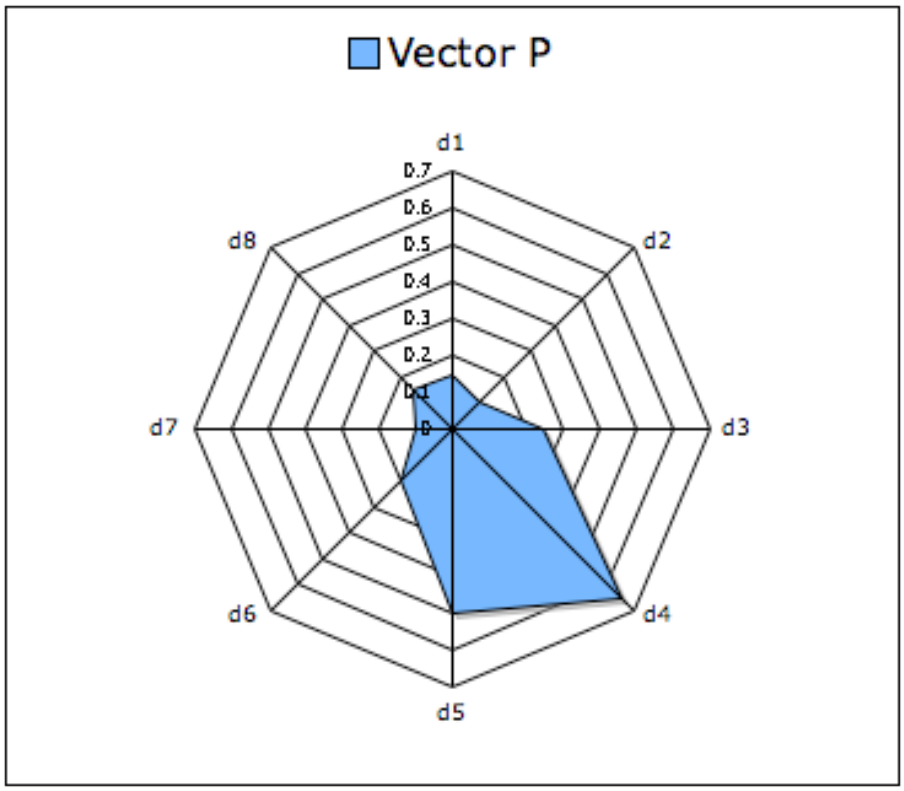

(a) Vector P plotted on a Kiviat diagram.

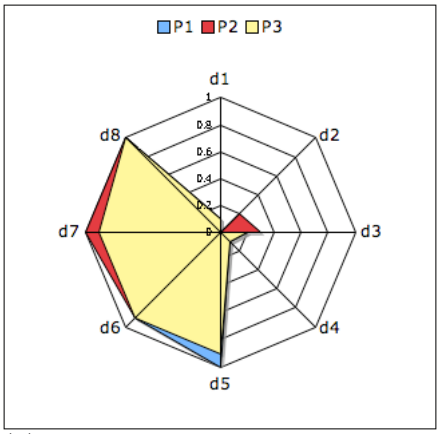

(b) Vectors P_1-P_3 on a Kiviat diagram.

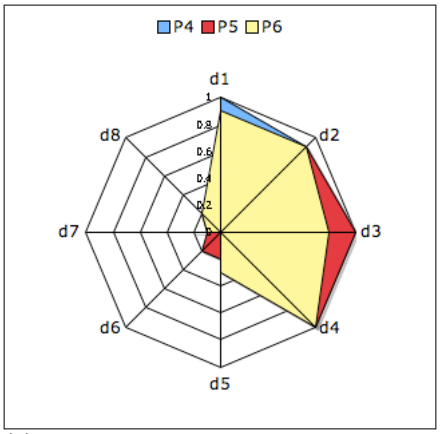

(c) Vectors P_4-P_6 on a Kiviat diagram.

Figure 3.20: $P_1 - P_6$ visualized on a Kiviat diagram. Notice that each vector P_i is represented by a closed polygon, in comparison to the Star-coordinates representations where each vector is represented as a point. The advantage of Star-coordinates over Kiviat diagrams increases significantly with an increase in the number of vectors that must be displayed simultaneously.

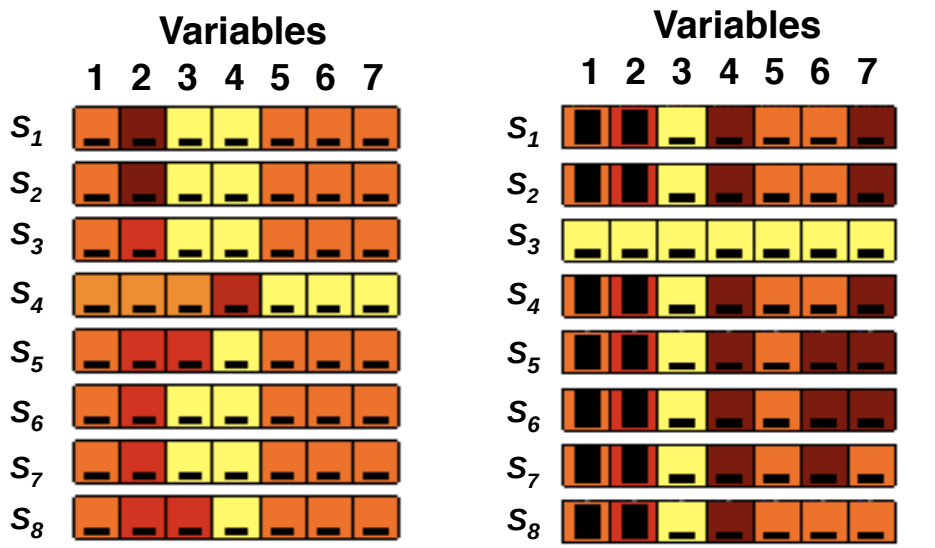

(a) Temporal signatures exhibiting low variance on all variables and various patterns on each variable.

(b) Temporal signatures exhibiting high variance on the first two variables and various patterns on each variable.

Figure 3.21: Visualization of groups of temporal signatures using our novel color matrix visualization.

Groups of temporal signatures displayed as color matrices may help inform a user or a system administrator about a possible problem in a given environment (system or application). While this is a first attempt at visualizing our feature vectors (i.e., our temporal signatures), there are great opportunities for research leveraging expertise from the user-interface and visualization communities in order to support *visual analytics* for performance monitoring data across distributed systems. Moreover, we do acknowledge that while we do use such visualizations in our specific framework to help represent multi-variate data, it is difficult in general to evaluate the quality of such visualizations that may be deployed in an on-line performance analysis system without extensive user studies targeted at system administrators or other human users.

3.5 Summary

We described the core data analysis and visualization methodologies employed in this framework. This chapter presented how we:

1. Select and extract relevant features from performance time series data in order to generate a compact representation of the data,
2. Build temporal signatures for scientific applications,
3. Use concepts from supervised learning to gather a knowledge base of qualitative performance states,
4. Evaluate the efficacy of our classifier for both qualitative performance validation and diagnosis, and
5. Employ multi-variate visualization techniques to aid in representation and analysis of our results.

Chapter 4

Qualitative Performance Analysis Framework

This chapter describes `Teresa`, (**Te**mporal **Re**asoning for **S**cientific **A**pplications), a general qualitative performance analysis framework that monitors *long-running tasks* of a scientific workflow to qualitatively validate and diagnose their performance in distributed Grid environments. `Teresa` has four high-level processing steps:

1. Selection of long-running computational tasks in workflows,
2. Collection of available performance time series data from environments where these tasks execute,
3. Analysis of data to extract characteristics correlated with well-performing and ill-performing executions of these tasks, and
4. Reasoning about the qualitative performance state of the workflow over time.

Figure 4.1 presents a diagram of the above high-level process.

4.1 Architecture

While Figure 4.1 presented a high-level, "black-box" view of our framework, we further elaborate on its composition. `Teresa` has three components: (1) a temporal signature design component, (2) a supervised learning component, and (3) a qualitative reasoning component. Figure 4.2 expands on the components within `Teresa`.

`Teresa` analyzes input data from a set of workflow monitoring tools, such as Grid infrastructure monitoring or workflow monitoring (e.g., execution engine, task

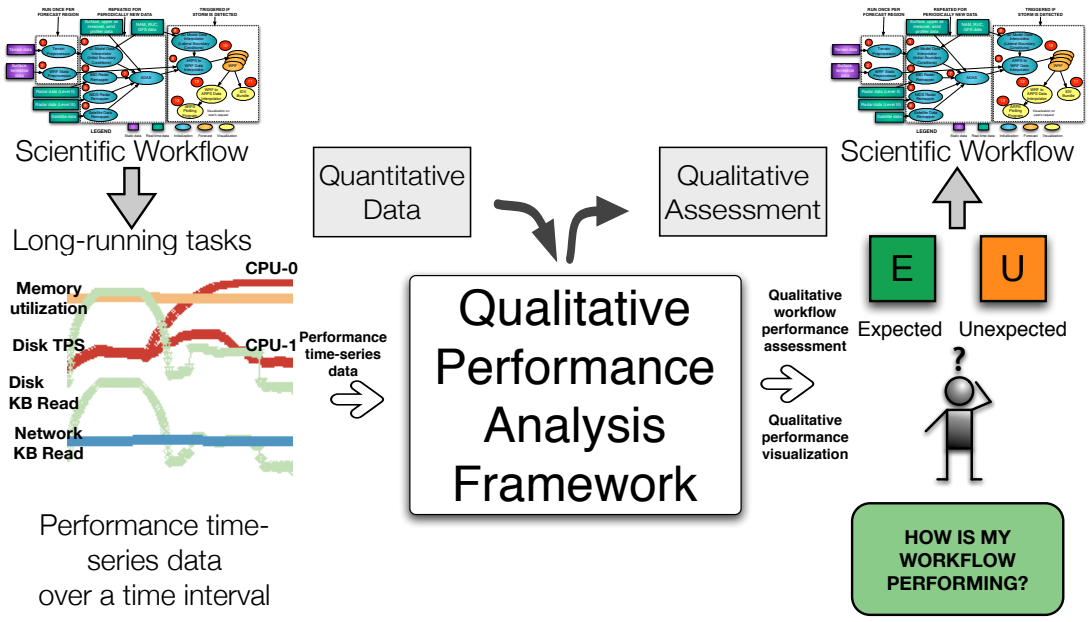

Figure 4.1: `Teresa`, qualitative performance analysis framework: high-level process overview.

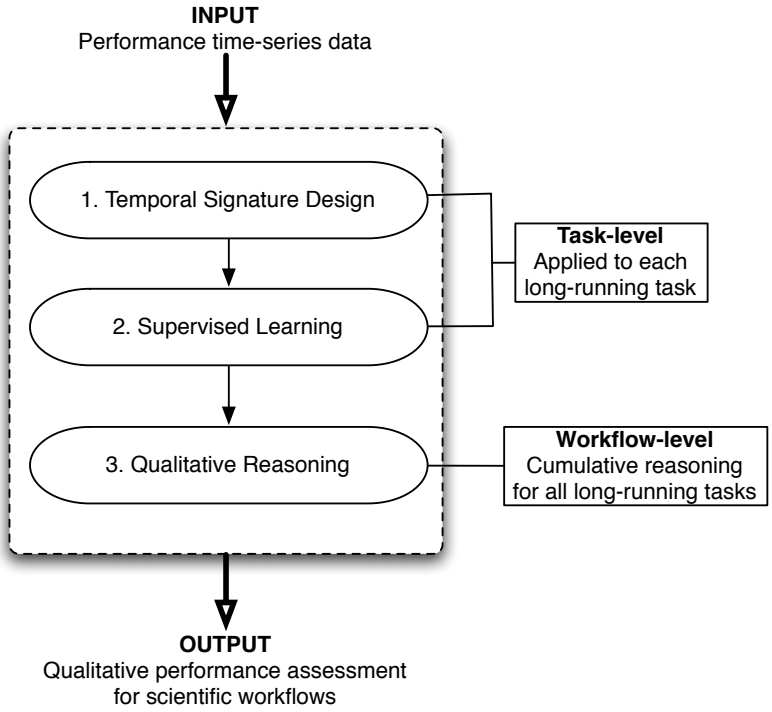

Figure 4.2: `Teresa`: framework components.

monitoring, etc). The *temporal signature design* component takes quantitative performance time series data over a specified time interval and transforms it into a temporal signature, $\mathcal{S}$, for each long-running task in a workflow. The *supervised learning* component assesses whether an application's temporal signature matches expected or unexpected behaviors. Previous application behaviors are learned in a training phase off-line. If the application behaves in an unexpected way, the *qualitative reasoning* component, which operates at the global workflow level, considers the implication to the global workflow performance of the unexpected behaviors of the flagged long-running tasks. A multitude of policies can be specified and invoked, depending on the characteristics of the scientific workflow (e.g., if 50% of the workflow tasks seem to be affected by a congested network, then checkpoint the application and restart in an hour).

We illustrate more detailed description of the framework, with the flow of information between components and their sub-components in Figure 4.3. The framework has on-line and off-line sub-components. On-line sub-components are utilized when the framework analyzes performance time series as they are received from monitoring software; the on-line sub-components are: (a) temporal signature generation, (b) on-line classification (of temporal signatures), and (c) qualitative reasoning.

The framework utilizes off-line sub-components in the configuration and training phases; the off-line sub-components are: (a) performance time series selection, (b) features selection, (c) temporal signature definition, (d) expected & unexpected temporal signatures training, and (e) policies for reasoning with qualitative diagnostic information.

Within the service oriented environment of Grids, the framework is a performance analysis service for scientific workflows, providing a periodic qualitative evaluation of performance of long-running tasks in a workflow. Grid infrastructure or workflow

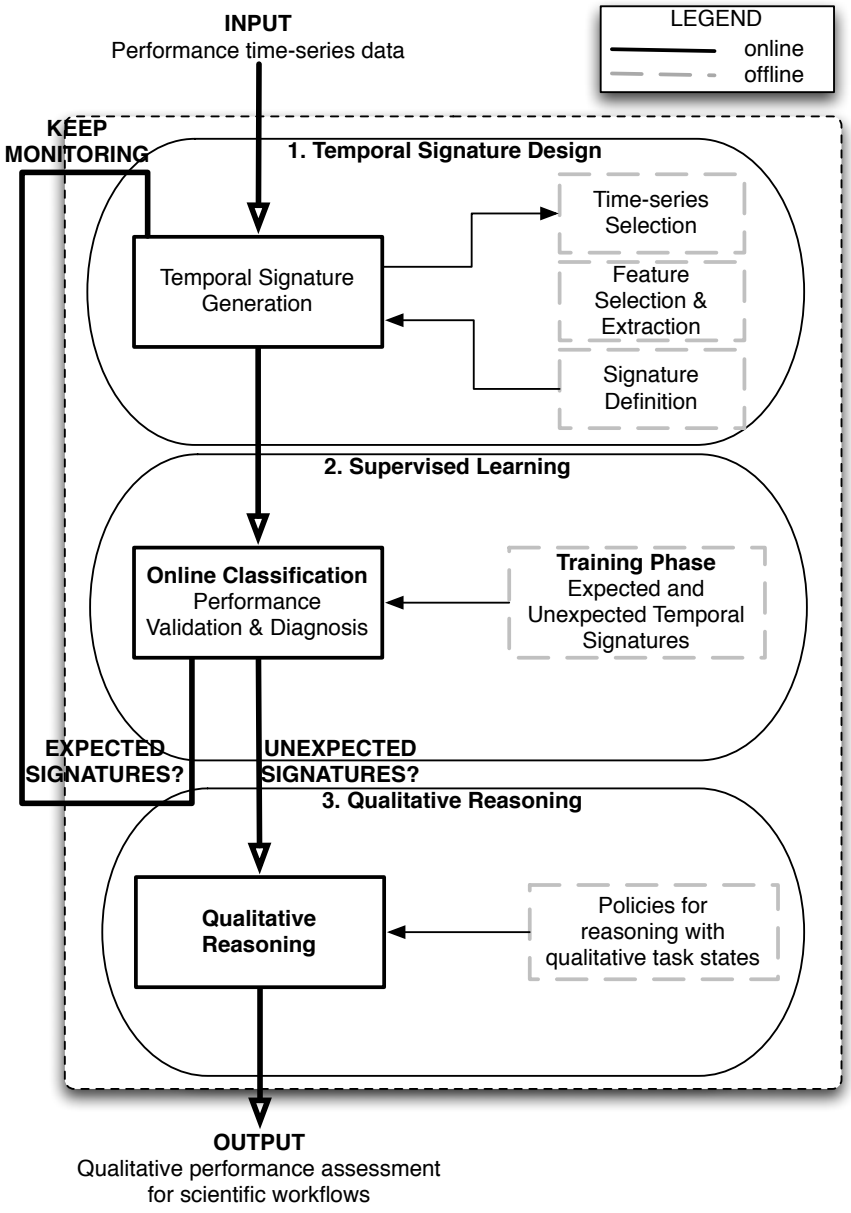

Figure 4.3: Flow of information through `Teresa`, its three components and its on-line and off-line sub-components.

monitoring services provide the performance time series data as input to the `Teresa` service, whose output can be utilized by a scheduling service and/or by a fault-tolerance service such as [54] to improve the performance of the monitored workflow, as shown in Figure 4.4.

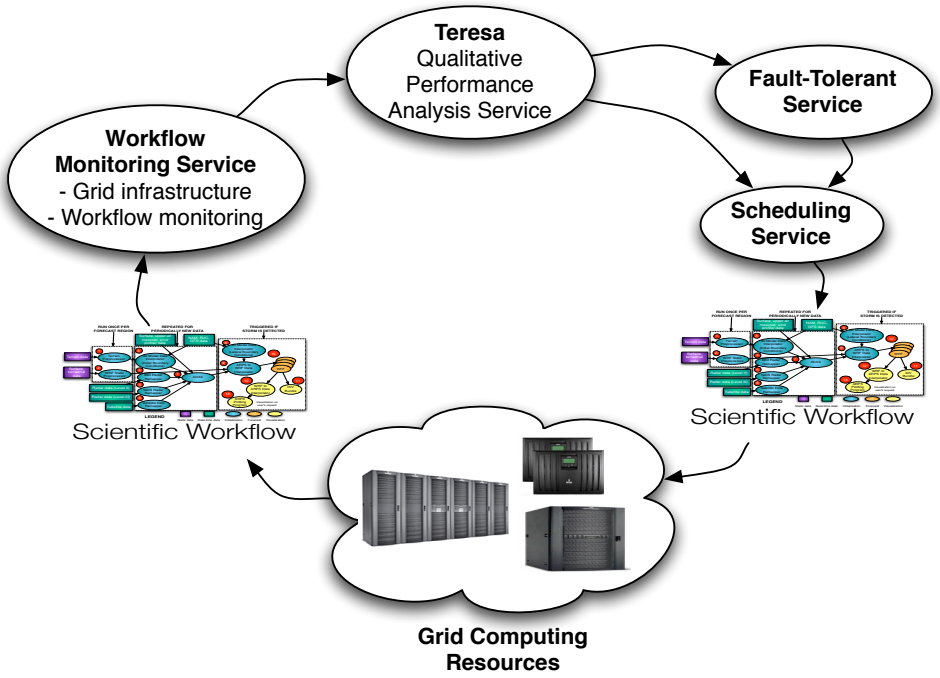

Figure 4.4: `Teresa`: a qualitative performance analysis service for scientific workflows.

4.2 Characteristics

The framework addresses a set of fundamental characteristics needed for a practical performance analysis tool operating on high performance computing environments and applications:

1. *Scalability.* Scientific workflows execute on Grids containing large numbers of computational resources. Therefore, `Teresa` must be scalable to accommodate processing data from all computational resources involved in supporting the execution of workflows. The monitoring infrastructure used must also be scalable, since the input is provided by Grid monitoring services. We address scalability by defining and generating temporal signatures of applications, which are very compact representations of information carried in time series performance data. With these temporal signatures we show how to achieve performance validation and diagnosis under certain cases.

2. *Metric independence.* The framework must be flexible; given a set of monitored metrics that reflect the temporal performance of the application, it must be possible to assess and diagnose the observed temporal behavior. However, if another set of metrics is deemed more representative of application behavior, the framework principles must still apply and behavioral reasoning must still be possible. We address this by including in our framework design the ability for the user to define different application signatures from different metrics. The off-line sub-component *time series Selection* allows for this flexibility.

3. *Accuracy of qualitative performance assessment.* The framework must make decisions based on qualitative data obtained by transforming/compressing large amounts of quantitative information. This process results in loss of information which may have implications on the accuracy of the qualitative transformations. However, the framework should provide simple and intuitive performance assessment answers, and should offer a statistical estimation of the correctness of the qualitative assessment. We address the issue of the accuracy of validation and diagnosis by associating with our framework an *accuracy-of-assessment* metric within the *on-line classification* sub-component. If the framework consistently falls below a specified accuracy threshold, T_a, then it will go into a training mode, until a better accuracy of performance assessment can be achieved.

4. *Assessment over appropriate time scale.* Due to the nature of the long duration of resource consumption by the distributed scientific workflows, the reasoning decisions made by the framework should similarly be made on a longer temporal scale, typically of the order of several tens of minutes. The framework's goal is to detect persistent behavioral violations and ignore small-scale variability, because the cost of performing any type of performance recovery mechanisms

for these applications is extremely high. We address this issue within each of the scientific application studied by generating temporal signatures only when specified percentage of the progress of the long-running application toward the scientific result has been reached. This specified percentage corresponds to a fixed time interval for performance evaluation. The interval can be different depending on the characteristics of the computational resource where the application executes.

4.3 Temporal Signature Component

The *temporal signature design component* receives performance time series data as input and generates a compressed temporal signature. It has four sub-components, shown in Figure 4.5: (1) a performance time series selection sub-component, (2) a feature selection and extraction sub-component, (3) a temporal signature definition sub-component, and (4) a temporal signature generation sub-component.

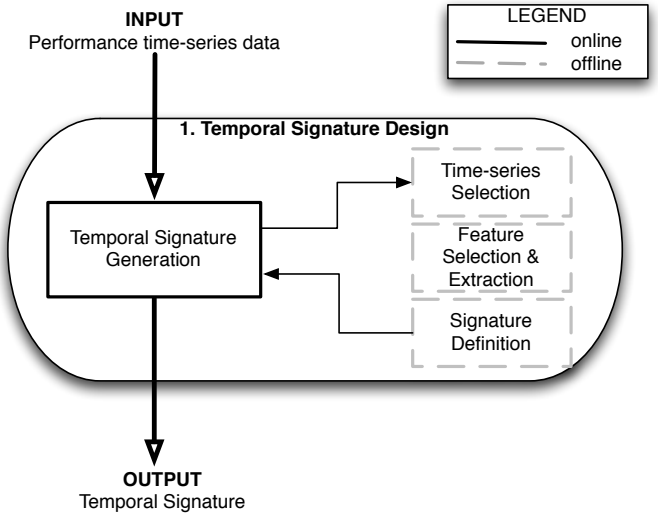

Figure 4.5: Temporal signature design component.

4.3.1 Performance Time Series Selection

Application users or system administrators can select a subset of performance metrics time series of interest, reflecting the performance of their workflows. Such a set is given in Table 4.1 and is justified because:

1. We are interested in capturing metrics easily available with standard monitoring tools (i.e., such as those coming from Grid infrastructure monitoring , NWS [115], Ganglia [69], and Monitoring and Directory Service (MDS) [24] or HAPI [97]), and easily available across a variety of platforms without requiring application instrumentation, and

2. The metrics reflect the resource usage of the application over time and are correlated with application performance over time.

A requirement of the selected set of metrics is that they must be as uncorrelated as possible. While total independence of metrics in a computer system is an unreasonable requirement, quasi-independent is satisfactory. If the user makes a selection that does not meet this requirement, principal component analysis as described in classical statistical analysis books [31], may be used as a tool to guide a more appropriate choice. Principal component analysis can transform a multi-dimensional data set to a lower dimensional one. The reduced data set contains the most important characteristics that contribute most to its variance.

Preprocessing

We preprocess the selected performance time series before analysis; in particular, the time series are smoothed and zero-mean normalized.

We perform smoothing because it filters out both the inherent noise present in the data collection process and potential significant transient changes (i.e., on the

Workload Metrics
Percentage CPU Utilization
Amount of Free Memory
Number of Local Disk Transactions per Second
Local Disk Number of Bytes Read per Second
Local Disk Number of Bytes Written per Second
Network Number of Bytes Read per Second
Network Number of Bytes Written per Second

Table 4.1: An example set of easy-to-collect, non-invasive performance time series metrics that can be used as input to the qualitative performance analysis framework.

scale of a couple of seconds or minutes), which are typically insignificant in the case of long-running scientific workloads (i.e., longer than 30 minutes).

We also normalize the time series to a zero-mean, to ease pattern analysis due to the metrics reflecting different measuring scales.

4.3.2 Features Selection and Extraction

We are interested in characterizing the selected performance time series such that we extract the maximum amount of information in the least amount of space. Our approach is to extract from the quantitative time series features that may correlate with performance variability, such as *amount of variability* and the *type of pattern* of the series. Both features are of interest because performance time series may have a similar amount of variability but different temporal patterns. The specific methodologies by which we perform the feature extraction are described in more detail in Chapter 3.

4.3.3 Temporal Signature Definition

Once the performance time series have been selected, together with the features of interest, we define the *temporal signature of a series*, s, to be a vector combining

the selected features:

$$s \quad = \quad [\text{Relative Variance}, \text{Pattern}].$$

Given M selected performance time series, (T_1 through T_M), we further define the *temporal signature of set of time series* $\mathcal{S}$ as the concatenated vector of the temporal signatures of all series:

$$\mathcal{S} = \{\text{Relative Variance}(T_1 \cdots T_M), \text{Pattern}(T_1 \cdots T_M)\}. \tag{4.1}$$

The $\mathcal{S}$ vector captures the features of interest for all selected performance time series; it represents a compressed quantitative vector that ideally should carry sufficient information to enable discrimination between series with different characteristics. For example, if a time series has a large amount of variance, that feature will be reflected in a larger quantitative value of its normalized,categorical variance $s^2_{n,c}$. Similarly, if another time series has a random pattern, that will be reflected in its corresponding pattern feature value.

Applications executing on varied Grid resources may exhibit over time different characteristics of these features. Some performance time series may be high varying and periodic while others may be low varying and flat; we hypothesize that these differences in temporal application behaviors can be captured via temporal signature vectors, $\mathcal{S}$.

4.3.4 Temporal Signature Generation

Given a definition for a temporal signature, the next step involves generating such signatures from performance time series. The temporal signature generation component generates $\mathcal{S}$ vectors from applications's performance time series data. It uses the configuration information set off-line in the previous three components (i.e., time series selection, feature selection & extraction, and temporal signature

definition). The resulting temporal signatures are received as input by the *supervised learning* component where they are further analyzed.

4.4 Supervised Learning Component

The *supervised learning* component receives temporal signatures as input. It has two different sub-components, as shown in Figure 4.6: (1) an offline training component, and (2) an on-line classification component.

4.4.1 Training: Learning Expected and Unexpected Signatures

The training sub-component of our framework must gather various instances of temporal signatures that are indicative of both well-performing and ill-performing application states. We conduct this necessary acquisition of training samples as explained in the following subsections.

Signatures Associated with Expected Application Behaviors

In a controlled environment, we conduct performance studies of long-running tasks within workflows to capture temporal signatures in instances where the tasks complete successfully and in a well-performing manner (i.e., no resource contentions or faults). The definition of a successful and well-performing experiment is further discussed in more detail in Chapter 5, with specific examples as to how it can be defined in the context of different scientific workflows.

We hypothesize that the temporal signatures of these tasks have similar characteristics that can be compactly grouped in classes of behaviors. The intuition behind our hypothesis stems from previous large-scale application performance studies showing a small number of equivalent classes of behaviors characterizing collected performance data [85, 23].

Therefore, via passively running experiments, we label a set of successful experi-

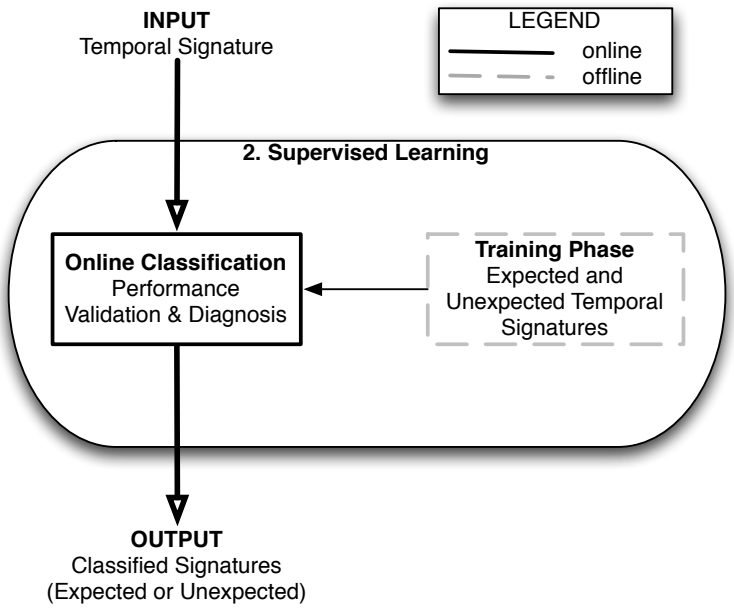

Figure 4.6: Supervised learning component.

ments with the qualitative label of *expected*, and generate temporal signatures which are also labeled in the training data set as being expected signatures for a specific application.

Signatures Associated with Unexpected Application Behaviors

Similarly, we perform various executions of long-running workflow tasks and capture temporal signatures in instances where stimuli affecting the application performance are introduced. One can learn *unexpected* or *diagnostic* temporal signatures in two modes:

1. utilize a benchmark application, such as [7, 82, 67] to generate known instances of issues affecting performance during application execution, and

2. manually label a set of performance time series known to have caused a specific type of failure in a real environment.

There are advantages and disadvantages to both approaches. The first approach enables us to acquire, in a controlled fashion and relatively quickly, instances of un-

expected temporal signatures for an application, and to label them with a known diagnostic state (e.g., signature was captured during known *memory leak* issue affecting the application). The disadvantage lies in potentially capturing signatures that will not have the same characteristics with signatures captured during a real performance problem. For the second approach, we are presented with the opposite situation: we capture within signatures real instance of performance problems, but are not able to learn these instances fast, as severe problems affecting the application may not occur frequently. Furthermore, we do rely on a third-party (e.g., such as a system administrator or application user) to correctly label the performance time series captured during such an event.

4.4.2 Classification: Performance Validation and Diagnosis

The *on-line classification* sub-component takes the temporal signature generated by the first component and assesses whether the signature matches expectations. Let us call this input temporal signature $\mathcal{S}$. The classification component applies the *knn* classifier method as described in Section 3.3.2 against the training data set, and assess whether $\mathcal{S}$ is closest to signatures in *expected* behavioral classes, E_i or to signatures in *unexpected* behavioral classes, U_i. The resulting classification label for $\mathcal{S}$ represents the qualitative temporal behavioral state of the application for the time interval of analysis. If $\mathcal{S}$ belongs to an *unexpected* behavioral class, the classification label represents the possible diagnostic problem affecting the performance of the application.

For example, consider that a set of long-running workflow tasks have three expected qualitative behaviors, $E = \{E_1, E_2, E_3\}$, and two unexpected behaviors $U = \{U_1, U_2\}$, characterized by different examples of temporal signatures labeled in the training phase with these class labels. The E_i classes represent *expected* labels while the U_i classes represent *unexpected* labels as follows: U_1 corresponds to temporal

signatures gathered under network contentions, while U_2 corresponds to temporal signatures gathered under near-disk failures. We monitor the workflow tasks on-line and observe behavior S for one of the task, which is not similar with any of the previously known expected behaviors E_1, E_2, and E_3. However, the unexpected behavior S resembles temporal signatures from class U_1 representing example signatures of network contention behaviors. Therefore, the currently analyzed temporal signature of the monitored task is classified as belonging to class U_1, and the qualitative diagnostic answer is that the tasks is performing unexpectedly due to a possible network contention.

4.5 Qualitative Reasoning Component

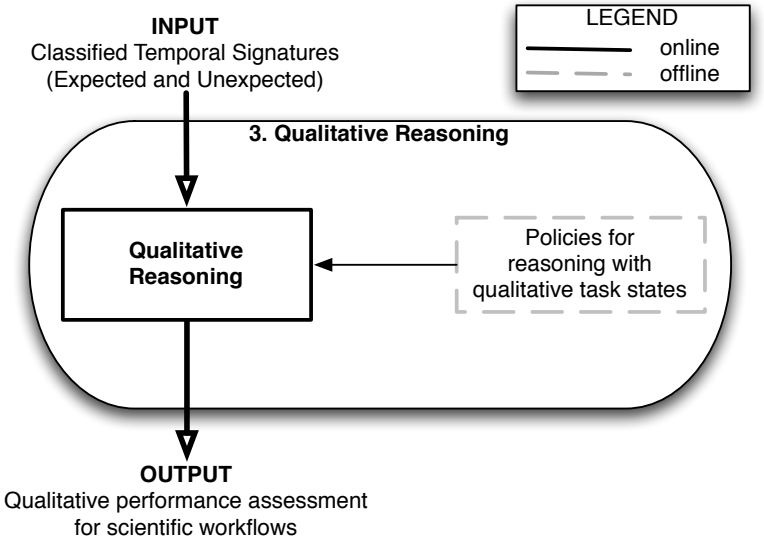

Figure 4.7: Qualitative reasoning component

While the *supervised learning* component analyzes data independently from each distinct long-running task in a workflow, the *qualitative reasoning* component sets the stage for interpreting the meaning of qualitative behaviors across all tasks in a workflow. Therefore, at the global workflow level, we interpret the cumulative qualitative states observed in all of a workflow's tasks, N, during a time interval.

In this work we show how to reason with qualitative behavioral information associated with each long-running workflow tasks; our focus is to demonstrate modes of utilization of our qualitative performance analysis framework and not explore the space of policies that may be developed within this context.

We describe in Chapter 5 a couple of simple policies for interpreting the global workflow performance by analyzing the number of tasks in *desirable* versus *undesirable* qualitative states for a given temporal interval of analysis. Within this context, global workflow performance validation checks the ratio of number of tasks in an undesired qualitative state, N_U, versus the tasks in an expected qualitative state, N_E:

$$R = \frac{\left(\frac{N_U}{N}\right)}{\left(\frac{N_E}{N} + 1\right)}. \tag{4.2}$$

For our evaluation, we assume the tasks analyzed have the same utility to the user: (1) they are all equally important to complete timely, and/or (2) they are on a workflow's critical path. Optimally, one desires N_U=0 and N_E=N, such that R=0 when all tasks are in an expected state and R=1 when they are not, as shown in Figure 4.8. The user needs to specify a threshold for R, T_R, that is acceptable to his or her workflow application.

Global performance diagnosis reports, when T_R has been surpassed, the types of unexpected behavioral states observed and the location of the task where the behavior occurred. A system administrator or application user can utilize this information to learn where the performance problem lies across the computational resource space used by the workflow; furthermore, the user can specify qualitatively remedy operations to be triggered such as: if the majority of the tasks in diagnostic mode are labeled with diagnostic problem U_1, class for network contention behaviors, for two consecutive analysis intervals, then check-point the application and try an alternate

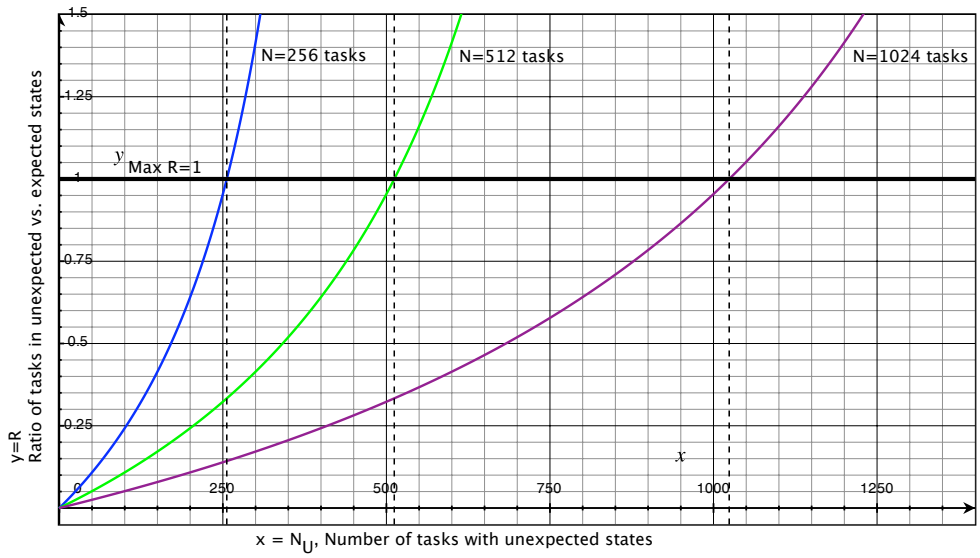

Figure 4.8: Values of R for workflows with 256, 512 or 1024 long-running tasks.

network location for reading or writing data.

4.6 Summary

This chapter described the architecture, components, sub-components and core characteristics of `Teresa`, a qualitative performance analysis framework, together with the set of methodologies which implement it. `Teresa` consists of tree components:

1. a temporal signature design component,
2. a supervised learning component, and
3. a qualitative reasoning component.

The components are configurable in an offline setting, and they jointly contribute to a qualitative performance assessment of scientific applications at both the task and global workflow level.

Chapter 5

Framework Evaluation

In this chapter we describe the data sets we use to evaluate our qualitative performance analysis framework, `Teresa`, as well as the results of the evaluation. We conduct benchmark experiments with long-running tasks from two different large-scale scientific workflows executing on four different architectural configurations of Grid resources.

We first describe characteristics of the computational environments from which we gathered our data sets, the performance time series metrics collected from each environment and characteristics of the scientific workflows studied. Next, we describe how to generate temporal signatures for our experimental data and study the differences in temporal signatures for application executions in cases of good qualitative performance versus cases of known degraded performance due to a performance stress factor or bottleneck. We then evaluate the efficacy of our framework by offering supporting evidence for our two hypotheses. For the first hypothesis we show how signatures based on temporal information are superior to signatures based on instantaneous values of the performance metrics. We show supporting evidence for the second hypothesis by computing the balanced classification accuracy for never-seen temporal signatures of different expectation labels (i.e., expected or unexpected), which is an indicator of how well our framework will be able to distinguish accurately and precisely both healthy and unhealthy application performance states. Finally, we discuss the performance impact of our framework, limits of our current evaluation, as well as limitations of our overall approach.

5.1 Execution Environment

We describe the Grid scientific applications, the computing environments, and the type of performance time series metrics collected.

5.1.1 Computational Resources

To validate our framework, we conducted experiments with two Grid scientific applications, Montage [81] and LEAD [29] on four different system configurations, shown in Table 5.1. We present more detailed architectural diagrams for the selected computational resources in Figures 5.1 and 5.2.

Resource Handle	**slowio**	**lowmem**	**himem**	**fastcpu**
Name	Dante	Mercury1a	Mercury1b	Mercury2
# Nodes	32	128	128	633
CPU Type	Intel Xeon	Intel IA64	Intel IA64	Intel IA64
CPU Speed	3.2 GHz	1.3GHz	1.3GHz	1.5GHz
# Processors	2	2	2	2
Memory	6 GB	4 GB	12 GB	4 GB
Disk	60 GB	60 GB	60 GB	60 GB
Interconnect 1	GigE	GigE	GigE	GigE
Interconnect 2	Infiniband	Myrinet	Myrinet	Myrinet
Network File Sys.	NFS	PVFS	PVFS	PVFS
Number NFS Servers.	1	54	54	54
***Net. Bandwidth**	1 GigE	40 GigE	40 GigE	40 GigE
OS Software	RedHat	SuSE	SuSE	SuSE
OS Version	3.2.3-42	2.4.21-309	2.4.21-309	2.4.21-309

Table 5.1: Architectural characteristics of computing resource sites.* indicates theoretical network bandwidth between application data location and location of the compute nodes.

While the type of selected resources are classified architecturally as clusters, similar experiments can be conducted on other categories of HPC architectures, such as Massively Parallel (MPPs) or Shared Memory Systems (SM). The choice of running experiments on clusters was based on the statistic that the cluster architecture represents a common computational resource in Grid environments today; as of November 2007, clusters represent 81.20% of the share of supercomputers in the world as categorized by the Top 500 Organization [71].

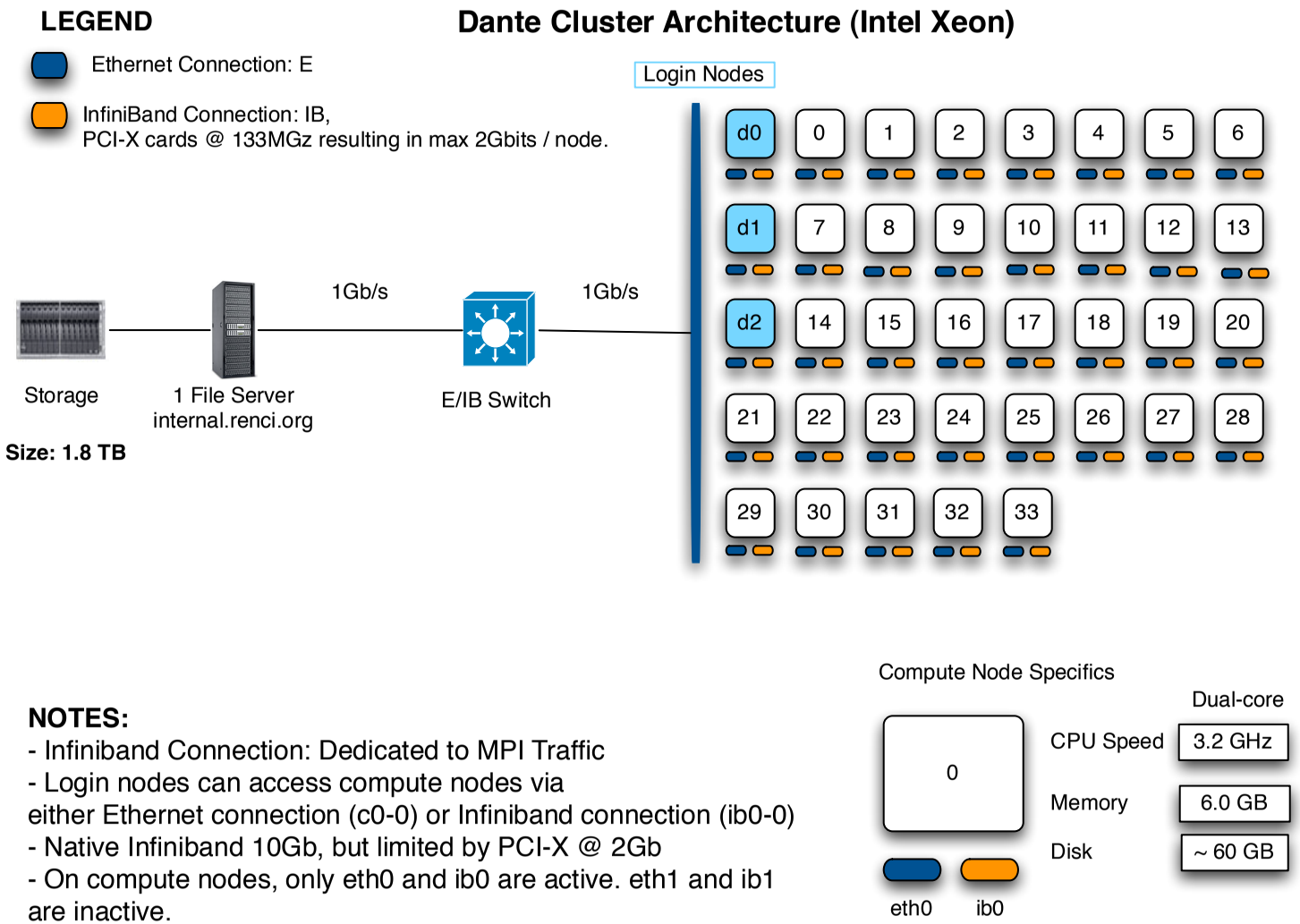

Figure 5.1: Architecture overview: Dante cluster.

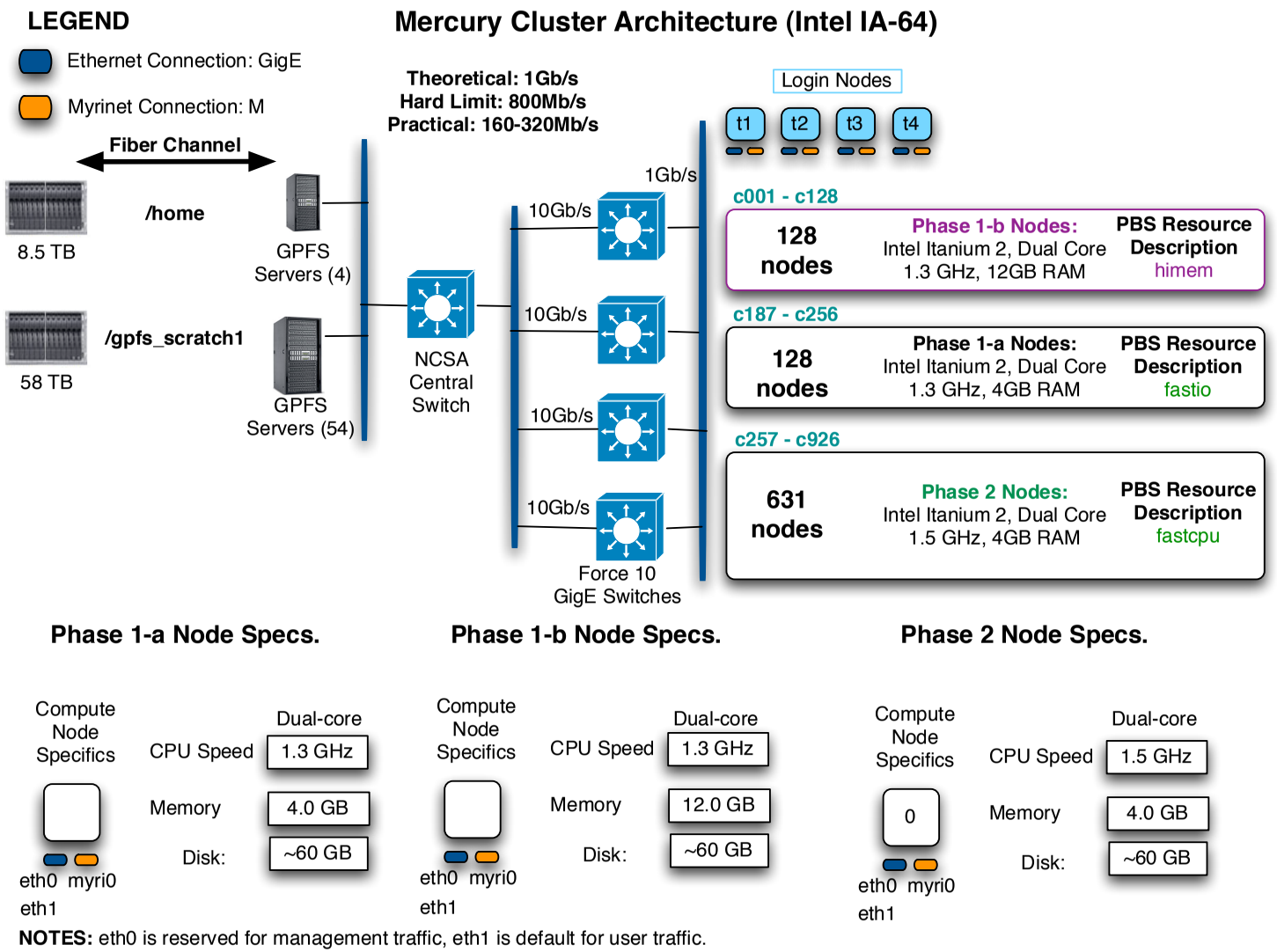

Figure 5.2: Architecture overview: NCSA TeraGrid Mercury Cluster.

5.1.2 Performance Time Series Data Collection

We gathered system-level performance time series data with `sar`[43], a utility commonly available on a variety of platforms that collects and efficiently stores in a binary data format various performance metrics. While we collected all the available metrics provided by `sar` on each system, we focus our analysis on a subset of metrics of interest. Furthermore, because different network interfaces are active on different clusters, we only analyzed network traffic on specific active network interfaces (e.g., on the Dante cluster, `eth0` is active for user application traffic, while on the Mercury clusters, `eth0` is active but dedicated for network management traffic, while `eth1` is active and dedicated to application traffic). Metrics names, units, and their abbreviations are identified in Table 5.2.

i	**Time Series Metric (T_i)**	**Unit**	**Abbr.**
1	Available CPU	%	CPU
2	Memory % Used	%	MPU
3	Swap % Used	%	SPU
4	Disk Blocks Read	KB/s	DBR
5	Disk Blocks Writ.	KB/s	DBW
6	*Eth 0 or 1 # Pkts. Recd.	pk/s	NPR
7	*Eth 0 or 1 # Pkts. Trans.	pk/s	NPT

Table 5.2: Set of system-level performance time series.* indicates we only analyze data for active Ethernet interfaces over which application traffic passes.

As all application executions are submitted via a batch scheduler controlling job executions on the specified cluster, we have carefully started the `sar` collection of data before application execution and have terminated it as soon as the job has finished execution.

5.2 Scientific Workflows

We conducted experiments with long-running computational tasks which are part of two large-scale scientific workflows from meteorology [29] and astronomy [60, 12].

Below we introduce each scientific workflow, we describe the longest running component application within each workflow, and we characterize the input application data sets.

5.2.1 Montage

Montage [81] is a set of modules that can collectively be used to generate large astronomical image mosaics by composing multiple small images. There are five high-level steps to building a mosaic with Montage which we show in Figure 5.3; they include (1) distributed data query, (2) image re-projection, (3) background modeling, (4) background matching, and (5) image co-addition, resulting in a final large-scale mosaic [81, 56].

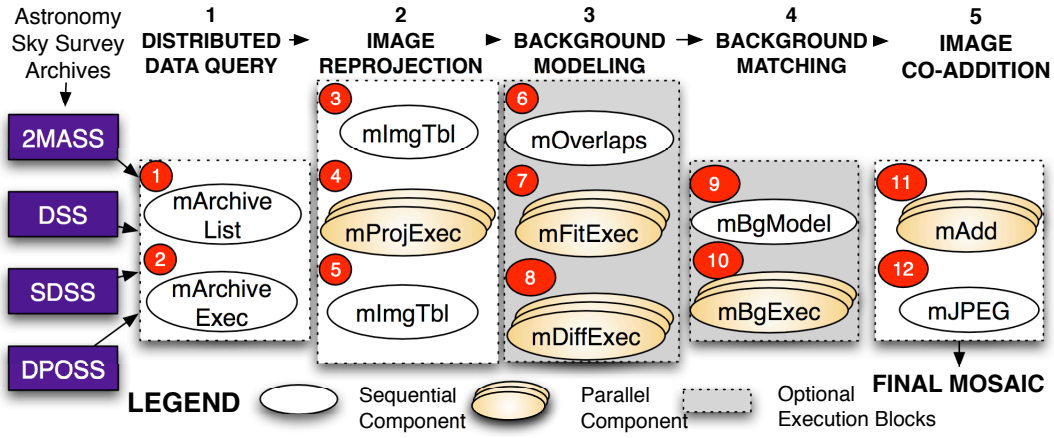

Figure 5.3: Montage workflow for astronomical data query, preprocessing and mosaic creation [56].

Long-running Component Application

Previous experiments with Montage showed that the image re-projection module, `mProjExec` (i.e., Task 4 in the Montage Workflow from Figure 5.3) dominates execution time [56]. `mProjExec` performs image re-projection on a set of astronomy data images downloaded from sky survey repositories. Each file is processed independently of all the other files in a given data set. The more files and the larger the size of each

file in the data set, the longer the time it takes for `mProjExec` to finish the required processing. We conduct experiments with this module on two different data sets, described in the following section.

Astronomy Data Sets

One data set, which we label `M101`, represents 7902 image files from a 15 ◦ area of the sky around the spiral galaxy, M101 in the U band obtained from the SDSS data archive. Each file has an approximate size of 5.8 MB, resulting in a total size of 45 GB for all the files in the data set. The application, `mProjExec` reads all these files and generates re-projections of these images, generating as output a data set of approximately 99 GB. The second data set, which we label `M57`, represents 7422 image files from a 15 ◦ area of the sky around the ring nebula, M57, in the J band obtained from the 2MASS data archive. Each file in the second data set has an approximate size of 2.0 MB, resulting in a total size of 15 GB for all the files in the data set. Similarly, `mProjExec` reads all these files and generates re-projections of these images, generating as output a data set of approximately 30 GB. All the experiments with data set `M101` are listed in Table 5.3, while all experiments with data set `M57` are listed in Table 5.4.

5.2.2 LEAD

Mesoscale weather causes hundreds of deaths, routinely disrupts transportation and commerce and results in significant economic losses [91]. Mitigating the impact of such events implies significantly changing the traditional weather sensing and prediction paradigm, where forecasts are static, linear workflows with no adaptive response to weather. The Linked Environments for Atmospheric Discovery (LEAD) project [29] addresses the fundamental technological challenges of real-time, on-demand, dynamically-adaptive needs of mesoscale weather research. Figure 5.4 shows an exam-

#	JobID	Cluster	N:PPN	Time(s)	Valid?	User Expectation
1	1336927	fastcpu	64:1	2748	Yes	Expected
2	1336939	fastcpu	64:1	2850	Yes	Expected
3	1337050	fastcpu	64:1	2854	Yes	Expected
4	1337063	fastcpu	64:1	2830	Yes	Expected
5	1337251	fastcpu	32:1	5281	Yes	Expected
6	1337321	fastcpu	32:1	5271	Yes	Expected
7	1337366	fastcpu	32:1	5271	Yes	Expected
8	1337411	fastcpu	32:1	5322	Yes	Expected
9	1337732	himem	64:1	3194	Yes	Expected
10	1337764	himem	64:1	3185	Yes	Expected
11	1337812	himem	64:1	3184	Yes	Expected
12	1337845	himem	64:1	3186	Yes	Expected
13	1337573	himem	32:1	6143	Yes	Expected
14	1337603	himem	32:1	6145	Yes	Expected
15	1337652	himem	32:1	6145	Yes	Expected
16	1337696	himem	32:1	6150	Yes	Expected
17	1338089	lowmem	64:1	3183	Yes	Expected
18	1338104	lowmem	64:1	3181	Yes	Expected
19	1338112	lowmem	64:1	3181	Yes	Expected
20	1338145	lowmem	64:1	3180	Yes	Expected
21	1338205	lowmem	32:1	6137	Yes	Expected
22	1338264	lowmem	32:1	6141	Yes	Expected
23	1338452	lowmem	32:1	6229	Yes	Expected
24	1338563	lowmem	32:1	6176	Yes	Expected
25	248416	slowio	30:1	6332	Yes	Unexpected
26	248418	slowio	30:1	5870	Yes	Unexpected
27	248420	slowio	30:1	5939	Yes	Unexpected

Table 5.3: `mProjExec` with data set `M101` on all four clusters. Column **-#-** represents the experiment number and column **-JobID-** represents the PBS job identification number assigned to the execution. Column **-Cluster-** indicates the resource on which the application was run. Column **-N:PPN-** represents the number of nodes the application was executed on and the number of assigned processors per node. Column **-Time-** represents the total execution time in seconds for the experiment. Column **-Valid?-** labels whether a valid scientific result was obtained for the application run. Column **-User Expectation-** labels the experimental application run as *expected* or *unexpected*.

ple of a LEAD workflow. Meteorological data sets and streams generated by radars, satellites, weather balloons and other weather instruments are transported via shared networks to computing resources for processing. The data types are integrated and

#	JobID	Cluster	N:PPN	Time(s)	Valid?	User Expectation
28	1345633	fastcpu	64:1	904	Yes	Expected
29	1345702	fastcpu	64:1	974	Yes	Expected
30	1345712	fastcpu	64:1	933	Yes	Expected
31	1345757	fastcpu	64:1	900	Yes	Expected
32	1345795	fastcpu	32:1	1643	Yes	Expected
33	1345800	fastcpu	32:1	1615	Yes	Expected
34	1345815	fastcpu	32:1	1647	Yes	Expected
35	1346744	fastcpu	32:1	1641	Yes	Expected
36	1347621	himem	64:1	1027	Yes	Expected
37	1347631	himem	64:1	1026	Yes	Expected
38	1347637	himem	64:1	1027	Yes	Expected
39	1347641	himem	64:1	1029	Yes	Expected
40	1348357	himem	32:1	1893	Yes	Expected
41	1348388	himem	32:1	1885	Yes	Expected
42	1348405	himem	32:1	1889	Yes	Expected
43	1348431	himem	32:1	1887	Yes	Expected
44	1347582	lowmem	64:1	1027	Yes	Expected
45	1347586	lowmem	64:1	1025	Yes	Expected
46	1347600	lowmem	64:1	1022	Yes	Expected
47	1347604	lowmem	64:1	1025	Yes	Expected
48	1347182	lowmem	32:1	1887	Yes	Expected
49	1347234	lowmem	32:1	1897	Yes	Expected
50	1347241	lowmem	32:1	1893	Yes	Expected
51	1347286	lowmem	32:1	1884	Yes	Expected
52	248471	slowio	30:1	3569	Yes	Unexpected
53	248475	slowio	30:1	5836	Yes	Unexpected
54	248476	slowio	30:1	6390	Yes	Unexpected

Table 5.4: `mProjExec` with data set `M57` on all four clusters. Column **-#-** represents the experiment number and column **-JobID-** represents the PBS job identification number assigned to the execution. Column **-Cluster-** indicates the resource on which the application was run. Column **-N:PPN-** represents the number of nodes the application was executed on and the number of assigned processors per node. Column **-Time-** represents the total execution time in seconds for the experiment. Column **-Valid?-** labels whether a valid scientific result was obtained for the application run. Column **-User Expectation-** labels the experimental application run as *expected* or *unexpected*.

transformed such that numerical weather forecast codes can be initiated. Automated data mining algorithms analyzing forecast output can dynamically request new real-time data from instruments when severe weather patterns are detected. The entire or

part of the workflow process is repeated following the arrival of new real-time data.

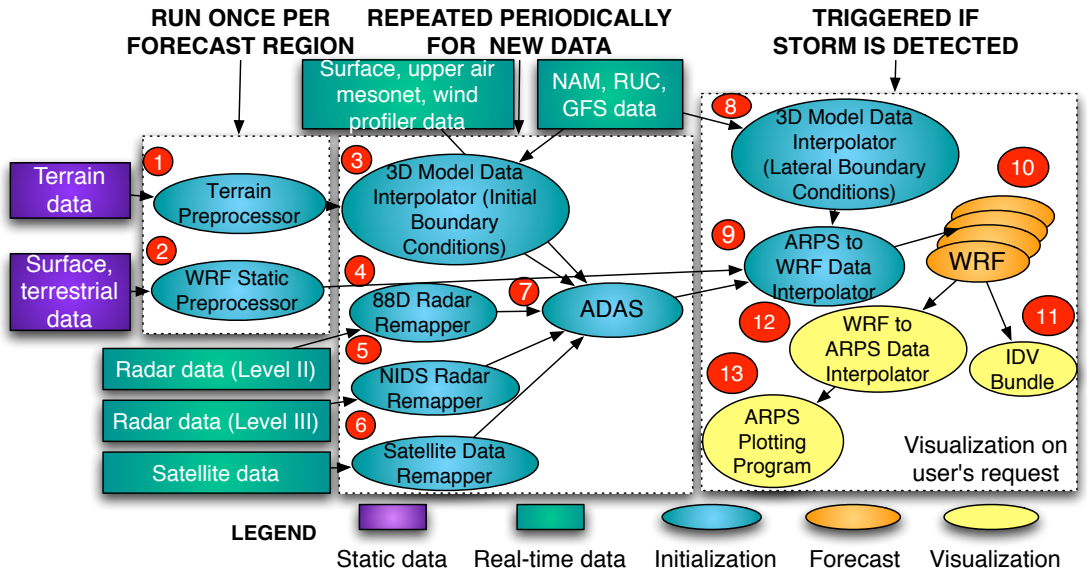

Figure 5.4: LEAD workflow for data ingestion, analysis and weather forecast. Source: LEAD project [29, 61].

The meteorological issues arising from the LEAD project are producing *accurate* and *immediate* severe weather forecasts. To obtain more accurate forecasts, scientists perform ensemble forecasts, which are grouped executions of the weather forecasting model numerical software, WRF [73]. One of the common use-case of running LEAD workflows is to initially run a wide-area, low-resolution forecast followed by a smaller-area, high-resolution forecast if a meteorological event of interest was detected in the first low-resolution forecast.

One experiment we performed involves executing WRF Version 2 [111] with the ARW dynamical core and with a benchmark real data set [116]. The initialization data set represents a 48-hours, 12 km resolution forecast of the weather over the continental U.S. domain. The data set is preprocessed by the WRFSI component and is provided as input to the ARW dynamical core. A default configuration file, `namelist.input`, accompanies the benchmark data, setting configuration parameters appropriately.

While this particular data set may run to completion on a couple of tens of computing nodes within a reasonable amount of time (i.e., 5396 seconds on 32 machines with an Intel Xeon 3.2 GHz, 6 GB RAM and Infiniband interconnect), hundreds of these data sets forming large ensembles will require a significant amount of resources to finish in time for the actual weather prediction to be useful. Larger Grids will provide the necessary computing power to process computationally intensive forecast ensembles processing streamed, distributed data sources.

Long-running Application Component

Within such LEAD workflows, the longest-running component is the numerical code, Weather Research and Forecasting (WRF) [73] (i.e., Task 10 in the LEAD Workflow from Figure 5.4). Therefore, we conduct experiments with WRF on two different data sets representing weather with different characteristics.

Weather Data Sets

One data set, which we label `mesoscale`, represents a 48-hour forecast during mesoscale weather from 24th October 2001, over a low-resolution of 12 km within the entire continental United States. The input files have an approximate size of 0.34 GB and the output data is 0.64 GB. The second data set, which we label `non-mesoscale`, represents a 24-hours forecast during non-mesoscale (i.e., good) weather from November 6th, 2007 over a high-resolution of 4 km in a grid of 1000 km^2 within the continental United States. The input files have an approximate size of 0.25 GB and the output data is 2.9 GB. All experiments with the `mesoscale` data set are listed in Table 5.5, and all experiments with the `non-mesoscale` data set are listed in Table 5.6.

#	JobID	Cluster	N:PPN	Time(s)	Valid?	User Expectation
1	1351014	fastcpu	60:2	1151	Yes	Expected
2	1351287	fastcpu	60:2	1085	Yes	Expected
3	1351292	fastcpu	60:2	1095	Yes	Expected
4	1351297	fastcpu	60:2	1187	Yes	Expected
5	1351634	fastcpu	30:2	1760	Yes	Expected
6	1351643	fastcpu	30:2	1694	Yes	Expected
7	1351702	fastcpu	30:2	1646	Yes	Expected
8	1351752	fastcpu	30:2	1682	Yes	Expected
9	1351487	himem	60:2	1214	Yes	Expected
10	1351581	himem	60:2	1219	Yes	Expected
11	1351625	himem	60:2	1211	Yes	Expected
12	1351628	himem	60:2	1214	Yes	Expected
13	1352492	himem	30:2	1866	Yes	Expected
14	1353639	himem	30:2	1870	Yes	Expected
15	1353659	himem	30:2	1858	Yes	Expected
16	1353833	himem	30:2	1852	Yes	Expected
17	1351337	lowmem	60:2	1210	Yes	Expected
18	1351348	lowmem	60:2	1214	Yes	Expected
19	1351467	lowmem	60:2	1293	Yes	Expected
20	1351469	lowmem	60:2	1208	Yes	Expected
21	1351860	lowmem	30:2	1874	Yes	Expected
22	1351880	lowmem	30:2	1877	Yes	Expected
23	1351887	lowmem	30:2	1863	Yes	Expected
24	1351899	lowmem	30:2	1884	Yes	Expected
25	248477*	slowio	30:2	4270	Yes	Expected
26	248478*	slowio	30:2	4223	Yes	Expected
27	248479*	slowio	30:2	4216	Yes	Expected
28	248480*	slowio	30:2	4219	Yes	Expected

Table 5.5: WRF2.2 and WRF2.0* with mesoscale data set on all four clusters. Column **-#-** represents the experiment number and column **-JobID-** represents the PBS job identification number assigned to the execution. Column **-Cluster-** indicates the resource on which the application was run. Column **-N:PPN-** represents the number of nodes the application was executed on and the number of assigned processors per node. Column **-Time-** represents the total execution time in seconds for the experiment. Column **-Valid?-** labels whether a valid scientific result was obtained for the application run. Column **-User Expectation-** labels the experimental application run as *expected* or *unexpected*. *While the data set for WRF2.2 and WRF2.0 is the same, the experiments from WRF2.2 executions should not be compared directly with the ones from WRF2.0 executions because these may represent different implementations of the numerical forecasting algorithms, and may represent WRF application binaries possibly compiled with different compilation options.

#	JobID	Cluster	N:PPN	Time(s)	Valid?	User Expectation
29	1343612	fastcpu	64:1	1973	Yes	Expected
30	1343619	fastcpu	64:1	1940	Yes	Expected
31	1344102	fastcpu	64:1	1980	Yes	Expected
32	1344269	fastcpu	64:1	2006	Yes	Expected
33	1351201	fastcpu	32:1	3042	Yes	Expected
34	1351228	fastcpu	32:1	3073	Yes	Expected
35	1351241	fastcpu	32:1	3056	Yes	Expected
36	1351275	fastcpu	32:1	2885	Yes	Expected
37	1349185	lowmem	64:1	2296	Yes	Expected
38	1349479	lowmem	64:1	2272	Yes	Expected
39	1349558	lowmem	64:1	2316	Yes	Expected
40	1349726	lowmem	64:1	2293	Yes	Expected
41	1349892	lowmem	32:1	3416	Yes	Expected
42	1350100	lowmem	32:1	3306	Yes	Expected
43	1350157	lowmem	32:1	3285	Yes	Expected
44	1350339	lowmem	32:1	3281	Yes	Expected
45	1347747	himem	64:1	2295	Yes	Expected
46	1348035	himem	64:1	2289	Yes	Expected
47	1348905	himem	64:1	2346	Yes	Expected
48	1349133	himem	64:1	2325	Yes	Expected
49	1351016	himem	32:1	3345	Yes	Expected
50	1351037	himem	32:1	3332	Yes	Expected
51	1351166	himem	32:1	3352	Yes	Expected
52	1351180	himem	32:1	3392	Yes	Expected

Table 5.6: WRF2.2 with `non-mesoscale` data set on all clusters except* `slowio`. Column **-#-** represents the experiment number and column **-JobID-** represents the PBS job identification number assigned to the execution. Column **-Cluster-** indicates the resource on which the application was run. Column **-N:PPN-** represents the number of nodes the application was executed on and the number of assigned processors per node. Column **-Time-** represents the total execution time in seconds for the experiment. Column **-Valid?-** labels whether a valid scientific result was obtained for the application run. Column **-User Expectation-** labels the experimental application run as *expected* or *unexpected*. We did not have `WRF2.2` compiled on the `slowio` cluster.

5.3 Labeling Application Performance Expectation

Our approach relies on a set of previously known labels of application behaviors to assess and diagnose the performance behavior of the application. We assume that a group of workflow users may label, over the time of their experiments, instances

of workflow executions where the application did not perform as *expected*. We define the *user performance expectation* as a set of conditions that must be met in order to correlate any instance of application execution with an expected performance behavior. Such conditions can include: (1) a valid scientific result for the application, and (2) total execution time within one standard deviation of previous execution times. We believe that in the case of long-running scientific applications, it is not sufficient to equate an application's successful completion (i.e., condition (1)) with an expected performance state, as the application may have a degraded performance over the course of its execution that can be attributed to multiple factors. Typically, a significantly degraded performance will manifest itself in significantly longer execution times, so we believe the example of the second condition described is justified in our context. Other conditions may be included in the definition. In our experimental results, we do use these two conditions to label an application's execution expected or unexpected.

Consider the running times of `mProjExec` with data sets `M101` and `M57` shown in Figures 5.5(a) and 5.5(b). From comparing the running times of either of the data sets for the 32 nodes executions on the `fastcpu, himem, lowmem` clusters with the 30 nodes execution on the `slowio` cluster, the user may expect the application to run at least as fast as the `fastcpu` executions, assuming nothing else is significantly different between the cluster configurations. Unfortunately, while the `slowio` cluster may be equipped with faster processors, the network bandwidth between the compute nodes and the location of the data on the network storage is unfit for the data intensive demands of this astronomy data mosaic application. While the application does produce a valid scientific result, it takes a considerable longer amount of time than if the cluster network architecture was adequate to its demands.

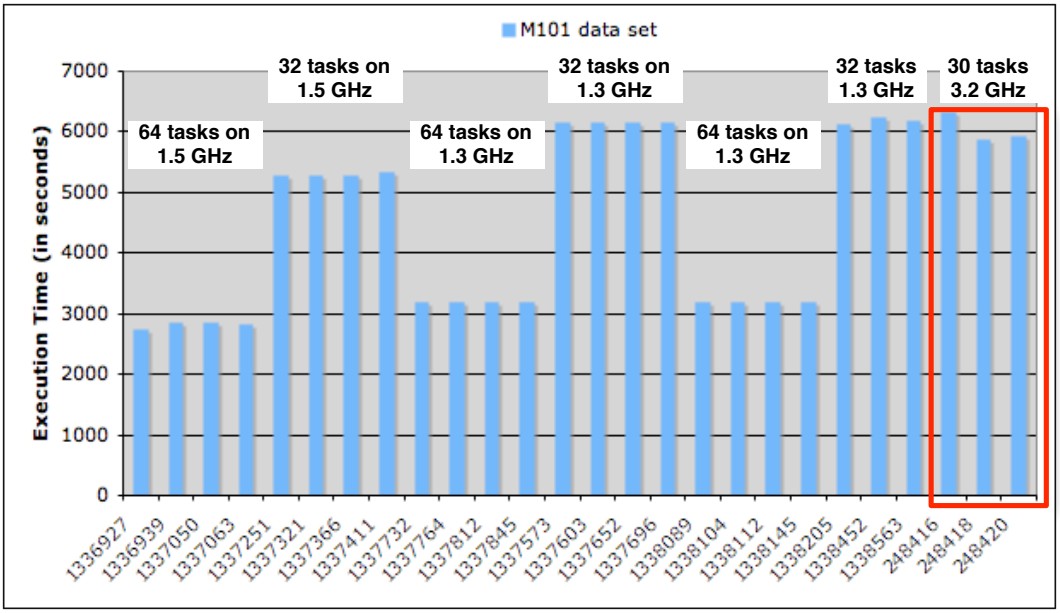

(a) Execution times for all experiments with M101 data set.

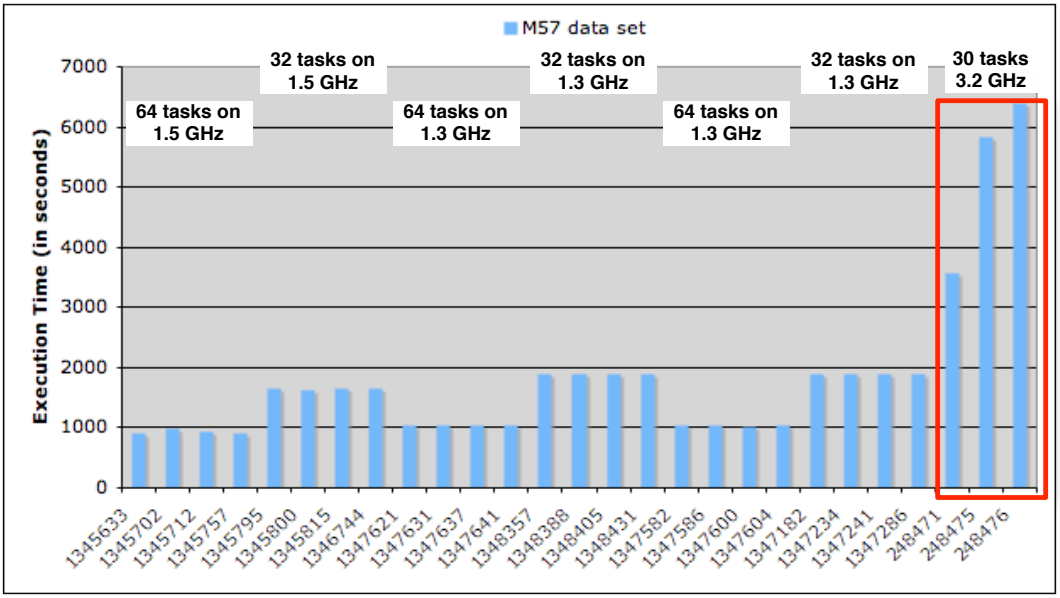

(b) Execution times for all experiments with M57 data set.

Figure 5.5: Execution times for all experiments with `mProjExec`. User may be expecting significantly faster execution times from the `slowio` - 3.2GHz nodes cluster. The last three marked bars in (a) and (b) represent the execution times for the application running on 30 nodes on the `slowio` cluster; these times are significantly longer than running times for the executions of the same application on the `fastcpu` - 1.5GHz nodes cluster.

5.4 Temporal Signatures of Expected Application Executions

We generated temporal signatures for all experiments listed for both workflow component applications `mProjExec` and `WRF`. In the following sections, we will take a bottom-up approach and show (1) characteristics of individual temporal signatures, (2) characteristics of groups of signatures for each of the component applications studied, and (3) characteristics of signatures across applications and execution platforms.

5.4.1 Temporal Signature for a Task Within an Experiment

We begin by illustrating in Figure 5.6(a) characteristics of the temporal signature for an expected behavioral task within one of the experiments performed, `mProjExec` Experiment #5. The temporal signature for the data is a vector of length 14, encoding the normalized, categorical variance and the pattern for each of the seven time series $\mathcal{S} = [1, 1, 1, 1, 1, 1, 2; 3, 1, 5, 5, 3, 3, 3]$. Two different visualizations of this signature are shown in Figures 5.6(b) and 5.6(c). The "bars" visualization on the left separates the two features and display the values as bars. The second "color vector" visualization encodes the five different patterns as five different colors, and it encodes the variance as a bar of 3 different heights within each color box.

Characterization

The data and its corresponding signature represent characteristics of the selected task for an instance of expected application behavior. Generally, there is low variance on all the metrics, with periodicity detected on the CPU, disk and network metrics.

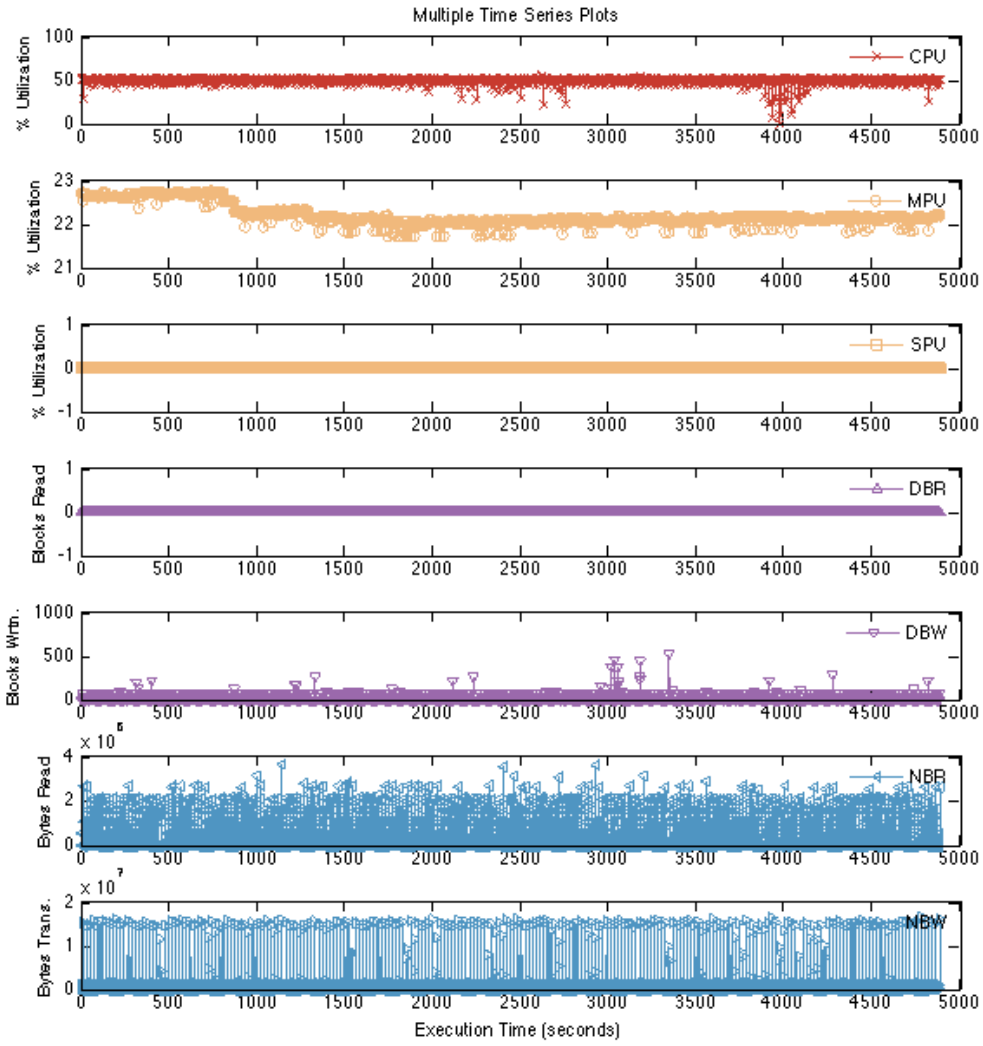

(a) Performance time series for one task from experiment `mProjExec` Experiment #5.

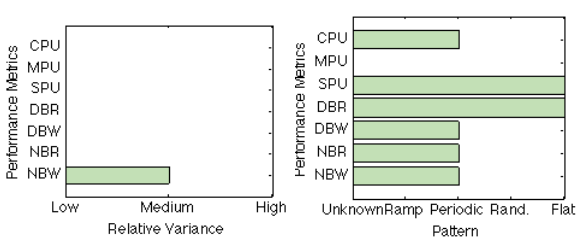

(b) Bars Visualization

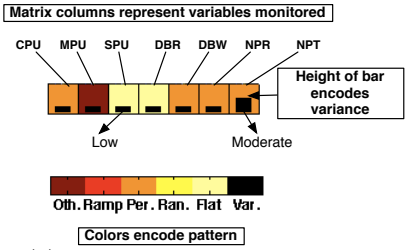

(c) Color Vector Visualization

Figure 5.6: Performance time series and temporal signature for one task from `mProjExec` Experiment #5. The performance data from which the temporal signature is generated has no smoothing applied (i.e. Smoothing Factor - S.F. = 1 second). We learn that the temporal signature of an expected application task has generally low variance on all the metrics, with periodicity detected on the CPU, disk and network metrics.

5.4.2 Temporal Signatures for a Group of Tasks in an Experiment

Next, we illustrate in Figure 5.7 how Experiment #5 `mProjExec`'s execution on 32 tasks in parallel can be characterized with temporal signatures. We generate a temporal signature for the entire duration of execution for each of these 32 tasks. The color matrix visualization summarizes the studied temporal features in all the time series data for this experiment.

Characterization

We generally observe for a group of tasks in an experiment the following characteristics: low variance on all the metrics except on the network-packets-transmitted metric, which has a moderate amount of variance. Furthermore, the CPU, the disk-writes and all the network metrics are periodic; the memory-swap, disk-reads and disk-writes are mostly flat while the memory utilized is detected as an unknown, periodic or ramp pattern.

5.4.3 Temporal Signatures Across Experiments

Next, we illustrate in Figure 5.8 how repeated experiments (i.e., # 5,6,7) of `mProjExec` are characterized via temporal signatures on the same architectural configuration. We observe how signatures of the entire application (i.e., all its tasks) are very similar to each other over repeated executions, when there is no known performance stress factor affecting the application. Figures 5.9 and 5.10 provide further proof that repeated experiments within the same architecture exhibit very similar characterizations in terms of the features selected by our temporal signature mechanism.

Similarly to the `mProjExec` application, we do obtain similar temporal signature characterizations for `WRF`. We illustrate one such example in Figure 5.11.

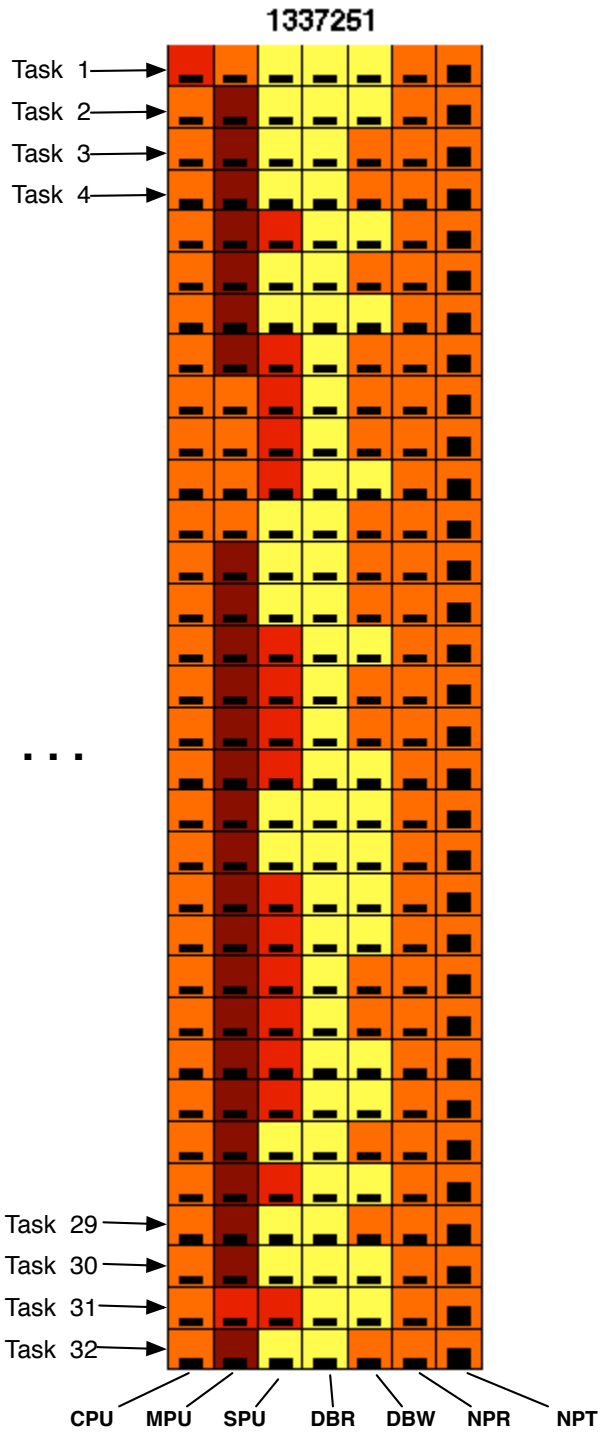

Figure 5.7: Temporal signatures represented as a color matrix for `mProjExec` Experiment # 5, with S.F.=1 second. Temporal signatures for all tasks in this experiment reveal how similar the tasks are with each other in terms of their temporal signature characteristics: low variance on most metrics and periodicity observed on the CPU, disk-writes and all the network metrics. The memory-swap, disk-reads and disk-writes are mostly flat, while the memory utilized is detected as an unknown, periodic or ramp pattern.

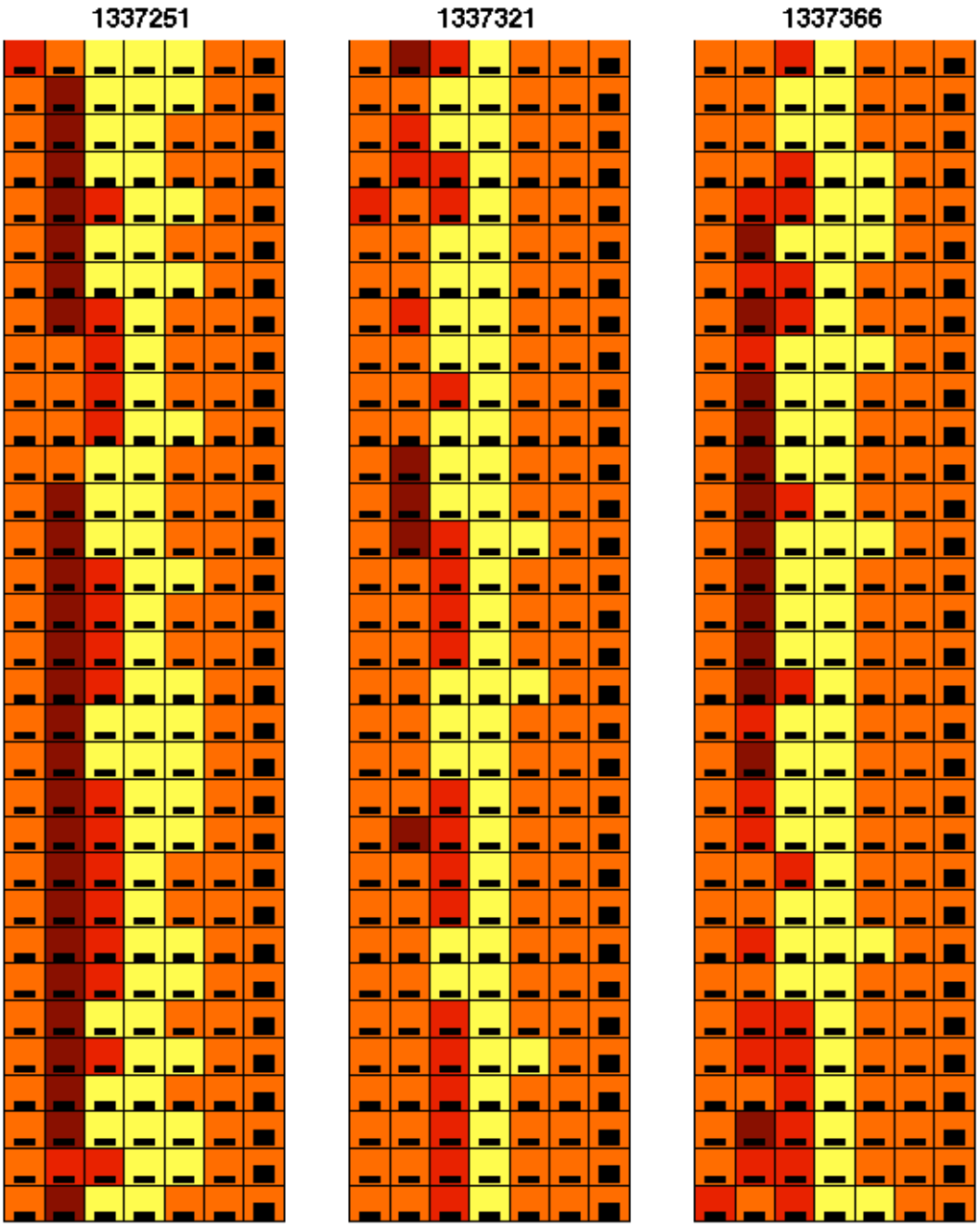

Figure 5.8: Temporal signatures across experiments: `mProjExec` experiments # 5, 6, 7, with S.F.=1 second. We learn from these repeated experiments and their corresponding temporal signature characterizations that signatures of expected behaviors are very similar over repeated executions of the application on the same architecture.

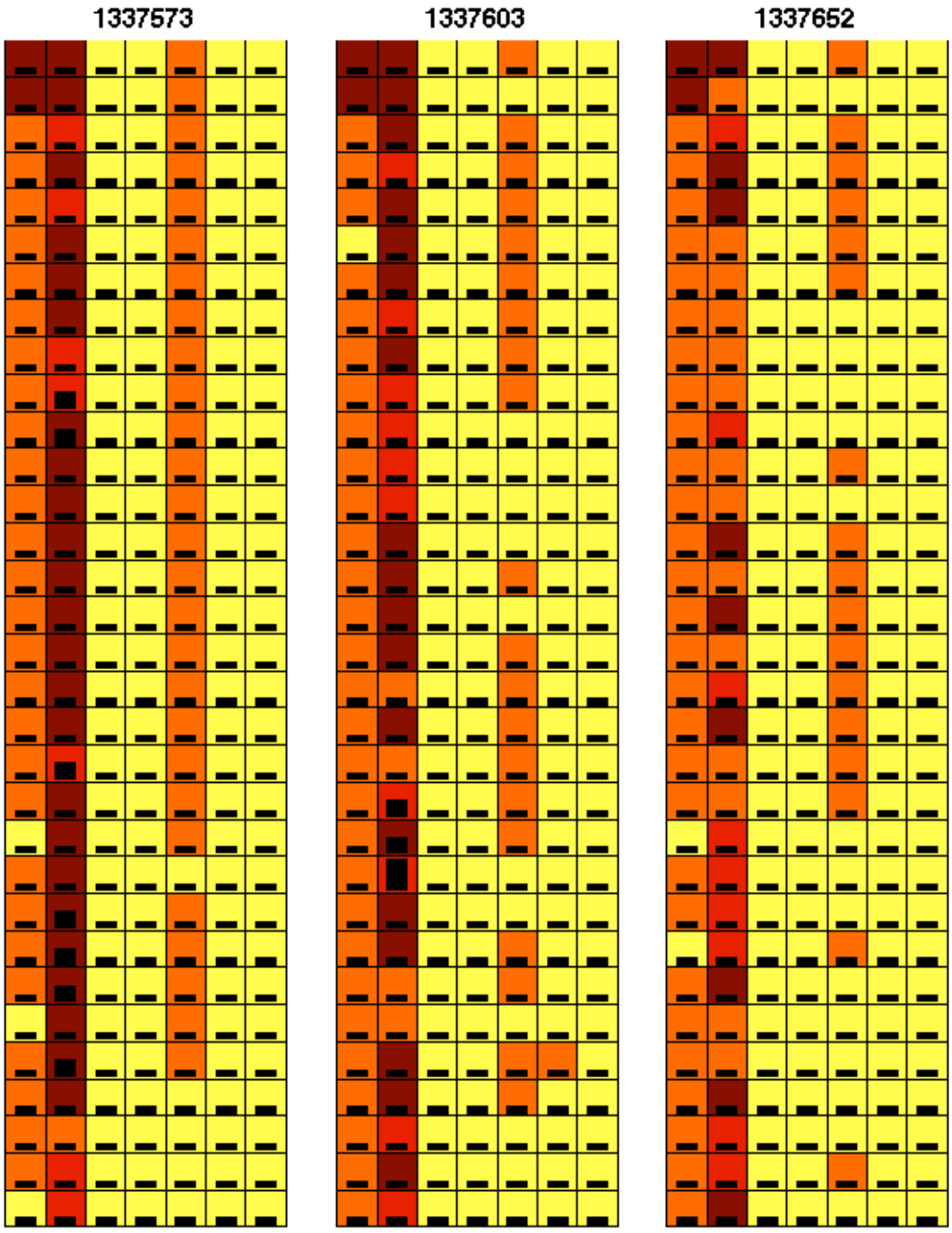

Figure 5.9: Temporal signatures across experiments: `mProjExec` experiments # 12,13,14, with S.F.=1 second. We learn from these repeated experiments and their corresponding temporal signature characterizations that signatures of expected behaviors are very similar over repeated executions of the application on the same architecture.

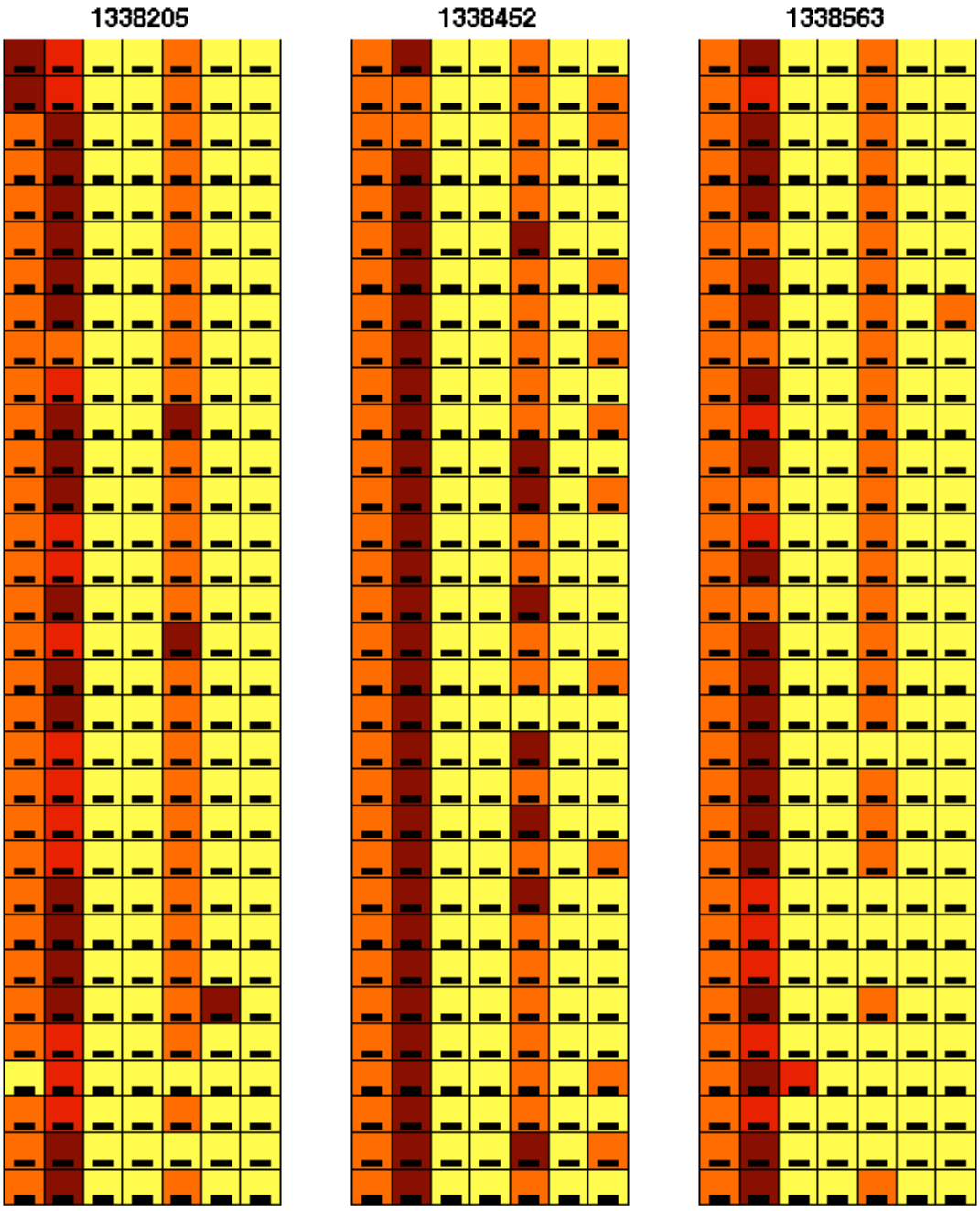

Figure 5.10: Temporal signatures across experiments: `mProjExec` experiments # 20, 21, 22, with S.F.=1 second. We learn from these repeated experiments and their corresponding temporal signature characterizations that signatures of expected behaviors are very similar over repeated executions of the application on the same architecture.

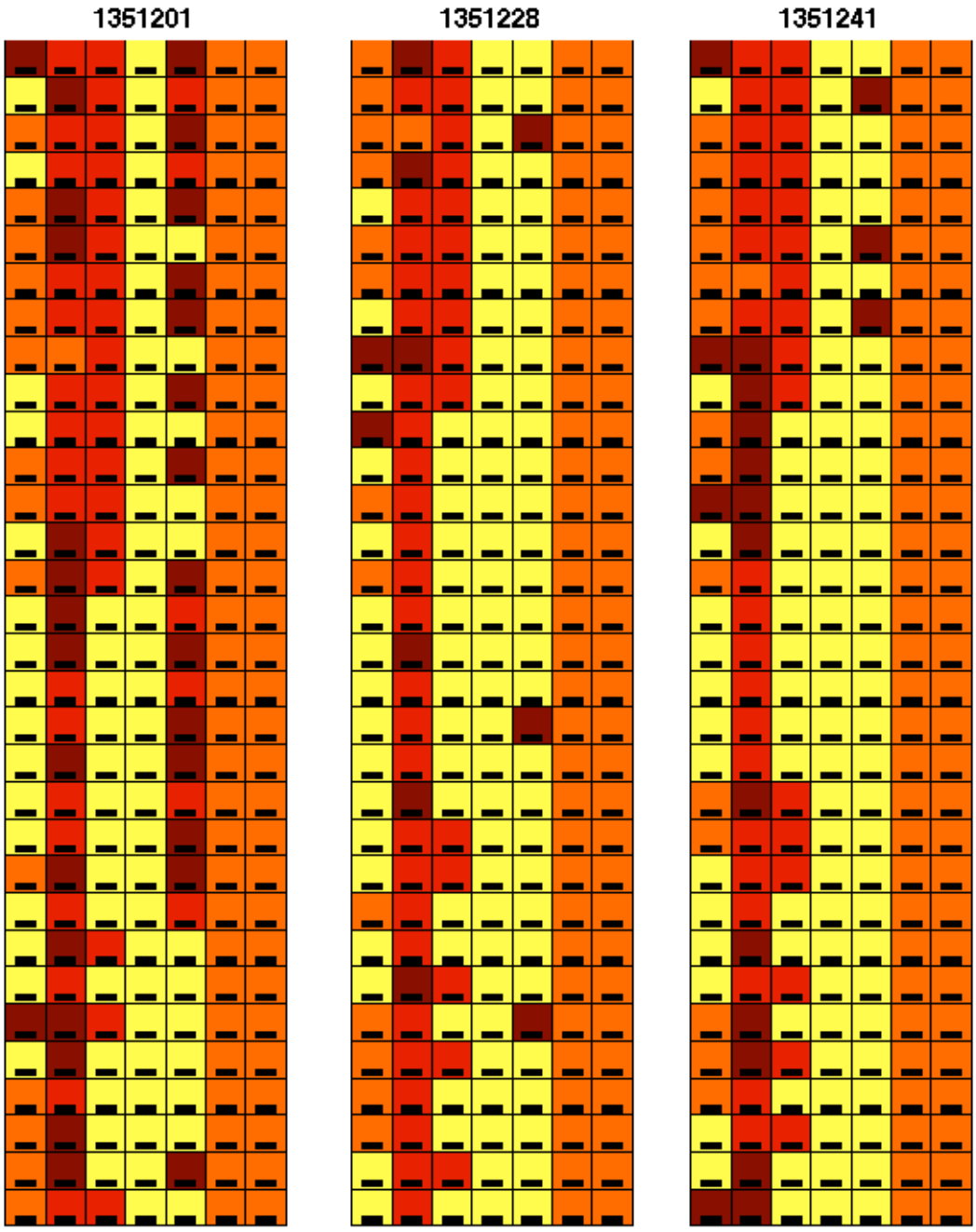

Figure 5.11: Temporal signatures across experiments: `WRF` experiments # 35, 36, 37, with S.F.=1 second. Similarly to `mProjExec`, we observe that repeated experiments and their corresponding temporal signature characterizations that signatures of expected behaviors are very similar over repeated executions of the application on the same architecture.

5.4.4 Summary

We have described characteristics observed in performance time series data collected from two different scientific applications during instances of expected performance. Generally, the temporal signature characterization of the time series data reveals low variance on the majority of metrics with some occasional moderate variance on the network metrics. In terms of patterns, we observe typically periodicity on the CPU, disk-writes, network-reads and network-writes metrics; we observe flat behaviors with low variance on the swap-memory, and on the local disk-reads metrics. Finally, the memory-utilization metric seems to vary considerably more in terms of the patterns we observe, as we observe ramp, periodic, flat and unknown patterns systematically across experiments and applications. This fact results from two sources: 1) the sensitivity of our pattern detection mechanism, and 2) other system processes or daemons running at the same time with the application, causing some fluctuation on the metric.

5.5 Temporal Signatures for Unexpected Application Executions

We describe two instances where we label the performance of application executions as unexpected or problematic, and describe the context. We also describe an instance where the temporal signatures are indicating a known problem on some resources (i.e., monitoring data corrupted on one specific node on the `slowio` cluster), and another instance suggesting a possible problem with a specific node in the Teragrid cluster. Both of these later instances do not seem to affect application performance for our experiments, but can help system administrators easily investigate reasons why certain resources do not behave similarly with other nodes in the cluster.

5.5.1 Case 1: Diagnosed Data-Intensive Application Running on Slow Network

We illustrate in Figure 5.12(a) the performance time series data collected during `mProjExec` Experiment # 23 executing on the `slowio` cluster. During this experiment, 30 compute nodes attempt to continuously read and write from the network 7902 files totaling 45 GB. While the application does produce a valid scientific result, as all images are processed correctly, the total execution time on these compute nodes is significantly longer than what a user may expect had the network configuration of cluster not be the bottleneck for processing. This mismatch case of running a data intensive application over an low-bandwidth network (i.e., there is one shared 1 Gb Ethernet link between all the compute nodes and the network file server) has the following effects on the application and environment: (1) the application's run time increases significantly because the CPU must wait for the data to arrive from the network (and this behavior is seen in the high variance and high amplitude periodicity of the CPU metric), and (2) the operating system keeps allocating memory buffers to handle the file IO requests submitted by the application. We believe that this allocation goes unbounded, as one observes the memory utilization on the system to be slowly but consistently increasing until all the memory of the system is fully utilized. While this behavior may be the result of a possible memory leak of the application, we believe that this is not the case, as the swap memory metric remains at zero even after all the memory on the system has been used. Figure 5.13 shows all signatures generated for each unexpected performance experimental run from `mProjExec` Experiments # 23, 24 and 25.

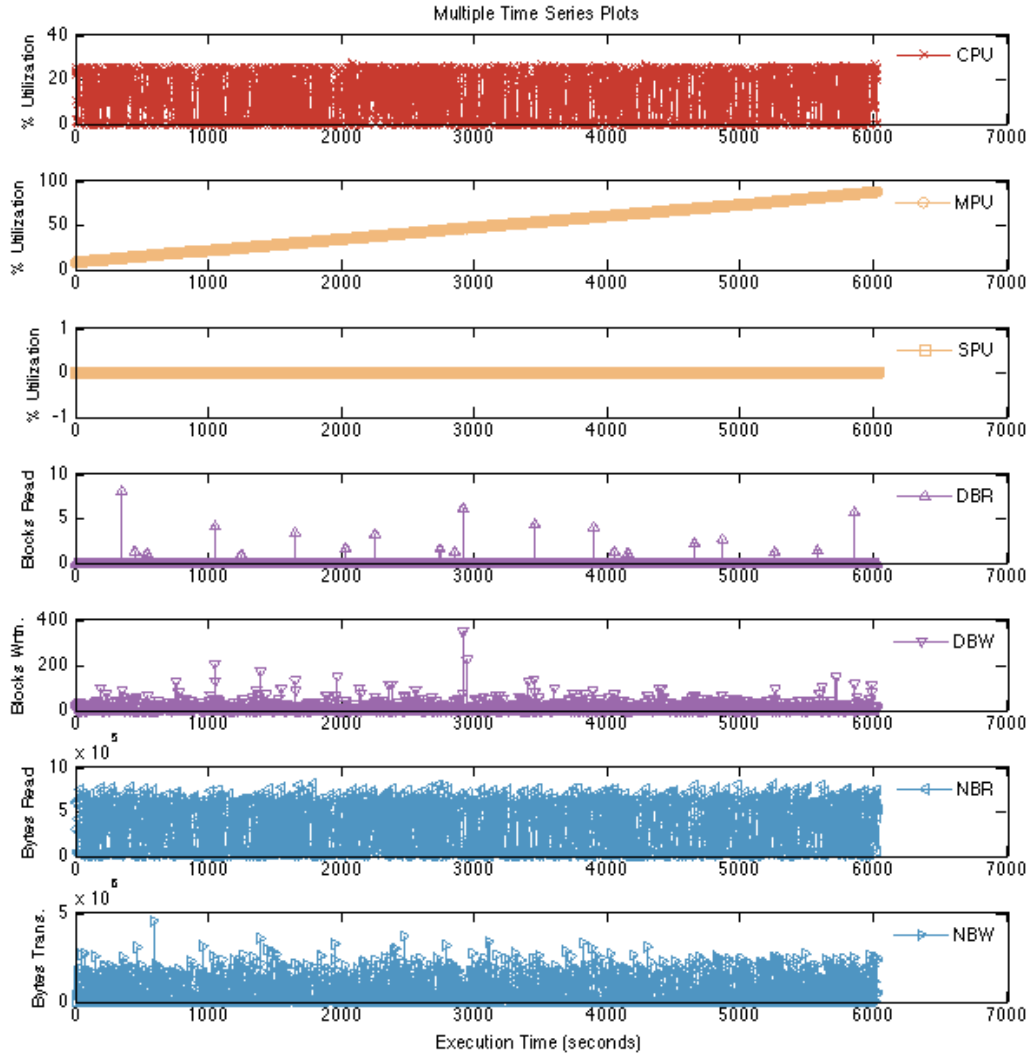

(a) Performance time series metrics of one task from unexpected `mProjExec` experiment #23.

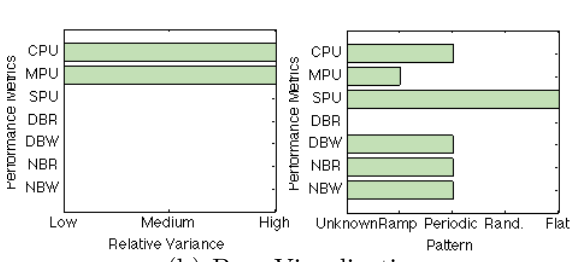

(b) Bars Visualization

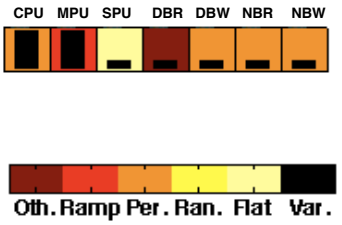

(c) Color Vector Visualization

Figure 5.12: Performance time series and temporal signature for one task from unexpected `mProjExec` experiment #23, S.F=1 second. We observe significant differences both in the data which are consequently reflected in characteristics of the temporal signature. The primary differences are the high variance, high periodicity of the CPU metric and the slow but gradually increasing memory utilization ramp.

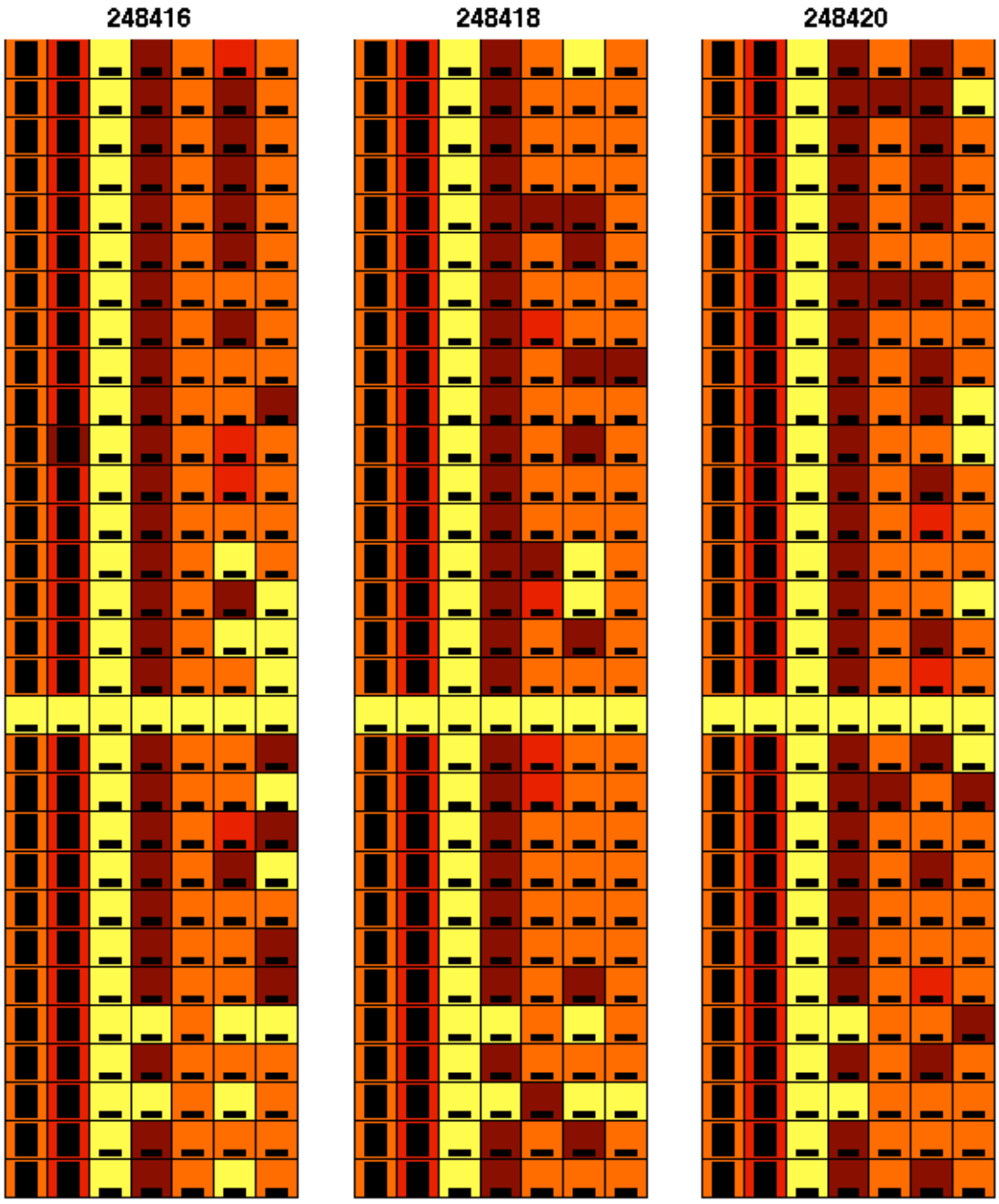

Figure 5.13: Unexpected temporal signatures for `mProjExec` Experiments # 23, 24, 25, with S.F. =1. We observe significant differences both in the data which are consequently reflected in characteristics of the temporal signatures. The main differences from samples of expected application performance are the high variance, high periodicity of the CPU metric and the slow but gradually increasing memory utilization ramp.

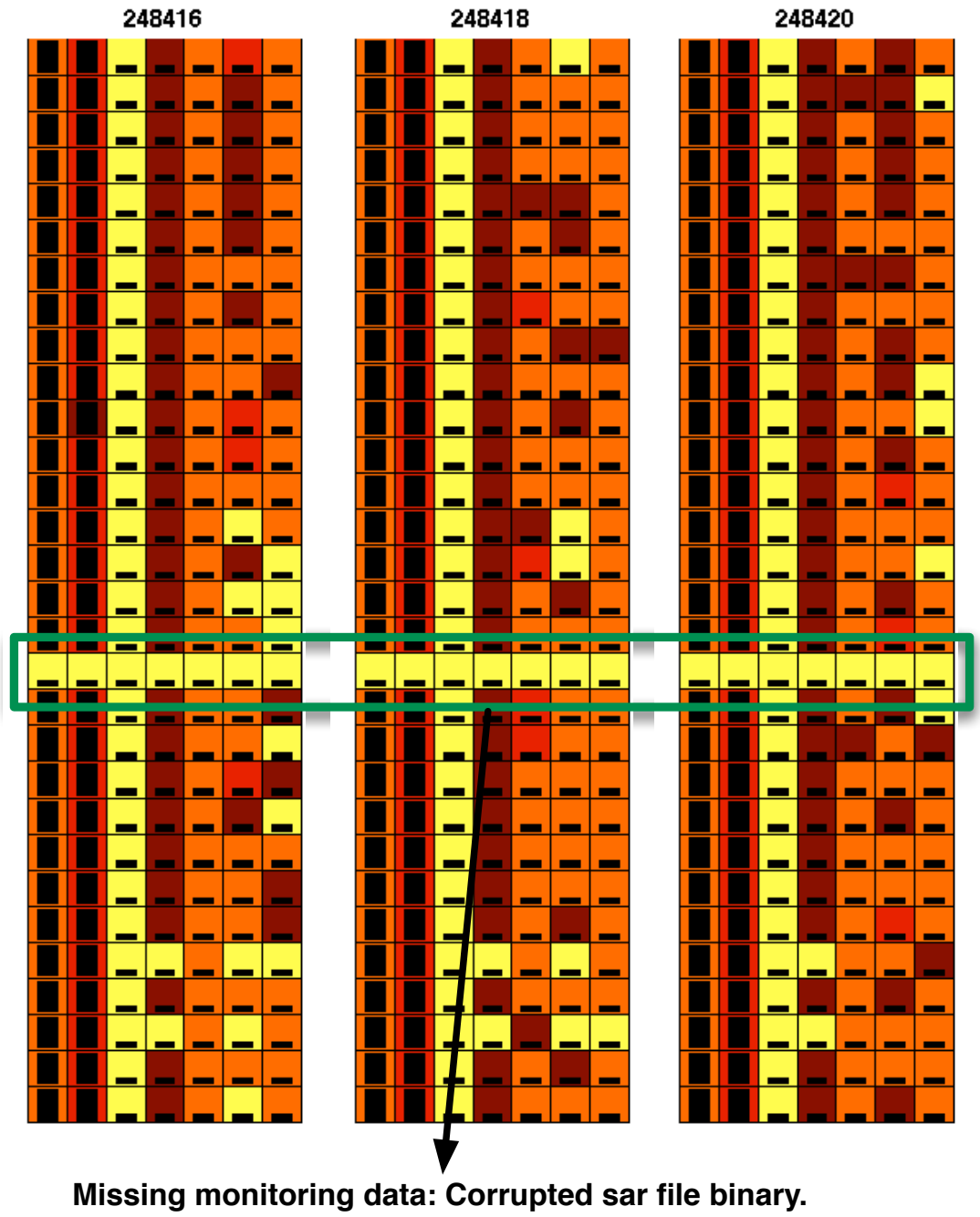

Figure 5.14: Temporal signatures across `slowio` cluster for unexpected `mProjExec` application executions. Missing monitoring data for task executing on compute node `c0-24`.

5.5.2 Case 2: Diagnosed Corrupted Monitoring Data File Binary

Compute node `c0-24` on the `slowio` cluster has been generating corrupted `sar` binary files (i.e., the performance monitoring data) for many of the experiments we have ran on the cluster, which results in empty monitoring data files or zero-time series for the performance metrics that we capture. The results of our scientific application experiments were not affected, though the presence of such a problem can be indicative to a system operator that configuration settings may not be properly set on that host or that the monitoring application's daemon may need to be restarted to produce valid monitoring data. Figure 5.14 shows how all the temporal signatures from the flat, zero-valued time series immediately indicate the lack of data.

5.5.3 Case 3: Undiagnosed Consistently Different Resource Characteristics Across Experiments

We have noticed during the execution of `WRF` on the `himem` cluster, Experiments # 51, 52 and 53, that the temporal signature of one task running across executions on the Teragrid node `tg-c256` is significantly different than most of the signatures for other tasks, as emphasized in Figure 5.15). When inspecting the performance time series data which generated those abnormal temporal signatures, we also noticed an abnormality on the memory metrics (MPU: percent-utilization and SPU: percent-swap-utilization), as they vary highly between 0 and 100%. While this behavior does not seem to affect our application and we do not know the source of this behavior, it may be prudent for a system operator to investigate such behaviors on the node, in order to prevent the node's possible future failure during a user's application execution.

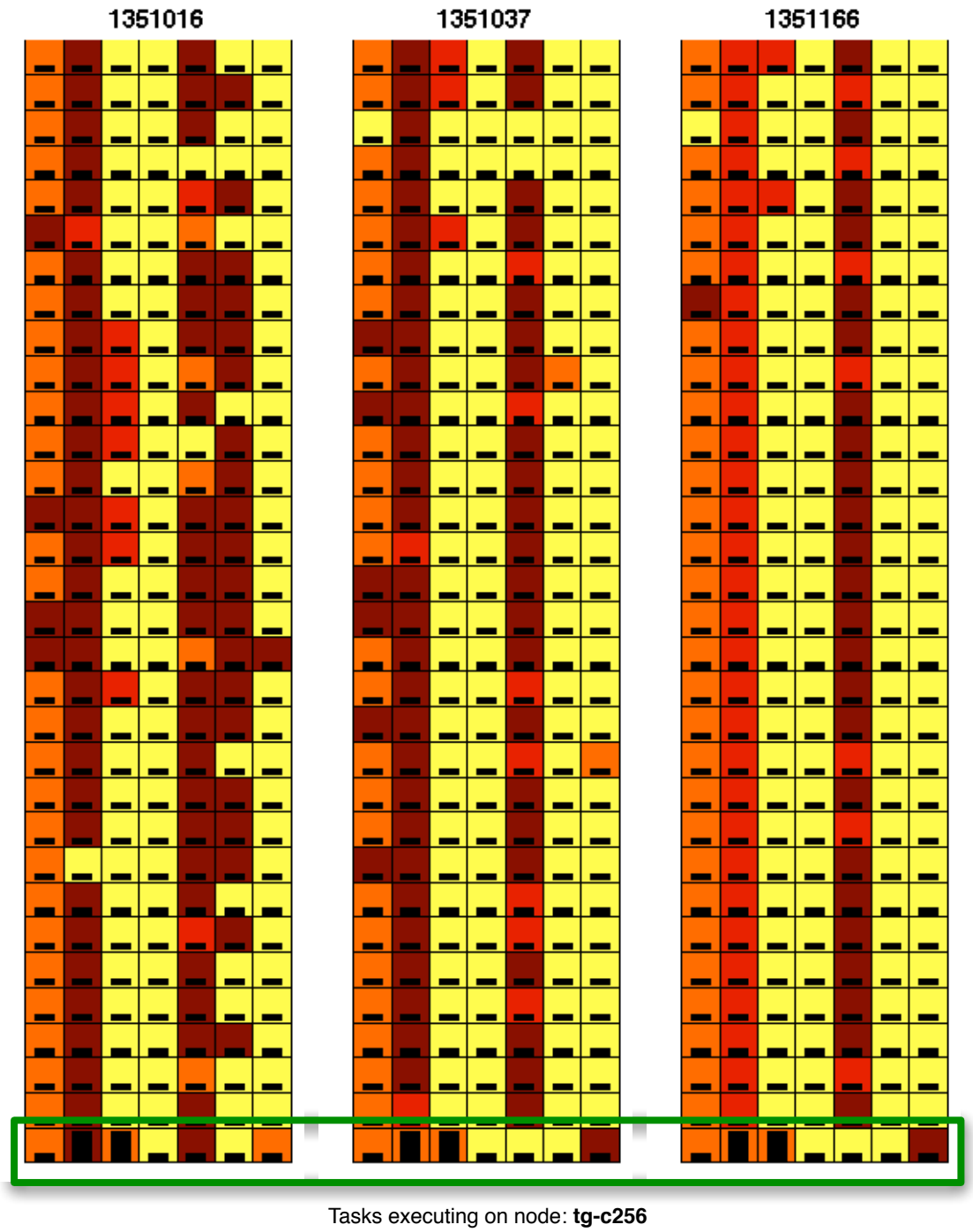

Figure 5.15: Unexpected temporal signatures on specific nodes during `WRF` experiments # 51, 52, 53. It is reasonable to assume from all the other temporal signatures generated for WRF during expected application states that behavioral characteristics manifesting in a high variance on both memory metrics is the likely result of some abnormality happening on the specific resource node, `tg-c256`, and its unlikely to be a characteristic of that specific task of the application. A system operator may want to investigate the cause of the abnormality.

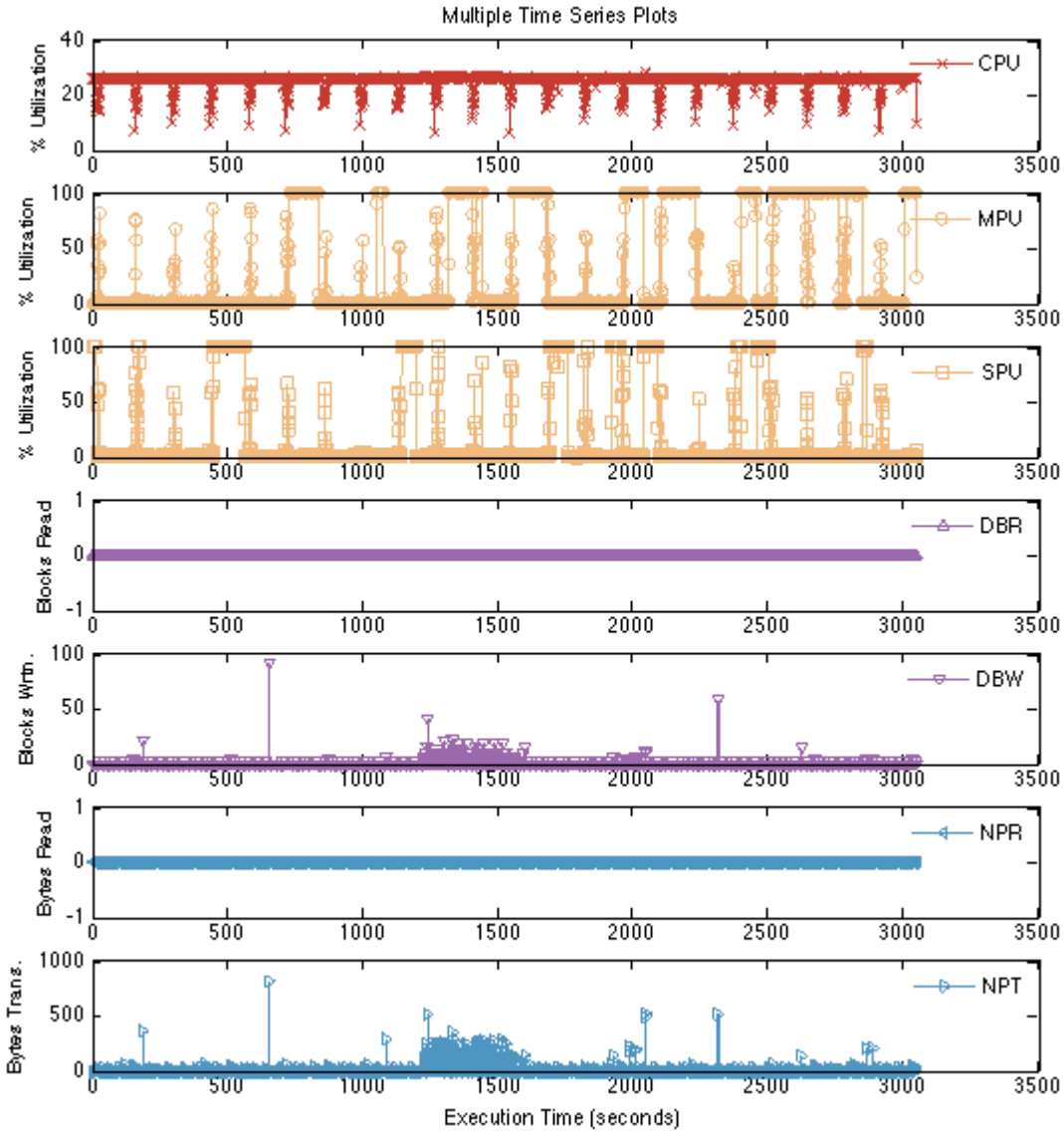

Figure 5.16: Time series data from `WRF` Experiment #51 for the compute node `tg-c256` exhibiting the abnormal behavior. We observe a very regular and marked periodicity on the CPU metric, and a very high oscillation between 0 and 100% on both the percent memory utiliztion and the percent memory swap metrics.

5.5.4 Summary

We have described characteristics observed in performance time series data collected from two different scientific applications during true instances of unexpected

performance. Generally, the temporal signature characterization of the time series data in degraded performance instances reveals higher variance on metrics on which the expectation was lower variance; similarly, in terms of patterns, we observe significant changes in patterns from cases of expected performance executions. The ability to make an automatic distinction between performance data collected during expected and unexpected behavior circumstances is fundamental to performance problem identification for applications and systems.

5.6 Qualitative Performance Validation and Diagnosis

We describe in the following sections the process of qualitative performance validation and diagnosis in scientific workflows using temporal signatures. We associate high-level, qualitative behaviors of applications with their corresponding temporal signatures and show how this correlation can provide, in a simple and intuitive manner, answers about the behavior of workflow components as well as interpret the global behavior of the application.

5.6.1 Task-Level

For the duration of each task within a workflow we can generate temporal signatures as illustrated in Figure 5.17. The evaluation epochs can be determined in several ways. In the case of scientific applications that output progress logs (i.e., logs recording the amount of work already performed -such as how many astronomy files have been reprojected or how many forecast hours have been computed), it is relatively simple to correlate the information in the logs with monitoring time-stamps in order to get evaluation time points across all tasks within a workflow instance. If the scientific application does not produce a progress output log that can be easily used for time-stamp generation, or in the case of a scientific application that cannot

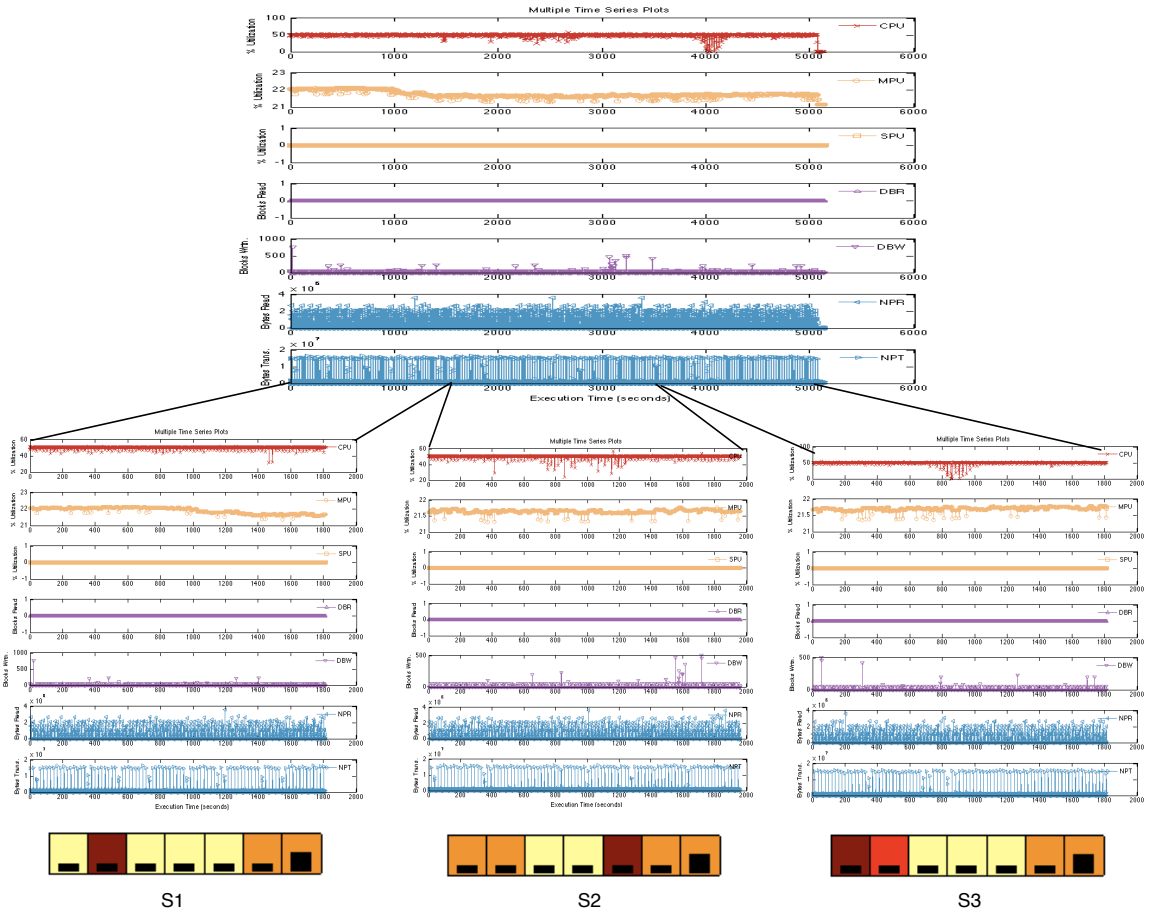

Figure 5.17: Time series data from `mProjExec` with `M101` on `fastcpu` from Experiment 1337251; Periodic evaluation of application behavior using temporal signatures generated when approximately 33% of the files have been processed.

estimate a progress-to-completion metric due to the nature of numerical algorithms (e.g., non-convergent), then the application can be instrumented with simple markers throughout the code that can serve as time-stamps for generating temporal signatures across tasks.

5.6.2 Workflow-Level

We present two scenarios that reflect how our qualitative performance analysis framework informs the workflow user with simple, qualitative descriptions of the

behavior of long-running workflows and how, in cases of degraded performance, a scheduler or a fault-tolerance mechanism may use such qualitative information for triggering appropriate remediation mechanisms to help improve the total workflow execution time.

Scenario 1: Expected Workflow Qualitative Behavior

Consider a simple instantiation of a LEAD workflow where 32 `WRF` tasks run in parallel on compute nodes on the `himem` cluster. Each task analyzes the same weather data set but with slightly different initial conditions. Each task is expected to output a weather forecast corresponding to the specified initial condition. At the completion of the workflow, the user inspects all the results from each task and analyzes the results. For this scenario illustrated in Figure 5.18, the total number of concurrently monitored tasks is 32. The user specifies a threshold value of $T_R = 0.1$, representing the ratio of unexpected to expected behavioral observations she is willing to tolerate. At periodic intervals correlated with application progress, the framework generates temporal signatures across all tasks. The following sequence of events illustrates global performance validation and diagnosis. During each analysis interval, 31 tasks are classified as expected and 1 task is classified as unexpected, reflecting the behavior of a possible problem computational node (i.e., compute node `tg-c256` of experiment #51 from the `WRF` experiments). The threshold value R is 0.02, which is well below the set $T_R = 0.1$; therefore, during all analysis intervals, the behavior of the workflow is deemed *expected*. In this scenario, notice that the tasks are independent of one another, and the possible performance degradation or failure of one task will not impact significantly the results the user expects. However, in circumstances where the performance degradation of one task can induce performance degradation in dependent tasks, the policy mechanism for interpreting the overall behavior of the workflow needs to be changed to reflect such dependencies. We address this issue

more in Section 5.9.1, which addresses limitations of the current evaluation.

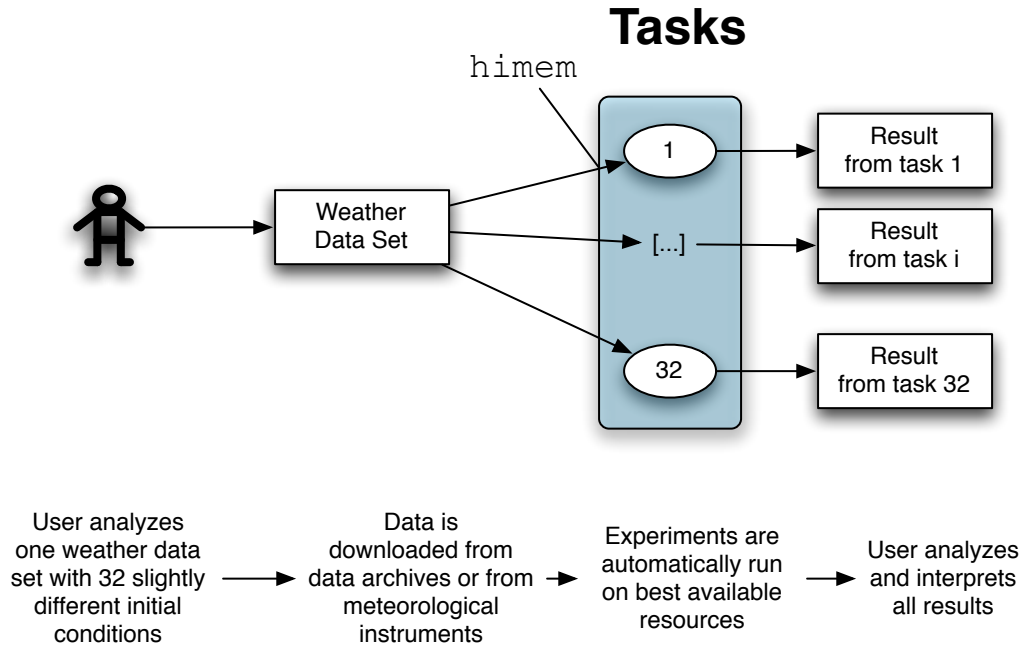

Figure 5.18: Scenario 1: Workflow instance with expected qualitative behavior.

Scenario 2: Unexpected Workflow Qualitative Behavior

Consider an instantiation of a Montage workflow illustrated in Figure 5.19,where 64 `mProjExec` tasks run in parallel on compute nodes on the `himem` cluster and 30 `mProjExec` tasks execute on the `slowio` cluster. The total number of concurrently monitored tasks is 94. The user specifies a threshold value of $T_R = 0.1$, representing the ratio of unexpected to expected behavioral observations he is willing to tolerate. At periodic intervals correlated with application progress, the framework generates temporal signatures across all tasks. The following sequence of events illustrates global performance validation and diagnosis. During the first analysis interval, all tasks executing on the `himem` cluster are classified as belonging to an expected behavioral state, while all tasks executing on the `slowio` cluster also belong to an expected behavioral class previously observed on that particular system. The threshold value R is zero because there are no unexpected states. Since $R \leqslant T_r$, the overall qualitative

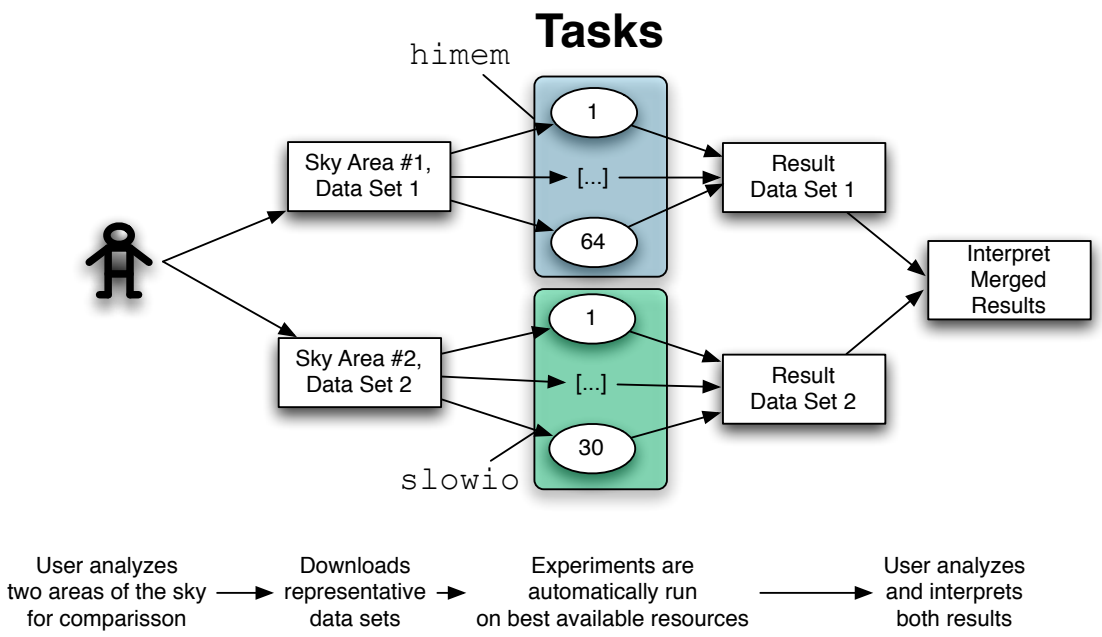

Figure 5.19: Scenario 2: Workflow instance with unexpected qualitative behavior.

performance of the workflow is deemed *expected*.

During the next analysis interval, all the qualitative signatures generated on the `slowio` cluster reveal a strong similarity with signatures from the unexpected behavioral signatures associated with perturbations due to an slow network. The threshold value $R = 0.19$ becomes greater than the user specified value $T_R = 0.1$. Our framework would report that the overall qualitative performance state of the workflow is *unexpected* with the possible diagnostic being a slow or shared network connection on the `slowio` cluster. A fault-tolerance service or a scheduler can take this information into consideration and may decide, based on a variety of factors (i.e., number of available resources, number of queued applications, time to completion of the application, etc), to migrate the application from the `slowio` cluster to another cluster with appropriate network bandwidth.

5.7 Framework Evaluation

We infer the efficacy of our framework based on temporal signatures from the main usage modality for signatures: classification. The evaluation criteria is based on the ability of a classifier to correctly classify a new, "never-seen" signature as belonging to the correct category of performance behaviors, *expected* and *unexpected*. Similarly to [22], to say that temporal signatures are accurate, meaningful and of high-quality is to imply that classification based on those signatures performs well.

Furthermore, in order to test the first hypothesis, we analyze a subset of the experimental data to show an example where performance data signatures based on temporal information are superior –in terms of accuracy of classification– to signatures based on instantaneous data values, which do not carry temporal information. To test our second hypothesis, we analyze all the experimental data for which we have examples of both expected and unexpected behaviors, and report the overall balanced accuracy obtained. For both cases of our evaluation, we use K-fold cross-validation[1] as the technique to help test the accuracy of our classifier in the absence of new experimental samples of behavior.

5.7.1 Comparison of Classification Accuracy Between Instantaneous Values Signatures and Temporal Signatures

In this section, we test the validity of our first hypothesis which states that it is necessary to extract temporal information in performance time series data for the case of long-running scientific applications. We show need by providing an example where instantaneous values of performance metrics are not able to accurately distinguish cases of expected and unexpected performance behaviors.

[1] Cross-validation is a statistical method of partitioning existing sample data into subsets such that learning is performed on a subset of the data, while validation of the learning is performed on another subset of the data. In K-fold cross-validation, the data is partitioned randomly into K subsets; training is performed on K-1 of the subsets, while the validation is done with the remaining subset. This process is repeated K times (or folds) such that each of the K subsets is used exactly once as a validation subset.

We make the following high-level deductive argument and substantiate it with experimental results. If instantaneous values signatures are sufficient for an accurate classification of expected and unexpected behaviors then temporal signatures are not probably needed for performance analysis. However, if we show at least some cases where instantaneous values signatures result in a significantly lower accuracy of classification than temporal signatures, then it is reasonable to conclude that temporal signatures help improve performance analysis and are therefore needed.

We use as a validating example the performance data collected from the `mProjExec` application during Experiment #25, which represents the *unexpected* behavior of 30 tasks for a duration of 6332 seconds. Because the characteristics of the environment (i.e., low bandwidth) do not enable us to collect an *expected* set of behaviors for the IO intensive application, we infer from the characteristics of the application observed on different environments that the expected behavior of `mProjExec` on the `slowio` cluster should look similarly to the expected behaviors found in the environments with a well-provisioned network. Therefore we generate a simulated data set for the `slowio` architecture that looks as shown in Figure 5.20(a). We generate simulated data resembling the expected behavior of 30 tasks and we compare the performance of instantaneous signatures with temporal signatures on these expected and unexpected data-sets.

We sample instantaneous, raw-values signatures for the same data by constructing a simple signature which incorporates the raw values of the seven selected metrics. An illustration of instantaneous signature extraction is shown in Figures 5.20(a) and 5.20(b). The "raw-values" are normalized for each metric by the maximum value ever seen, such that the highest value in a instantaneous, "raw-value" signature can be 1 and the lowest value can be 0. We perform this normalization as is customary in data analysis methodology in order to be able to correctly compare signatures

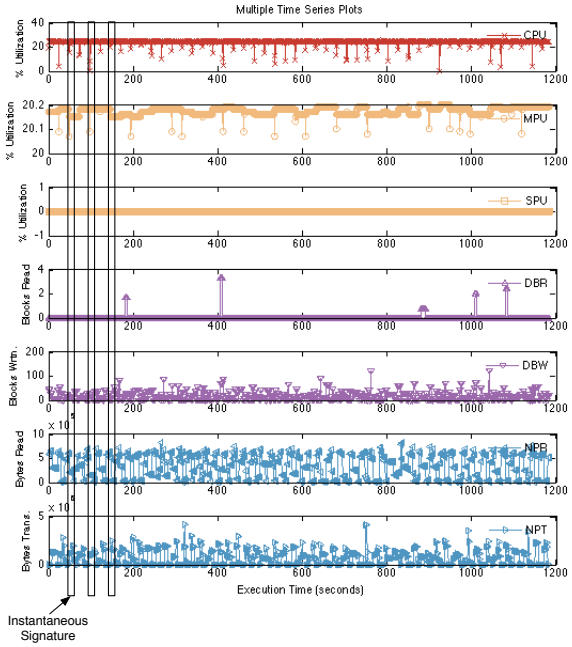

(a) Examples of instantaneous signatures for expected performance data.

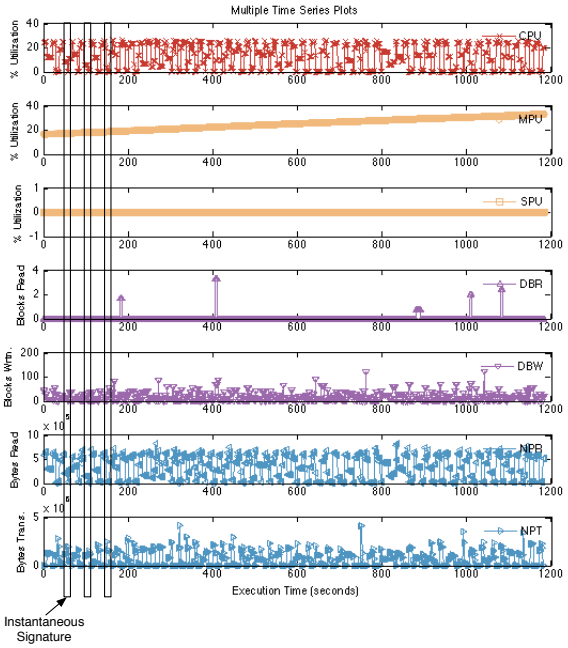

(b) Examples of instantaneous signatures for unexpected performance data.

Figure 5.20: Examples of instantaneous signatures extracted from both expected and unexpected performance data. Performance data is smoothed with a window size of 60 seconds and instantaneous signatures are extracted every 60 seconds. Some of the instantaneous signatures sampled from the unexpected data are very similar to instantaneous signatures sampled from expected data which will likely reduce the ability of the classifier to correctly classify this data based on this information alone.

and to rely on classification results. We also extract temporal signatures from the same data as described in the previous sections and compare the results of accuracy classification. The distance metric used for instantaneous signatures is the Euclidean distance while for temporal signatures it is the normalized Hamming distance, as each distance metric is appropriate given each signature definition.

The performance data sets are analyzed as an example for the first 1000 seconds of the duration of the experiment, in order to reduce the number of instantaneous samples collected. The data is smoothed with a window of 60 seconds for each task in both expected and unexpected data, resulting in 30 temporal signatures and 480 instantaneous signatures for each behavioral class.

We use cross-validation with $K = 10$ on the database of both instantaneous and temporal signatures and compare the results of classification using the `knn` classifier with $k = 1$ in Figure 5.21. In this example data set, temporal signatures outperform instantaneous signatures considerably, as the balanced accuracy for using temporal signatures is 0.9858 while the balanced accuracy for using instantaneous signatures is 0.7848. Analyzing the sensitivity and the specificity values for the classification results, we note that the temporal signature classification is able to classify, equally well instances of expected (i.e., high specificity–close to 1) and unexpected (i.e, high sensitivity–close to 1) behaviors. However, in the case of instantaneous signatures, while the sensitivity is relatively high, the specificity is a lower 0.6174, implying that it is more difficult to distinguish unexpected behaviors, because there are samples of instantaneous signatures which, although they are labeled as unexpected due to the poor performance of the application, are very similar to instantaneous signatures of known expected behaviors. This result could have been predicted as instantaneous signatures tend to give a local view of behaviors, not the needed longer, temporal one. We therefore conclude that these results show an initial support for our first

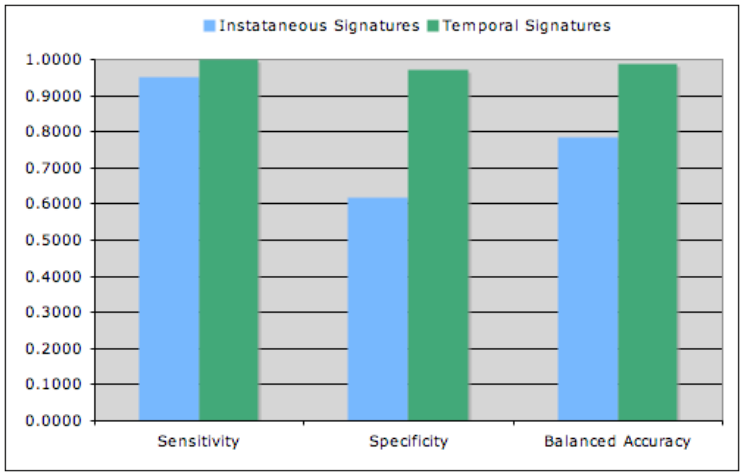

Figure 5.21: Balanced accuracy results for classification with instantaneous signatures and with temporal signatures.

hypothesis that temporal information is necessary, under certain circumstances, to help a performance analysis framework better assess application behavior. While we have shown the potential utility of our temporal signatures, we note that, depending on the characteristics of the application and of the performance data, there will likely be experimental data cases where simpler signatures may perform as well or better than temporal signatures. Therefore, for a full validation of our hypothesis, more experiments would need to be conducted, supported by more examples of both expected and unexpected instances of long-running application behaviors.

5.7.2 Classification Accuracy Using Temporal Signatures

In this section, we test the validity of our second hypothesis which states that temporal signatures based on qualitative variance and pattern as instances of temporal information are sufficient for an *accurate* performance validation and diagnosis. We quantify the *accuracy* of our framework by testing how well new samples of temporal signatures are classified into the expected or unexpected behavior categories. As previously noted in the methodology chapter, we use as the classifier the k nearest-neighbor algorithm with $k = 1$ and with the normalized Hamming distance

as the similarity metric between temporal signatures. The classification of temporal signatures corresponds to performance validation (i.e., deciding whether the label is expected or unexpected), and diagnosis (i.e., deciding which type of unexpected behavior is detected).

We generate a temporal signature for the entire duration of each task from each experiment described in Tables 5.3 and 5.4, resulting in a total of 1242 signatures for the first Montage data set, and 1242 signatures of the second Montage data set. Out of these signatures, there are 90 instances of unexpected behaviors and 1152 instances of expected or good-performance behaviors. We note that the ratio of samples of expected to unexpected behaviors is 1142:90 which represents approximately 13:1. This ratio strongly supports our choice of balanced accuracy as a measure of evaluating framework efficacy, because a simpler accuracy metric may inflate accuracy results due to a larger sample of expected signatures.

Cross-validation with $K = 20$ partitions all 1242 signatures from each Montage data sets into subsets, where training is performed on approximately 1085 signatures and validation is performed on the remaining 157 signatures. Both the training and validation data sets are randomly chosen each time from both sets of expected (1152) and unexpected signatures (90).

Table 5.7 shows supportive evidence for our secondary hypothesis that qualitative variance and pattern as instances of temporal information are sufficient for the creation of performance signatures that can accurately –with accuracies higher than 98.66%– detect instances of expected and unexpected behaviors in long-running scientific applications.

Although these results reflect a very good, high-accuracy of detection, we cautiously note that the accuracy of our framework will most likely decrease as more experimental data from more applications, configurations and different instances of

unexpected behaviors are included. However, our current results offer an initial valid substantiation of the utility of temporal signatures for performance validation and diagnosis in long-running scientific applications.

	`mProjExec` with `M101`	`mProjExec` with `M57`
Average B.A. (S.F.=1 s)	0.9979	0.9976
Average B.A. (S.F.=10 s)	1.0000	0.9947
Average B.A. (S.F.=60 s)	0.9975	0.9929
Average B.A. (S.F.=300 s)	0.9934	0.9866

Table 5.7: Evaluating the efficacy of our framework with K-fold cross-validation, where $K = 20$ and with various smoothing factors applied to the data before signature generation. The maximum variance ever-seen for each metric is also calculated on correspondingly smoothed data. It is ideal to obtain a balanced accuracy of 1.0, which means the classifier does a good job of classifying equally well both expected and unexpected instances of behaviors.

Considerate Use of Smoothing

We note that smoothing must be carefully applied to the performance time series data as its misguided application may have a significant impact on our framework's accuracy. We describe below an instance showing the effect of mis-application.

Smoothing the performance data prior to calculating the qualitative variance and normalizing by the maximum variance ever-seen that has not been computed from similarly smoothed data, will significantly decrease the accuracy of the framework. The reason for this is because the variance feature contributes to distinguishing the expected from the unexpected performance behaviors. Normalizing the variance by a higher maximum value (i.e., the maximum variance value will be higher when computed from raw data versus smoothed data) will reduce the ability of a temporal signature to capture the difference between our experimental examples of expected and unexpected behaviors. We support this statement by running the same type of cross-validation experiments as done in the previous section, in which we obtain

the balanced accuracy rates for this instance of calculating the qualitative variance. Table 5.8 shows the accuracy results obtained for the unfit application of smoothing and the impact on the framework efficacy. Figure 5.22 compares the accuracy levels between the appropriate (i.e., the two top curves), and the inappropriate application (i.e., the two lowest curves) of smoothing on the calculation of the qualitative feature variance and shows the significantly reduced accuracy in the case of the inappropriate use of smoothing.

	`mProjExec` with `M101`	`mProjExec` with `M57`
Average B.A. (S.F.=1 s)	0.9993	0.9975
Average B.A. (S.F.=10 s)	0.9326	0.6867
Average B.A. (S.F.=60 s)	0.6839	0.6072
Average B.A. (S.F.=300 s)	0.7164	0.6150

Table 5.8: Considerate use of smoothing: impact of unfit application of smoothing for calculation of variance feature. Evaluating the efficacy of our framework similarly as before, with K-fold cross-validation, where $K = 20$. Accuracy decreases with smoothing because the temporal features of the diagnostic problem manifest themselves at the raw data sampling rate (S.F.=1 s); smoothing, as applied in this case, reduces the variability and amplitude of the periodicity present in the diagnostic data and effectively creates signatures more similar to previously known expected states.

While we do not specifically study in this work the effect of smoothing the data on the pattern feature and its direct impact on the efficacy of the framework, our experiments with accuracy of the pattern identification mechanism suggest that while smoothing will increase the accuracy of the pattern identification, over-smoothing can significantly change the patterns observed. This can lead to an overall decrease in accuracy of the framework, because some patterns that are present in data for some level of smoothing may be transformed into different patterns belonging to a different performance expectation category.

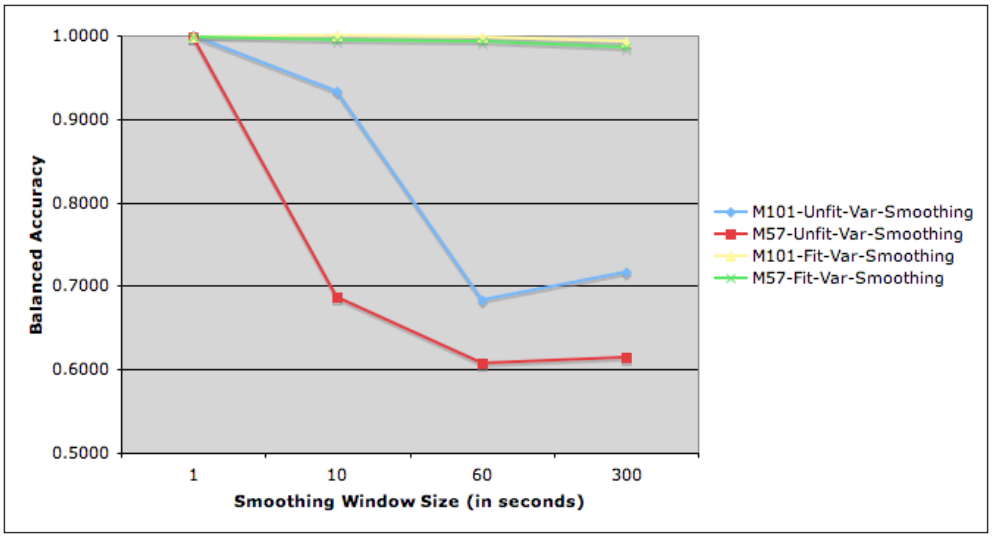

Figure 5.22: Impact of smoothing on the variance feature calculation and the direct impact on framework accuracy. When the qualitative variance feature is calculated from smoothed performance data normalized by the maximum variance ever-seen that has not been computed from similarly smoothed data, the accuracy of the framework decreases significantly, because the variance feature contributes to distinguishing the expected from the unexpected performance behaviors.

5.8 Performance Impact of Framework

There are three factors within our approach that may add a computational, data storage or time cost to any system or application using our proposed framework. The three factors are:

1. Overhead of collecting the data (Overheads: computational and storage),
2. Temporal signature computation (Overheads: computational, storage), and
3. Temporal signature classification (Overheads: computational, storage, and time).

The performance time series data is collected by a widely available and deployed system monitoring tool, `sar` [43] which has a low overhead (i.e., observed and reported overheads for CPU memory resources $< 0.1\%$). The overhead may increase and may affect slightly the disk and the network resources, depending on the sampling rate and on the duration of monitoring (i.e., writing the collected data to the binary monitoring

	mProjExec with M101	mProjExec with M57	WRF 2.0 with meso	WRF 2.2 with non-meso
Epoch Length (min)	2748 s	900 s	4216 s	1940 s
Epoch Length (max)	6332 s	6390 s	4270 s	3416 s
# Generated Signatures	1242	1242	150	1152
Time to Generate All Signatures	183.23 s	88.24 s	24.49 s	121.76 s
Classification of ONE signature	< 1 s	< 1 s	< 1 s	N.A.

Table 5.9: Performance impact of temporal signatures and their subsequent classification. All timing measurements were done on a Mac Book Intel Core Duo, with 2.0 GHz processor speed and 1 GB RAM. All algorithms were implemented using Matlab 7.4.0 Release 2007a.

file). However, we plan to take snapshots of the monitoring data at small intervals, such as 30 - 60 minutes, and automatically generate the compressed signatures from the data, meaning that we automatically eliminate the cost involved in storing large amounts of monitoring data that may accumulate over the long-running execution of a scientific workflow. Only performance time series data representing failed or important diagnostic cases may be stored, since diagnostic raw data sets are very valuable for future detection of potential problems.

The temporal signatures are very fast to compute as shown in Table 5.9, and there is sufficient time to compute hundreds or thousands of signatures during each epoch of periodic evaluation of performance. Also, the classification of a signature is done in under a second on a Intel Dual Core 2.0 GHz notebook. We conclude from this information that signature generation and classification is fast enough to be done as needed during the performance evaluation of workflows on distributed resources.

The last significant overhead to consider relates to the amount of time needed to capture samples of expected and unexpected application behavior. Currently, our framework takes a passive learning approach, where signatures are labeled with *expected* or *unexpected* labels as experiments are performed. This passive approach can take a long period of time to learn a statistically significant database of samples

of behavior. However, this can be remedied by using an active learning approach such as proposed by [101], where known stress factor can be applied to the applications of interest in a controlled fault-injection test-bed, and signatures of diagnostic states can be generated at a much faster rate and with more accurate labels.

5.9 Limitations

We address limitations of our current framework evaluation as well as higher-level limitations of the approach. First, we list and describe ways in which our framework could be improved by further evaluation and expansion. Last, we describe circumstances that will likely cause our approach to perform poorly and may require significant changes in operating assumptions, implementation techniques, and evaluation.

5.9.1 Limitations of the Current Evaluation

We list and describe several avenues which we believe would significantly improve the current framework and expand on its current evaluation.

Passive Learning of Behaviors

Currently, we have passively learned instances of expected and unexpected behaviors for our experimental data sets. The major disadvantage of a passive learning approach is that gathering a representative sample of behaviors will be slow. An alternative approach can leverage an active learning technique, such as that proposed in [101]. We could construct a fault-tolerance test bed where we inject a variety of common faults known to affect the performance of long-running applications in production environments.

This approach would enable us to acquire, in a controlled fashion and relatively quickly, instances of expected and more importantly –unexpected– temporal signa-

tures for an application, and to label them with a known diagnostic state (e.g., signature was captured during known *memory leak* issue affecting the application). The disadvantage of using temporal signatures of applications under a controlled, fault-tolerance test bed lies in the fact that such signatures may not have the same characteristics with signatures captured during a performance problem occurring in real production environments.

Adaptation to Change

The current framework assumes that once a set of behaviors has been learned, the overall accuracy of validation and diagnosis will remain constant due to the assumption that behaviors drawn from the same distribution with the training data set will be analyzed. Because the space of parameters that can affect temporal signatures and application behaviors is large and complex, it is likely that new application behaviors will cause a reduction in framework's accuracy because they are not captured in the baseline learning set. Under this circumstance, `Teresa` would need to be enhanced with a dynamic learning mechanism that would re-learn baseline behaviors once the overall accuracy decreases below an accepted user value.

Workflow Tasks Independence

While the use of temporal signatures is independent on the dependence relationship in a set of workflow tasks, we currently evaluate workflow-level behavior under the assumption that behaviors of the tasks do not have a significant dependence on the temporal observed behavior. The current time series collected and analyzed may not specifically expose dependent behaviors in a group of tasks (e.g., MPI communication patterns), but such performance time series may be captured and characteristics of the temporal signatures can be further studied, together with the implication on variation of observed temporal signatures for a set of interdependent tasks.

Alternate Signature Definitions

In this work we have defined and presented results for a specific instance of a temporal signature, containing structural and temporal features of performance time series with two discrete features: relative variance and pattern. There are many other possibilities of defining signatures for performance time series data. For example, a continuous feature version of our current signature may capture as one feature, f_1, the continuous normalized variance $[0, 1]$ as well as a feature for each of the pattern of interest, f_2 for the periodic pattern, f_3 for the ramp pattern, f_4 for the flat pattern, and f_5 for the random pattern, each varying from $[0, 1]$, where the values in the interval may represent confidence levels for the detection of each pattern (i.e., 0: non-confident, and 1: complete confidence). The signature would encode five features for each of the selected time series.

Additionally, signatures could be also created by varying the number of time series for which features are extracted. Coupled with the metric attribution work by Cohen [21], we can use different subsets of times series for different signatures targeted at identifying different performance problems. For example, time series $M = \{1, 2, 3, 4, 5\}$ with the discrete features f_1 and f_2 may be used to identify problems related to memory and disk, while time series $M = \{1, 2, 6, 7\}$ with the same discrete features, may be used to identify problems related to the network.

Impact of Smoothing the Data on Signatures

Smoothing must be carefully applied to the raw performance data, as it has a direct impact on the two features we selected for our particular signature definition, as discussed in Section 5.7.2. If the data is unprocessed, with no smoothing filter applied, small amounts of variance may have an impact on the pattern identification mechanism, as patterns may be incorrectly classified. At the other extreme, too much smoothing can significantly reduce the amount of variance in the series, and

may change patterns.

As smoothing will often be used to pre-process monitored data in order to reduce noise or local variations, care must be taken in applying it because smoothing over large windows of time may hide some important variations in the data which are correlated with a significant and persistent performance problem. To support identification of problems without worrying about finding an optimal smoothing window, signatures can be generated for different windows, and performance validation and diagnosis can be done on all these signatures, potentially triggering performance problem identification for some smoothing levels and not for others.

Transferability of Temporal Signatures

One question that arises from the characteristics of temporal signatures for Montage and LEAD is whether temporal signatures are transferable – that is, if we learn a set of expected and unexpected temporal signatures for an application, can we use them to validate the performance for a new application that exhibits expected signatures similar to a known application? A further study expanding on this issue could be of great value in providing further evidence for the practicality and general applicability of such a qualitative performance analysis approach.

5.9.2 Limitations of the Approach

There are two main circumstances of our approach under which if the operating assumptions change, they will likely impact the accuracy of our framework. The contexts refer to our approach's (1) reliance on an expert for supporting the initial learning of expected and unexpected behavioral instances, and (2) assumption that the behaviors of the applications are not dependent on the scientific data analyzed and on the application's configuration. Furthermore, there is an inherent loss of accuracy of validation and diagnosis because we correlate a limited set of performance

metrics with higher-level application states. We describe these issues in the following subsections.

Reliance on Expert for Learning Behavior Instances

Our framework does rely on a human expert or a semi-automated expert to label samples of performance data associated with both good and degraded performance behaviors. This setting allows our framework to assess performance via classifiers in an on-line setting. However, the disadvantage of relying on a human or semi-automated experts for gathering of training data sets is that accurate labels of behaviors are very hard (in terms of time and expertise) to acquire.

In the absence of training data, the alternative is to use unsupervised learning techniques (i.e., clustering) that may automatically discover groups of behaviors, which over time, can be associated with various qualitative behavioral descriptions for a given application. Neither technique (classification or clustering) lacks disadvantages. While the disadvantage of the supervised learning technique is that it requires an expert's pre-labeled instances of behaviors, the disadvantage of the unsupervised learning technique is that deciding how many behavioral clusters truly exist in a sampled training set and their practical meaning is typically hard to interpret. These disadvantages suggest that maybe combining both techniques in an effort to strengthen their individual advantages may be most practical under certain contexts.

Application Data and Configuration Dependence

`Teresa` currently assumes that the scientific applications executions do not exhibit parameter or data dependent behavior. If this assumption is removed, our framework needs to allow for two modifications: (a) a methodology for deciding the appropriate time interval for generating signatures periodically, and (b) a characterization how differences in application data characteristics impact the performance time series collected and the generated temporal signatures.

Characteristics of temporal signatures under these changed assumptions can be learned by analyzing the impact of various parameters and the contents of the input data on the time series analyzed. Our work can be expanded by including methods to map such dependencies described in work by [33, 103].

Non-uniqueness of Diagnostic Signatures

Our temporal signatures correlate symptoms of performance problems in scientific applications and their execution environments. There could be many problem root causes that manifest themselves in similar symptoms; therefore, temporal signatures associated with one symptom may represent different causes or types of problems. The goal of our framework is to offer guidance in identifying the most likely type of problem affecting the application and not necessarily to find the root-cause of the problem. Because it is likely that different behaviors will exhibit similar signatures, this will reduce the ability with which our framework can pinpoint the most likely problem affecting an application. We discuss more about the related issue of correlation and causation in the concluding Section 7.2.4.

5.10 Summary

This chapter demonstrated how `Teresa` reasons qualitatively about temporal behaviors for long running components within two large-scale scientific workflows. We described the scientific applications, their components, and characteristics of the computational environment where we conducted data collection experiments. We further showed instances of temporal signatures for applications during good performance executions and during degraded performance executions, and described scenarios of how the qualitative performance information can be used in practice to reason about application behavior.

We have presented evidence supporting the hypothesis that temporal information

is necessary to extract and analyze in order to achieve performance validation and diagnosis for the class of long-running scientific applications. Furthermore, temporal signatures incorporating variance and pattern information generated for these applications reveal signatures that have distinct characteristics during well-performing versus poor-performing executions. This leads to the framework's accurate classification of instances of similar behaviors, which represents supporting evidence for the second hypothesis that it is sufficient to extract variance and pattern as instances of temporal information available in performance data.

We described the performance impact of using our framework in practice and addressed both limitations of our current evaluations and limitations of the overall approach.

Chapter 6

Related Work

This thesis uses concepts and techniques spanning several areas, including time series analysis, pattern recognition, dimensionality reduction and compression, learning algorithms for problem diagnosis, methodologies for multi-variate data analysis, and visual analytics. We apply the framework in the context of performance analysis of *Grid scientific applications*[1]. Figure 6.1 shows a visual map of the techniques borrowed from related areas, and how we combine them to achieve a qualitative performance assessment in scientific workflows.

The following sections describe some of the more relevant examples of approaches similar to our own as they have been used in the analysis of distributed systems and applications.

6.1 Temporal Signatures

Our framework generates a compressed representation of data in performance time series during application execution. For this purpose, it uses some methodologies employed in classical time series analysis as well as techniques for feature extraction from time series data.

While there is a significant body of research in computer science, engineering and other fields employing similar methodologies, we describe only the ones most similar with our proposed work.

[1]Used interchangeably with *scientific workflows* or *scientific Grid workflows*.

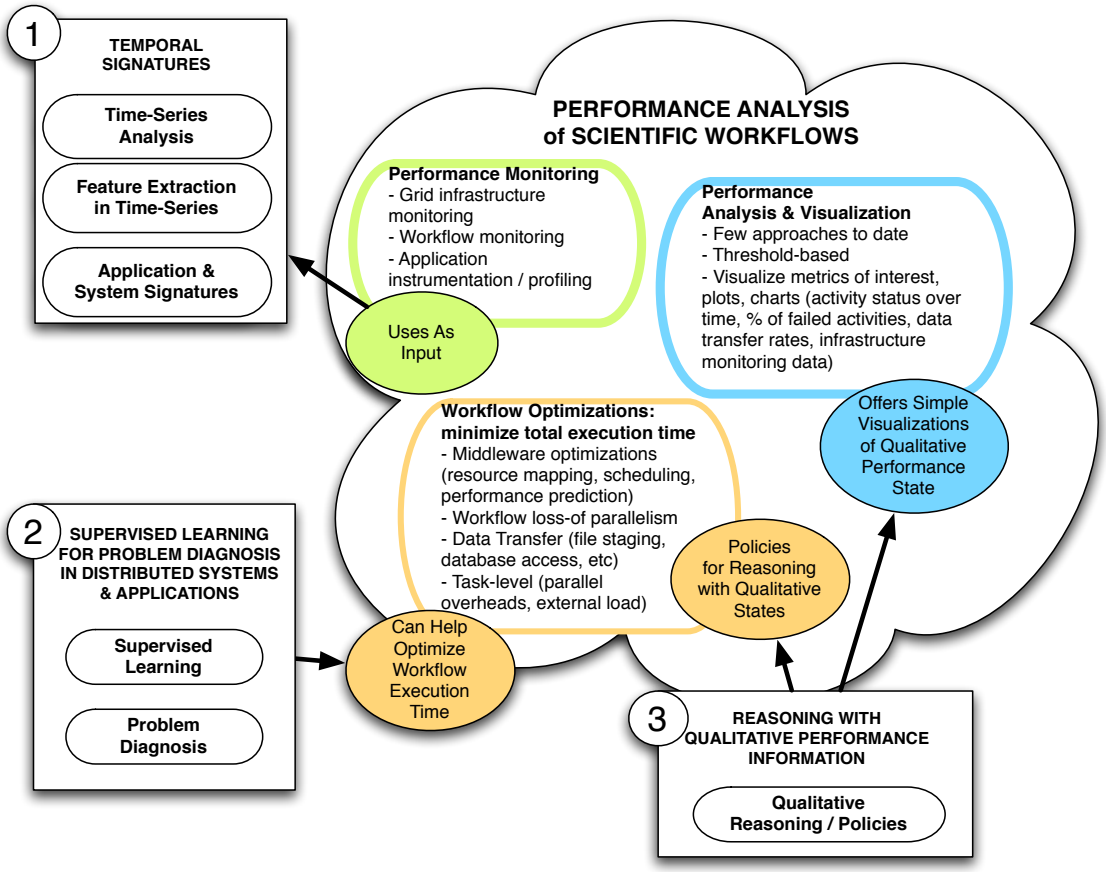

Figure 6.1: Qualitative performance analysis framework: related areas and problem context.

6.1.1 Time Series Analysis

A time series is an ordered sequence of values for a variable at specific, often equidistant, time intervals. Time series analysis focuses on: (1) understanding the structure and underlying forces that produced the data, and (2) finding a model that fits the given time series data as well as possible in order to correctly forecast future values of the variable [35]. Our framework focuses only on the former part of classical time series analysis; we strive to understand characteristics and special features present in the observed performance time series during application execution. We do not attempt to fit a model to the series and/or make predictions about future

performance metric values.

There are two common classes of techniques applied to time series analysis: *frequency domain* techniques and *time domain* techniques. Frequency domain methodologies, such as spectral analysis or wavelet analysis, investigate a given time series with respect to frequency, while time-domain ones, such as auto-correlation and cross-correlation analysis, investigate the series with respect to time. In our work, we rely primarily on using *time domain* methodologies, in particular we make use of auto-correlation analysis for pattern detection.

Examples of Time Series Analysis for Performance Analysis

Various time series analysis methodologies have been widely employed in understanding and improving the performance of applications and systems. We present a small subset of such examples and discuss similarities and differences with our approach.

Tran addresses in [105] the Input/Output (I/O) performance in high-performance computing (HPC) systems. An adaptive framework, called TsModeler, automatically models I/O requests using auto-regressive integrated moving average (ARIMA) time series models to predict temporal patterns of I/O requests. The resulting time series models coupled with spatial Markov model predictions enable more efficient prefetching of blocks in I/O systems. Our framework uses similar time series analysis techniques, in particular aspects related to auto-correlation analysis for automatic time series model identification. However, mathematical properties of the ACF are only used for a heuristic pattern identification mechanism, instead of more complex methods, such as periodicity detection mechanisms [4, 34]. We do not attempt to find a best model for any of the performance time series; we are only interested in extracting a small set of features from the series that we hypothesize can be used for problem diagnosis in long-running scientific Grid applications.

Brutlag [18] proposes a mathematical model based on exponential smoothing and Holt-Winters forecasting for the automatic aberrant behavior detection in network time series. Aberrant network behavior in performance time series data is decomposed in three components: (1) an algorithm for predicting values of a time series one time step into the future, (2) a measure of deviation between the predicted and observed values, and (3) a mechanism to reason if one or more observed values are "significantly deviant" from the prediction. A similar approach is also described in [112], where the focus is to detect as soon as possible network performance failures by studying deviations in the performance time series data of number of Internet service requests processed over a specific time interval. While they do not use specific time series model fitting for forecasting as in [18], they do use the expected mean and variance of each process to identify whether the observation is within expected norms. While we are also interested in detecting *unexpected* or *aberrant* behavior in time series, we do not take the same approach with [18]. As previously stated, we do not use techniques for time series forecasting. Furthermore, we analyze characteristics of a set of time series, not only an individual time series, as we are interested in an application's behavior as it utilizes necessary resources within a system (e.g., CPUs, memory, disk, network).

6.1.2 Dimensionality Reduction for Time Series Data

Massive data sets have become common in many applications and pose new challenges for knowledge discovery. When dealing with massive multi-variate time series data, we must employ specific techniques that analyze these data as automatically as possible and provide us with the needed information to make a specific decision within a specific context. This general problem is known as *dimensionality reduction*, and various techniques have been developed to address it. The techniques are broadly classified in two categories: (1) *variable selection*, and (2) *feature selection*

& extraction. The process of *variable selection* refers to identifying a small set of time series metrics variables that are most useful in identifying or detecting a specific objective function. *Feature selection* refers to the automatic process of identifying a small set of relevant features or characteristics within the selected variables that can be of further use for the same objective function; *feature extraction* is the process by which a selected feature can be extracted from the data. There are significant benefits to using techniques for dimensionality reduction. Benefits include: (1) making easier data understanding and visualization, (2) reducing the measurement and storage requirements, (3) reducing the time needed to train a classifier for the data, and (4) defying the curse of dimensionality to improve the classifier efficacy [46].

In this work we assume that variable selection has been already performed by either a domain expert or by an automatic technique such as the metric attribution described by Cohen [21]. Our focus is on deciding on a set of features in time series that would be most useful and relevant to distinguish between possible persistent problem states affecting application performance.

The types of features that one can select and extract form time series data can be broadly classified in two categories: (1) statistical features, and (2) structural features.

Statistical features are extracted using established concepts from statistical decision theory to discriminate among data from different groups based on quantitative features of the data [87]. Common techniques for statistical feature extraction include various time series transformations, including the identity transformation, Fourier transformations and wavelet transformations. Examples of statistical features in time series data include mean, variance, frequency counts, auto-correlation coefficients, wavelet transform coefficients and so on.

Structural features are extracted using methods relied on syntactic grammars to

discriminate among data from different groups based upon the morphological interconnections present within data. Examples of structural features in time series include the extraction of presence of straight lines, parabolas, peaks, sinusoidal, triangular or rectangular patterns.

Limitations of using statistical features for classifications include the difficulty of extracting structural patterns or sub-patterns from the data using only quantitative features, while the limitation of using structural features for classification include the difficulty of implementing the feature extraction in general, in the absence of specific domain knowledge.

Below we give some selected examples from both approaches using both types of features to achieve classification of time series data.

Use of Statistical Features for Time Series Classification

Nurmi and Floréen [86] propose a method to selecting features in time series data that is generated in adaptive, context-aware systems. Data available in these contexts include time series data from a user's GPS, cellular phone, car accelerometer reading. Other sensors may measure physical characteristics of the user context, and the potential for data generation is enormous. Therefore, the authors devise a scheme involving feature selection in time series in order to reduce communications and computational costs. The features used are statistical measurements of the time series and include the mean, variance, auto-correlation and absolute magnitude and they various subsets of them are selected for transmission at different times, t_i, based on their relevance to the user activity.

Mierswa [74, 75] describes a methodology that extracts and uses a set of statistical features from audio data. Statistical features extracted include the average loudness, average distance and variance between extreme values, tempo and variance of the auto-correlation, k highest peaks after a Fourier transfomration and so on. The

features are used to identify the genre of a set of users' music files, in order to make automatic music recommendations to users of "Internet" music players (e.g., Itunes, Musicmatch).

Use of Structural Features for Time Series Classification

We present an example of structural pattern recognition [87] in time series that comes from the medical domain, specifically electrocardiogram diagnosis. Each time series records the electrical activity recording during a patient' heartbeat by a single electrode. The electrocardiogram of a healthy patient looks similarly to the time series from Figure 6.2(a) while the electrocardiogram of a patient who may suffer from a cardiac condition called myocardial infarction resembles the time series from Figure 6.2(b). The structural features present in the time series (e.g., peaks and valleys) have been encoded using symbols and a grammar, which helps identify automatically the expected versus the unexpected cardiac condition.

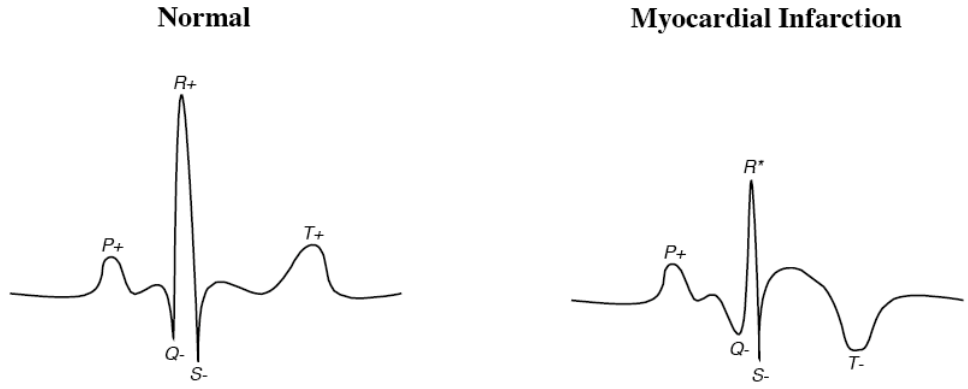

(a) Normal Electrocardiogram: Parse string: P+ Q- R+ S- T+.

(b) Abnormal Electrocardiogram: Parse string: P+ Q- R* S- T-.

Figure 6.2: Examples of time series from a cardiogram of a healthy patient (a) and a patient suffering from an unhealthy condition (b). Structural features are encoded in a parse string representing peaks (+) or valleys(-) in the data and a specific grammar describing the expectation of a specific symbol with respect to time. From [87].

Xie and Yan [51] recently proposed a structural (or qualitative) feature extraction

method for time series data from the financial domain. The authors use the domain knowledge from the financial field with respect to analyzing stock prices: that is, they try to identify shapes of the price patterns, in particular they identify *convex* or *concave* features in the time series data. These qualitative features are independent of the actual numerical values of the time series. Identifying these features in time series data can guide the decision on when to buy or sell various stocks in order to maximize profit.

Other Approaches for Dimensionality Reduction in Time Series

Within the context of very large time series, there are an abundance of techniques that have explored methods for time series clustering and compression based on feature extraction and representation; a notable recent technique is SAX [64]. We believe there are vast amount of opportunities for using techniques developed in the space of time series clustering and compression together with multi-dimensional data visualization designed for user-centric performance analysis approaches.

Our Approach

Methodologies and applications for feature selection and extraction in time series abound in many domains. Within our framework, we employ structural feature extraction from time series data. The structural features of interest, (e.g., pattern in the time series data: random, flat, periodic, ramp) are based on specific knowledge of characteristics of large-scale scientific applications. Furthermore, we also extract a "qualitative feature" from the time series data, which is the relative variance of a metric given a scientific application's execution in a given computational environment. The choice of a structural feature selection versus the more common statistical feature selection was guided by the hypothesis that we could extract information from performance time series data that could be used to compare and understand the behavior of scientific applications across different computational systems. Notice that

the structural/qualitative features provide independence on the actual numeric value of a time series, suggesting the possibility of multi-environment behavioral comparison.

6.1.3 Application and System Signatures

Our work analyzes time series data and strives to extract a compressed representation or *signature* that may help in problem diagnosis and remediation. There are many existing techniques which have been developed that analyze data and extract a signature from it for the purpose of problem identification (e.g., intrusion detection, system health, application performance, to name a few). In essence, application and system signature approaches are another form of dimensionality reduction in data, calibrated to specific domain knowledge. Below, we highlight some of these approaches.

Jain [49] describes examples of *visual signatures* of performance problems, displayed with the help of Kiviat graphs. Kiviat graphs of different systems or of the same system at different times allow the system administrator to detect resource bottlenecks and imbalances. These simple visual performance signatures represent an early approach of qualitatively describing a good (i.e., graph has star-like appearance as shown in Figure 6.3(a)) versus a bad (i.e., graph looks more like a polygon than a star Figures 6.3(b) and 6.3(c)) system state.

Lu and Reed [66] describe *compact application signatures* for parallel and distributed scientific codes, an approach that summarizes using poly-lines, as shown in Figure 6.4, the time-varying resource needs of applications from historical trace-data. Applications of interest are instrumented to collect event traces as well as to insert markers that aid in comparing signatures across executions and platforms. Application signatures are used in combination with performance contracts [109] to validate execution performance.

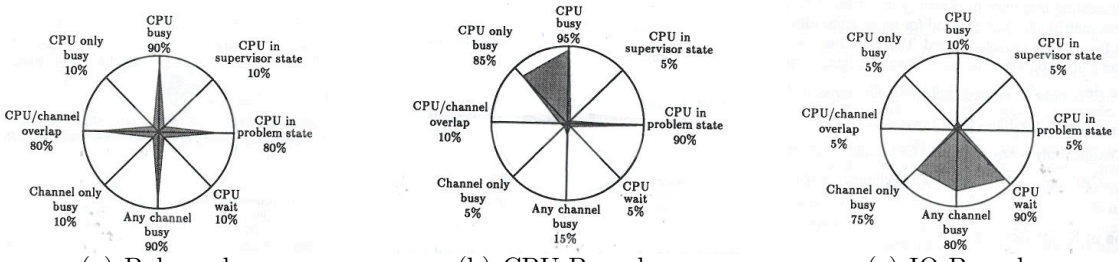

(a) Balanced. (b) CPU-Bound. (c) IO-Bound.

Figure 6.3: Examples of Kiviat graphs for visually detecting performance issues in a system. Kiviat graphs having a star-shape as in a) are ideal cases.

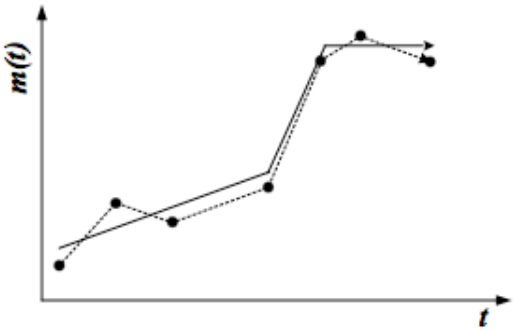

Figure 6.4: Example of a performance time series metric (dashed line) and its compressed, poly-line representation (solid line), from [66].

Mirgorodskiy et al [77] describe an approach for locating causes of certain types of abnormalities in distributed applications that contain multiple identical processes executing similar activities. They instrument the application and use function-level traces to capture behavioral information of the processes during execution. The core of the approach is using time profiles for each process for possible problem identification. A time profile p for a given host h where a process executes is defined as a vector of length F, where F represents the total number of functions in the application. The time profile, $p(h)$ simply counts the cumulative amount of time spent in each of the process' functions $f_1, \cdots, f_i, \cdots, f_F$ and could be easily thought of as a *compact representation* or *signature* of the performance data collected. Because

the processes are assumed to be doing the same activities, each process should have about similar time profiles for each f_i. If one of the process deviates from the time profiles of all its peers, the approach signals the process as problematic. Figure 6.5 illustrates the time profile approach.

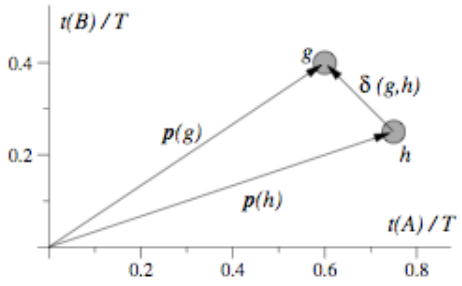

Figure 6.5: Example of two simple time profiles of identical processes that have only two functions, A and B. The time profile for $g = (0.6, 0.4)$ while for $h = (0.8, 0.2)$. Processes experiencing performance problems tend to have dissimilar time profiles. From [77].

Jones and Li [52] build temporal signatures of application to perform intrusion detection. A temporal signature in this context is defined as a system-call sequence augmented with time-stamp of the system-call. Figure 6.6 shows two temporal signatures of system-calls where one signature is flagged as a potential security risk due to the large delay between certain system-calls. Possible intrusions are simply detected by comparing the signature of the intrusion with an *expected* temporal signature of a normal application.

A: C1---------C2----------C3------C4
B: C1---------C2--------------------------------C3--
----------C5

Figure 6.6: Example of two temporal signatures of system-calls used for intrusion detection; signature B is anomalous. From [52].

Cohen et al. [21] propose the use of Tree-Augmented Bayesian Networks (TAN) to identify combinations of system-level metrics and threshold values that correlate with

high-level performance states in a three-tier Web service. TAN models are further used for offline forensic diagnosis and in limited settings for performance forecasting. More recent work by Cohen et al. [22] presents a method for automatically extracting an indexable signature that distills the essential characteristics from a system state. The technique clusters system states corresponding to similar problems, allowing diagnosticians to identify recurring problems and to characterize the core features of a group of problems.

6.2 Learning Techniques for Problem Diagnosis

There exist two fundamental approaches by which one can learn from performance data cases of expected or unexpected behavior. One approach, called supervised learning (or classification), relies on an expert to provide samples of behaviors that correspond to healthy and unhealthy performance states. The other approach, called unsupervised learning (or clustering), attempts to discover groups of data that correlate with performance states. While there are a large number of works employing such techniques, we only present a few examples to illustrate the techniques as applied to performance data.

6.2.1 Classification Techniques

A component of our framework includes a supervised-learner (or classifier) that trains to distinguish good versus bad performance cases. In an on-line-setting, it helps to distinguish possible problem states affecting application performance.

Classification techniques used for a wide range of data abound in literature [32, 47]. Methods include k-nearest-neighbor search, neural networks classifiers, fuzzy classifiers, Bayesian classifiers, or support vector machines. The current work uses a classifier based on the k-nearest-neighbor algorithm. In the next section, we will describe some approaches that use classification to help with problem diagnosis in

distributed systems and applications.

Yuan et al [117] describe a technique based on supervised learning to identify reproducible failures from system call traces of applications. Similarly to the approach we take in our framework, the label of the trace determines the type of observed problem and in the case described the root cause of the problem.

6.2.2 Clustering Techniques

In [77], the authors use dynamic instrumentation to collect control-flow traces of each process in a distributed application that contains multiple identical processes performing similar activities. Because the processes are assumed to behave similarly by having the same control-flow, problems such as fail-stop[2] are detected by identifying processes that stopped earlier than the rest, while non-fail-stop problems are detected using outlier detection techniques to identify processes that behave differently from the rest.

Roth and Miller [98] introduce a scalable performance diagnosis approach for finding performance problems in applications with a large number of processes. The approach employs two techniques: (1) a well-established technique for methodically examining the solution space and (2) a Sub-Graph Folding Algorithm for bottleneck search, that dynamically clusters application processes based on their qualitative behavior.

6.3 Context: Performance Analysis of Scientific Workflows

The fundamental metric that defines performance in the case of workflow applications is the total time to execute the entire instance of a workflow, $T_{workflow}$. This time depends on several factors, including (1) the amount of resources allocated to it,

[2]A problem in which some processes stop earlier than the rest.

(2) the type of computational resources assigned (e.g., CPU speed, memory size, disk and network resources), and (3) characteristics of the workflow/application executing on these resources.

Because of these factors, researchers have employed a variety of techniques to improve the overall execution time, including mechanisms that optimize the amount and types of resources available to the workflow before and during execution as well as methodologies to understand characteristics of the specific application and optimize for those specific characteristics (e.g., load imbalance, communication, external load, etc). Moreover, very recent approaches have looked at building the infrastructure and required tools to provide performance monitoring data, analysis and visualization for scientific workflows at multiple levels of abstraction, ranging task-level monitoring to global workflow level monitoring.

In the following section, we present an overview of some of these key approaches. We then present our framework within this larger context and discuss similarities, differences and interactions between our framework and these related approaches.

6.3.1 Performance Monitoring

There are many distributed performance monitoring tools available for Grids; a detailed categorization and comparison of the tools is done in [41]. Our focus is to be aware of performance monitoring tools that have been made available to support performance monitoring of scientific workflows, as this data can be used as input by our framework.

SCALEA-G [108] is one of the few unified monitoring and performance analysis for Grid applications. The framework offers support for both source code and dynamic instrumentation for profiling and monitoring events of Grid applications. The performance monitoring data is used by methodologies for performance analysis and

visualization for scientific workflows. Some of these approaches are detailed later, in Section 6.3.4. Another performance monitoring framework is MonALISA [62], which is a widely used distributed service for collecting and processing monitoring information for Grids and distributed applications. The monitoring information gathered can be used by higher-level services to provide decision support, in order to maintain and optimize workflow through the Grid.

Another widely used performance data monitoring for clusters and Grids is Ganglia [69]. Ganglia utilizes a hierarchical design to gather data from federations of clusters. It employs the use of commonly used technologies for data representation (XML), data compaction and transport (XDR), and for storage and visualization (RRDtool). It utilizes carefully designed data structures and algorithms to have a low overhead at both the individual node resource level and for groups of resources. Ganglia is currently used on thousands of clusters around the world [1].

Our methodology can easily integrate with any Grid application performance monitoring system and provide a qualitative performance analysis service to the Grid application users.

6.3.2 Workflow Optimizations

Because there are many different levels at which a scientific workflow's execution time can be improved, we present a brief overview of related work studying efficient resource selection and mapping, scheduling strategies, methods to detect loss of parallelism in workflows, optimizations for data transfers, as well as comprehensive methods attempting to optimize workflow performance by optimizing at multiple levels at once.

Resource Mapping and Workflow Refinements

Resource mapping refers to finding a best set of available resources that match an application's needs. A number of frameworks have been developed to address these issues for scientific workflows. They include Pegasus [25], the Virtual Grids Execution System (VGES) [57] - which exposes techniques for resource allocation and execution, and flexible resource selection via qualitative description of resources [20, 48], GridARM [102] - which negotiates, reserves and allocates best available resources.

Another related technique helping the effort of appropriate resource mapping refers to the concept of *workflow refinements*, where a workflow is analyzed, before resource mapping and allocation, to determine whether some of the workflow components do not require computing resources, as they may already been computed. Such an technique is used by Pegasus within Montage - an astronomical workflow application for computing sky mosaics. In Montage's case, existing data catalog information is used to discover whether intermediate sky mosaics have previously been computed.

Workflow Scheduling

Workflow scheduling refers to the act of scheduling the set of a workflow's task on the set of mapped resources. The workflow scheduling engine typically maps a workflow instance to actual Grid resources. A workflow scheduler typically implements a variety of Directed Acyclic Graphs (DAGs)-based scheduling heuristics which can have varying levels of accuracy and different optimization goals. Scheduling algorithms take as input information about predictions of execution times for every workflow task or activity[3], as well as predictions about the availability and quality of resources to be used (i.e., predicted bandwidth on each data link in a workflow)

[3]From this point forward, we will refer interchangeably to workflow *task* and *activity*.

and output a static schedule.

Given the uncertainty and varied availability of resources on Grids, allowing a workflow execution system to respond to changes in the execution environment can significantly improve the overall performance of a workflow. Below are some techniques based on specifying and monitoring performance or execution contracts of workflow tasks.

Threshold-based approaches supporting adaptive scheduling

In [93], the authors specify and monitor a fixed set of performance metrics for each workflow task. The metrics include: (1) structural assumptions within a workflow (e.g., such as dynamic expansion of the workflow, due to the need to compute more calculations on-demand), (2) external load on processors, (3) processors no longer available, (4) low-bandwidth, high-latency networks and (5) new Grid sites available. When any of these metrics are above or below a specified threshold and violate initially specified contracts, a rescheduling event is triggered that makes the scheduler to re-evaluate current workflow and execution environment conditions and output a new schedule.

Similarly to the above, the authors in [96] describe performance contracts [109, 9], and real-time adaptive control, two possible mechanisms to realize soft performance guarantees for Grid applications. Performance contracts formalize the relationship between application performance needs and resource capabilities. Contract monitors use performance data to verify quantitatively (i.e., using performance metric thresholds) if expectations are met. If contract specifications are not met, the system adapts the application accordingly.

More recently, the authors of the K-WfGrid and DIPAS projects [106, 107] study how performance problems in Grid workflows can be determined by examining the value of thresholds specified for a set of workflow performance metrics of interest to

the user. A performance problem occurs when the value of the metric is greater than the threshold. For example, they define a set of workflow performance metrics that track various overheads for workflows [84], such as those resulting from scheduling or resource management overhead or data transfers. The authors define a global workflow performance metric called *performance severity* that indicates the importance of a performance overhead to the total execution time of the workflow, $T_{workflow}$. When the performance severity passes a predefined threshold, an alarm is triggered and the user or some workflow service can provide a specific solution to reducing or eliminating the source of the overhead.

Fault-tolerance and Recovery

In [54], the authors propose a Fault-Tolerance and Recovery (FTR) service which uses information from application performance models, resource availability models, network latency and bandwidth, and queue wait times for batch queues on compute storage to determine whether application over-provisioning or migration is the better strategy to reduce individual workflow task failure rates. Their results show that such recovery mechanisms can help improve the overall failure rate of a meteorological-based large-scale workflow, LEAD [29] considerably (e.g., from 79.39% to 23.03%).

6.3.3 Comprehensive Workflow Performance Analysis

In [84] and more recently in [94], the authors propose an overhead analysis model for scientific workflows executing on Grids. The total execution time of a workflow, $T_{workflow}$ is defined as the sum of a theoretical *ideal* time, T_{ideal}, and a set of temporal overheads originating from various sources, $T_{overheads}$. In this setting, the analysis efforts focus on describing, classifying and measuring sources of overheads in a systematic manner in order to minimize the overhead time. Scientific workflow overheads are classified into four main types: middleware (e.g., impact of resource

brokerage, scheduling algorithms, performance prediction, security, service latency), loss of parallelism (e.g., load imbalance, serialization, replicated job), data transfer (e.g., file staging, database access, input from user) and workflow task/activity (e.g., parallel overheads or external load). Their experimental analysis for one workflow scientific workflow application, WIEN2K [13], results in five major types of overheads due to: (1) serialization due to a limited Grid size, (2) loss of parallelism due to load imbalance of the application, (3) job preparation overhead for compression and decompression of a large amount of files, (4) data transfer overhead and (5) external load overhead depending on the number of Grid sites used by the workflow and also depending on the nature of the SMP architecture that executes workflow tasks or activities concurrently. The overhead on this specific architecture stems from remote memory accesses and contention on the shared memory bus, parallel process management and cache coherency protocols. If compute clusters are used, the external load overhead for their specific application is insignificant because of dedicated access to individual compute nodes within a cluster.

6.3.4 Performance Analysis and Visualization

SCALEA-G [108] is a recent effort towards a unified monitoring and performance analysis for Grid applications. The framework exposes data within a workflow environment from multiple levels, including (a) monitoring of events from Grid applications, (b) profile data from both source code and dynamic instrumentation, and (c) from Grid infrastructure monitoring tools such as Ganglia [69], the Network Weather Service (NWS) [115], or Monitoring and Discovery Services (MDS) [24]. The authors in [17] use the foundation provided by SCALEA-G and provide the scientific workflow user with the ability to monitor different kinds of data about their workflow and to inspect graphs that visualize metrics of interest, such as status of various workflow events (e.g., activity has been initialized, queued, failed), data transfer rates between

Grid sites, analysis and comparison of activity distribution for Grid sites as well as querying of infrastructure monitoring information during execution (e.g., what is the CPU load on host A at a specified Grid site).

Another similar project aimed at expanding the number of performance monitoring and analysis tools for scientific workflows is the K-WfGrid project, [106]. It exposes the monitoring and analysis of workflows and the corresponding computational infrastructure through a Web portal. The difference from [17] appears to be the introduction of XML-based representations for describing application structures and specifying instrumentation requests, to ease the interaction between the many services and clients involved in providing monitoring data and analysis services.

6.3.5 Discussion

In our research, we assume that the workflow application has already been mapped and scheduled on the best computational resources available. Furthermore, we do not address the issue of distributed performance monitoring for a scientific workflow, as our framework strictly analyzes easily available time series data correlated with workflow or task performance. For example, our approach can use data provided at the workflow level by an integrated Grid performance monitoring tool such as SCALEA-G [108] or that in the related K-WfGrid project [106], and transform it to a compact representation so as to learn essential characteristics of data that correlate well with workflow performance states. Performance monitoring and visualization tools such as those in [17] are very valuable since they enhance the support provided to a scientific user to understand the performance of a workflow. However, they do rely on the user to "analyze" the data charts, plots and other visual information. This analysis process may be reasonable for a user with prior experience to performance analysis tools and for inspection of moderate amounts of data and plots. However, when the workflow scales to thousands of nodes, and the amounts of data monitored is

very large, even experienced performance analysts will have difficulties understanding the performance of the analyzed workflow. Our approach represents a small-step towards a self-assessing and self-diagnosing performance framework, where we rely a user's notion of a successful and well-performing workflow or activity execution to learn patterns in the performance data associated with these qualitative performance states.

The qualitative performance analysis framework we propose in this thesis is intended to help minimize the total workflow execution time, $T_{workflow}$, by analyzing, during execution, performance data characteristics of the longest-running workflow tasks, and offering qualitative and intuitive interpretations of performance to both the scientific application user and a fault-tolerance and recovery service, such as [54], which can use the information to trigger recovery/scheduling events based on specific policies.

Comprehensive Workflow Performance Analysis

Using the overhead terminology introduced by [84], this thesis concentrates on understanding the overhead involved only in long-running activities (or tasks) within a scientific workflow, the reasoning being that since long-running components constitute a significant time of the total running time, optimizing this subset of tasks will result in the optimization of the overall execution time of a workflow, $T_{workflow}$. Our framework can analyze activities that are either individual programs or parallel programs; we only require a labeling of whether the long-running activity was successful, as well as performance monitoring data of interest collected from where each studied activity executes.

Threshold-based Approaches

Threshold-based approaches such as those in [93, 96, 106], are definitely useful to a user who knows (1) the key metrics to monitor, and (2) the best value of the threshold

that would capture the most important performance problems without triggering false alarms. The major weakness of threshold-based approaches that rely on static, non-adaptive thresholds is the assumption that these meaningful threshold values are known in advance. This is seldomly true in practice. Furthermore, in a complex and dynamic environment such as a Grid on which different scientific workflows with varied characteristics execute, finding meaningful performance metric thresholds for a scientific workflow is extremely difficult.

While there are no formal service-level agreements (SLA) for scientific workflows as in the commercial Grid domain (though specific threshold methods could be considered in essence, SLAs for workflows), we attempt to define the concept of an SLA in terms of the qualitative notion of performance as understood by the scientific user. Our approach will integrate well with self-healing, fault-tolerance and recovery approaches for scientific workflow tasks as described in [54], because in the cases of long-running workflow tasks, the FTR framework does not need to wait for the task to fail in order to initiate a remedy action. The qualitative performance output of our framework can notify FTR of persistent performance problems/degradations affecting long-running activities and various policies for triggering an FTR action can be implemented, depending on each tasks's effect on the global workflow performance.

Problem Diagnosis in Large-Scale Distributed Environments

Because of the assumption of process similarity, the methodology in [77] does not require learning a database of reference data to distinguish good versus anomalous behaviors. On the contrary, our approach relies on a supervised learning technique to identify in a training phase well-performing versus poor-performing application states. The performance data we collect is also different in two ways: (1) it does not come from sources involving application instrumentation (static or dynamic), and (2) it is collected at much coarser time scales then instrumentation traces. As a result,

the types of diagnostic problems we are able to detect are dependent on whether the specific problem will manifest itself persistently over a longer period of time within the data we analyze.

6.4 Summary

We described in this chapter selected works spanning three main domains: time series analysis and dimensionality reduction, supervised learning for problem diagnosis and qualitative reasoning. We have discussed how our proposed framework compares and contrasts with these selected works.

The performance analysis framework we propose in this thesis is different from existing approaches supporting the performance scientific workflows in several ways:

1. We focus only on the performance of long-running tasks within a scientific workflow,

2. We analyze and extract information only from performance time series data and not qualitative variables such as those describing the execution status of a task (e.g., running, started, failed),

3. We do not currently analyze data that require instrumentation of application code,

4. We target the scientific workflow user who does not have the experience of using traditional performance analysis tools for the science applications,

5. We show how to correlate qualitative behavioral task states to performance time series metrics and how to use it for problem diagnosis and remediation.

While similar methodologies at the intersection of machine learning, statistical induction, and systems [44] have been previously applied in different domains [21, 22,

15], we believe, to the best of our knowledge, this to be a first work looking at a user-centric, qualitative performance evaluation and failure detection by automatically deriving correlations from the data in the context of scientific workflows executing in Grid environments.

Chapter 7

Conclusion and Future Directions

This thesis presented a general *qualitative performance analysis* framework that incorporated (a) techniques from time series analysis and machine learning to extract and learn from data, features of interest associated with application performance in order to reach a qualitative interpretation of the application's behavior, and (b) mechanisms and policies to reason over time and across the distributed resource space about the qualitative behavior of the application.

7.1 Conclusions

Our empirical evaluation with two real Grid applications from meteorology and astronomy on diverse physical computing resources showed support for our two stated hypotheses: (1) for the class of long-running scientific applications it is necessary to analyze temporal information present in performance data, and (2) that variance and pattern as specific instances of such information are sufficient for accurate performance validation and diagnosis.

The proposed framework's ability to generate a qualitative assessment of performance behavior for scientific applications using temporal information present in performance time series data represents a step towards simplifying and improving the quality of service for Grid applications.

7.2 Future Directions

We look forward to future research that will strive to achieve a comprehensive qualitative performance analysis of scientific workflows, by transforming information found in performance metrics into meaningful, qualitative information useful to both

a workflow user and a performance analyst/or performance analysis service.

Additionally, it would be very interesting to test the efficacy of our approach given variations on the techniques we proposed, as shown in the x-axis, and variations on context, as described in the z-axis of Figure 7.1.

Below we discuss four potential directions for improvement specific to our context: scientific workflow applications executing in distributed Grid environments.

7.2.1 Variable and Feature Selection for Performance Data

In this thesis we have chosen a set of variables (e.g., system-level time series data), and a set of features of the variables (e.g., relative variance and pattern) to build temporal signatures of applications for performance validation and diagnosis. Our choices were guided by specific domain knowledge of scientific applications. However, many performance time series variables can be collected and used for analysis. For this purpose, the analyst may want to consider existing techniques for automatic variable and feature selection in order to build a good predictor of application performance. Guyon et al [46] present a good overview of available techniques, which include *independent variable* ranking based on correlation criteria or information theoretic criteria, *variable subset* selection based on wrappers and embedded methods or filters, and *feature selection* methods employing clustering or matrix factorization techniques. More specifically to feature extraction in time series data, the work of Olszewski [87] presents a good overview of existing statistical and structural feature extraction techniques for time series; the author also proposes a generalized approach for automatic structural feature extraction, which would be especially useful in domains where one may not know *a priori* features of interest to investigate.

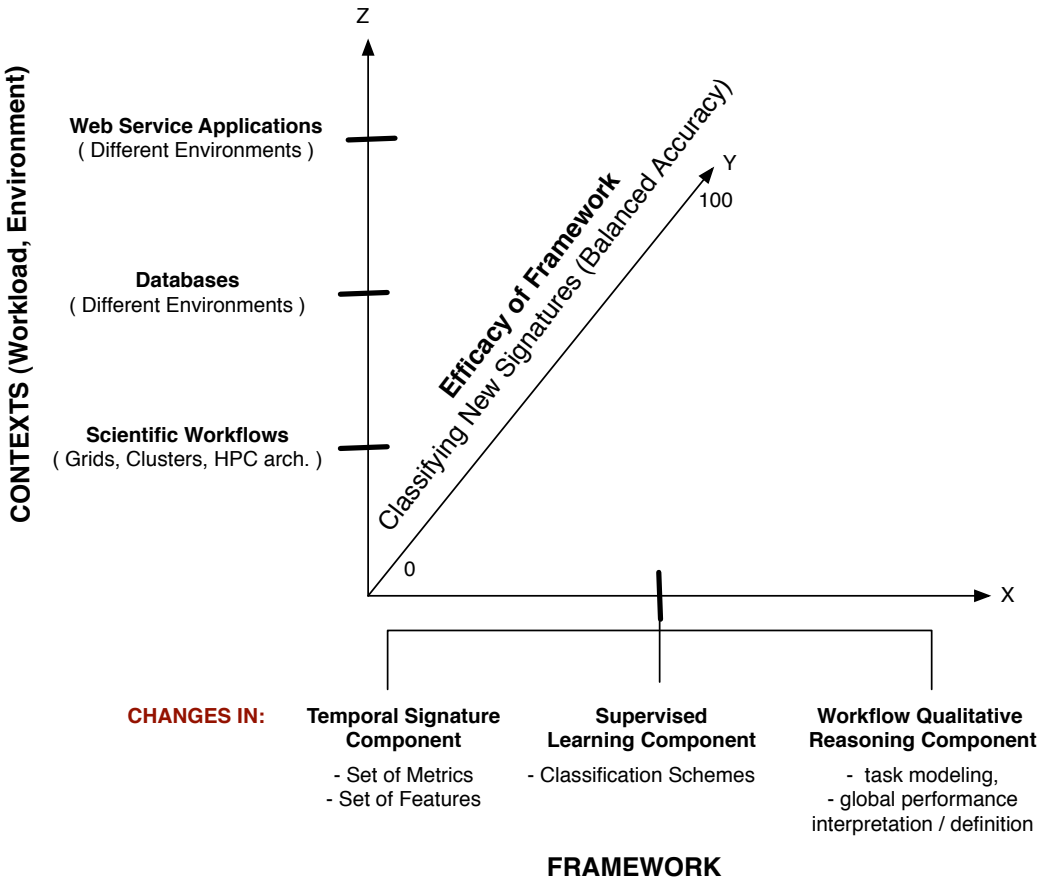

Figure 7.1: Other contexts where `Teresa` may be applied. Variations within both framework techniques and definitions, as well as the context of applicability can be explored.

7.2.2 Learning Techniques

Our framework relies on previously labeled samples of performance data to make the distinction between good and degraded application behaviors. Therefore, we employ the use of classifiers to assess performance in an on-line setting. Depending on the definition and size of a temporal signature, different classifiers may yield better accuracy rates; exploring the impact of various classifiers on the framework with various signature definitions may be further investigated.

A practical disadvantage of employing a supervised learning technique (i.e., classification) is that it relies on the availability of a "good" training set of data and

signatures for classification. In the absence of training data, the alternative is to use unsupervised learning techniques (i.e., clustering) that may automatically discover groups of behaviors, which over time, can be associated with various qualitative behavioral descriptions for a given application.

7.2.3 Reasoning with Qualitative Information

In this framework, we have only presented a couple of simple examples of how one can implement global workflow policies based on the performance states of a workflow's long-running tasks to reason about workflow behavior over time, and to trigger an adaptive re-scheduling if needed. We have assumed that each task within a workflow has the same utility to the user; this however can be expanded in order to reflect alternate scenarios.

Towards a Comprehensive Qualitative Performance Analysis for Workflows

We presented a prototype framework that uses easy-to-collect, non-instrumented performance time series, and makes a qualitative assertion about the performance of the long-running tasks in a workflow. It would be ideal to extend our current framework so that other qualitative information can be extracted from performance data correlated with factors causing different types of workflow performance overheads as described in [84], such as middle-ware, loss of parallelism, or data transfer.

7.2.4 Problem Diagnosis: Correlation and Causation

In diagnosis problems across science and engineering domains, it is important to achieve two goals:

1. distinguish between normal and abnormal data within the target domain, and
2. identify the cause of the abnormal/ symptomatic data observation (and possibly

the chain of events from cause to symptom).

As applied to the domain of computing systems, the first goal is called problem *diagnosis* or *identification*, while the second goal is called *root cause analysis*. The task of root cause analysis is in general more difficult than problem identification because, in essence, reverse-engineering the system that produced the diagnosis symptom data is more challenging than observing expected and symptomatic states and building a predictor. The crux of the problem lies in the distinction between *correlation* and *causation*.

The performance time series data analyzed in this work allows our framework to observe correlations between temporal features in time series data and symptoms of performance for long-running scientific applications. Our work could be expanded by addressing the challenging root-cause problem and incorporating techniques from the causality inference literature [90].

Appendix A

Upper Bound Calculation for Sample Variance

Given a time series $Z = z_1, \cdots, z_t, \cdots, z_N$ sampled at a fixed interval of time, h, we define the sample mean, m as:

$$m = \frac{1}{N}\sum_{t=1}^{N} z_t \tag{A.1}$$

and the sample variance, s^2 as:

$$s^2 = \frac{1}{N}\sum_{t=1}^{N}(z_t - m)^2. \tag{A.2}$$

If the time series Z is bounded, that is $z_t \in [z_{min}, z_{max}]$, so is its mean, m:

$$z_{min} \leqslant m \leqslant z_{max} \tag{A.3}$$

$$-z_{min} \geqslant -m \geqslant -z_{max} \tag{A.4}$$

$$-z_{max} \leqslant -m \leqslant -z_{min}, \tag{A.5}$$

but,

$$z_{min} \leqslant z_t \leqslant z_{max}. \tag{A.6}$$

We add (A.5) and (A.6):

$$\begin{aligned} z_{min} - z_{max} &\leqslant (z_t - m) \leqslant z_{max} - z_{min} \\ -(z_{max} - z_{min}) &\leqslant (z_t - m) \leqslant z_{max} - z_{min} \\ |z_t - m| &\leqslant (z_{max} - z_{min}) \\ (z_t - m)^2 &\leqslant (z_{max} - z_{min})^2 \\ s^2 = \frac{1}{N}\sum_{t=1}^{N}(z_t - m)^2 &\leqslant \frac{1}{N} \cdot N(z_{max} - z_{min})^2. \end{aligned}$$

Therefore, the sample variance will also be bounded:

$$s^2 \leqslant (z_{max} - z_{min})^2. \tag{A.7}$$

Bibliography

[1] Ganglia Web Site. http://www.ganglia.info, 2008.

[2] The Two Micron All Sky Survey. http://www.ipac.caltech.edu/2mass/, 2006.

[3] M. Adya, F. Collopy, J. S. Armstrong, and M. Kennedy. Automatic Identification of Time Series Features for Rule-Based Forecasting. *International Journal of Forecasting*, 17:143–157, 2001.

[4] M. Ahdesmaki, H. Lahdesmaki, R. Pearson, H. Huttunen, and O. Yli-Harja. Robust Detection of Periodic Time Series Measured from Biological Systems. *BMC Bioinformatics*, 6(117), 2005.

[5] The Amazon Elastic Compute Cloud (EC2). http://www.amazon.com/b/?node=201590011, 2008.

[6] Amazon Simple Storage Service (Amazon S3). http://www.amazon.com/gp/browse.html?node=16427261, 2008.

[7] D. Anderson and J. Chase. Fstress User Manual. http://www.cs.duke.edu/ari/fstress/, 2002.

[8] R. L. Anderson. Distribution of the Serial Correlation Coefficients. *Annals of Mathematical Statistics*, 8(1):1–13, 1941.

[9] R. Aydt, C. Mendes, D. A. Reed, and F. Vraalsen. Specifying and Monitoring GRaDS Contracts. Technical report, University of Illinois at Urbana-Champaign, July 2001.

[10] S. Baker. Google and the Wisdom of Clouds: A Lofty New Strategy Aims to Put Incredible Computing Power in the Hands of Many. http://www.businessweek.com/magazine/content/07_52/b4064048925836.htm?chan=magazine+channel_top+stories, December 13th 2007.

[11] F. Berman and T. Hey. The Scientific Imperative. In *The Grid 2: Blueprint for a New Computing Infrasctructure*, pages 13–24. Morgan Kaufmann, 2004.

[12] B. G. Berriman, E. Deelman, J. C. Good, J. Jacob, D. Katz, C. Kesselman, A. C. Laity, T. Prince, G. Singh, and M.-H. Su. Montage: A Grid Enabled Engine for Delivering Custom Science-Grade Mosaics on Demand. In *Proceedings of SPIE: Astronomical Telescopes and Instrumentation*, volume 5487, Glasgow, Scotland, 2004.

[13] P. Blaha, K. Schwarz, G. Madsen, D. Kvasnicka, and J. Luitz. Wien2k: An Augmented Plane Wave Plus Local Orbitals Program for Calculating Crystal Properties. Technical report, Institute of Physical and Theoretical Chemistry, Technische Universitat, 2001.

[14] G. Box and G. Jenkins. *Time Series Analysis: Forecasting and Control*. Holden-Day, 1970.

[15] D. Breitgand, E. Henis, and O. Shehory. Automated and Adaptive Threshold Setting: Enabling Technology for Autonomy and Self-Management. In *Second International Conference on Autonomic Computing (ICAC'05)*, 2005.

[16] K. Brewster. Application of a Bratseth Analysis Scheme Including Doppler Radar Data. In *Proceedings of the 15th Conference on Weather Analysis and Forecasting*, pages 92–95, 1996.

[17] P. Brunner, H.-L. Truong, and T. Fahringer. Performance Monitoring and Visualization of Grid Scientific Workflows in Askalon. In *High Performance Computing and Communications*, volume 4208, pages 170–179. Springer Berlin / Heidelberg, 2006.

[18] J. Brutlag. Aberrant Behavior Detection in Time Series for Network Monitoring. In *Lisa XIV*, New Orleans, LA, USA, 2000.

[19] K. Chen and L. Liu. Vista: Validating and Refining Clusters Via Visualization. *Information Visualization*, 3(4):257–70, 2004.

[20] A. Chien, H. Casanova, Y.-S. Kee, and R. Huang. The Virtual Grid Description Language: VgDL. Technical report, University of California San Diego, UCSD, 2005.

[21] I. Cohen, M. Goldszmidt, T. Kelly, J. Symons, and J. Chase. Correlating Instrumentation Data to System States: A Building Block for Automated Diagnosis and Control. In *Proceedings of the OSDI*, 2004.

[22] I. Cohen, S. Zhang, M. Goldszmidt, J. Symons, T. Kelly, and A. Fox. Capturing, Indexing, Clustering, and Retrieving System History. In *In Proceedings of SOSP*, Brighton, United Kingdom, 2005.

[23] P. E. Crandall, R. A. Aydt, A. A. Chien, and D. A. Reed. Input/Output Characteristics of Scalable Parallel Applications. In *Proceedings of the 1995 ACM/IEEE Supercomputing Conference*, volume 2, page 1643, San Diego, CA, USA, 1995. ACM.

[24] K. Czajkowski, S. Fitzgerald, I. Foster, and C. Kesselman. Grid Information Services for Distributed Resource Sharing. In *Proceedings of IEEE International Symposium on High Performance Distributed Computing*, page 181, San Francisco, CA, 2001. Institute of Electrical and Electronics Engineers Inc.

[25] E. Deelman, G. Singh, M.-H. Su, J. Blythe, Y. Gil, C. Kesselman, G. Mehta, and K. Vahi. Pegasus: A Framework for Mapping Complex Scientific Workflows onto Distributed Systems. *Scientific Programming*, 2005.

[26] S. G. Djorgovsky, R. R. Gal, S. C. Odewahn, R. R. de Carvalho, R. Brunner, G. Longo, and R. Scaramella. The Palomar Digital Sky Survey (DPOSS). `http://www.citebase.org/cgi-bin/citations?id=oai:arXiv.org:astro-ph/9809187`, 1998.

[27] J. Doyle and M. McGeachie. Exercising Qualitative Control in Autonomous Adaptive Survivable Systems. In *Self-Adaptive Software: Applications*, pages 1–6. 2003.

[28] K. Droegemeier. Linked Environments for Atmospheric Discovery. Technical report, University of Oklahoma, 1st July 2005.

[29] K. Droegemeier, D. Gannon, D. Reed, B. Plale, J. Alameda, T. Blatzer, K. Brewster, R. Clark, B. Domenico, S. Graves, E. Joseph, D. Murray, R. Ramachandran, M. Ramamurthy, L. Ramakrishnan, J. A. Rushing, D. Weber, R. Wilhelmson, A. Wilson, M. Xue, and S. Yalda. Service-Oriented Environments for Dynamically Interacting with Mesoscale Weather. *Computing in Science and Engineering*, 7(6):12–29, 2005.

[30] S. Duan and S. Babu. Processing Forecasting Queries. In *Proceedings of the 33rd international Conference on Very Large Data Bases (VLDB).*, Vienna, Austria, 2007.

[31] R. O. Duda, P. E. Hart, and D. G. Stork. Chapter 10: Unsupervised Learning and Clustering. In *Pattern Classification*, pages 568–573. John Wiley & Sons, 2001.

[32] R. O. Duda, P. E. Hart, and D. G. Stork. *Pattern Classification*. John Wiley & Sons, Inc, 2nd edition, 2001.

[33] L. Eeckhout, H. Vandierendonck, and K. De Bosschere. Quantifying the Impact of Input Data Sets on Program Behavior and Its Applications. *Journal of Instruction-Level Parallelism*, 5:1–33, 2003.

[34] M. Elfeky, W. Aref, and A. Elmagarmid. Periodicity Detection in Time Series Databases. *IEEE Transactions on Knowledge and Data Engineering*, 17(7), 2005.

[35] NIST/SEMaTECH E-Handbook of Statistical Methods. http://www.itl.nist.gov/div898/handbook/index.htm, 2003.

[36] B. S. Everitt and G. Dunn. Chapter 3: The Initial Examination of Multivariate Data. In *Applied Multivariate Data Analysis*. Edward Arnold; A division of Hodder & Stoughton, London, 1991.

[37] T. Fahringer, R. Prodan, R. Duan, J. Hofer, F. Nadeem, F. Nerieri, S. Podlipping, J. Qin, M. Siddiqui, H.-L. Truong, A. Villazon, and M. Wieczorek. ASKaLON: A Development and Grid Computing Environment for Scientific Workflows. In Ian J. Taylor, Ewa Deelman, Dennis B. Gannon, and Matthew Shields, editors, *Workflows for E-Science: Scientific Workflows for Grids*, pages 450–471. Springer-Verlag, 1st edition, 2006.

[38] I. Foster. What Is the Grid: A Three Point Checklist. *Grid Today*, 2002.

[39] I. Foster, C. Kesselman, and S. Tuecke. The Anatomy of the Grid: Enabling Scalable Virtual Organizations. *International Journal of High Performance Computing Applications*, 15(3):200, 2001.

[40] D. G. Galati and M. A. Simaan. Automatic Decomposition of Time Series into Step, Ramp, and Impulse Primitives. *Pattern Recognition*, 39:2166–2174, 2006.

[41] M. Gerndt, R. Wismuller, Z. Balaton, G. Gombas, P. Kacsuk, Z. Nemeth, N. Podhorszki, H. L. Truong, T. Fahringer, M. Bubak, E. Laure, and T. Margalef. Performance Tools for the Grid: State of the Art and Future, Apart White Paper. Technical report, Technische Universitaet Muenchen, 2004.

[42] T. Gneiting and A. E. Raftery. Athmospheric Science: Weather Forecasting with Ensemble Methods. *Science*, 310(5746):248–249, 2005.

[43] S. Godard. The Sysstat Utilities. http://perso.orange.fr/sebastien.godard/.

[44] M. Goldszmidt, I. Cohen, A. Fox, and S. Zhang. Three Research Challenges at the Intersection of Machine Learning, Statistical Induction, and Systems. In *10th conference on Hot Topics in Operating Systems*, volume 10, Santa Fe, NM, 2005.

[45] GridPP: UK Computing for Particle Physics. http://www.gridpp.ac.uk/, 2008.

[46] I. Guyon and A. Elisseeff. An Introduction to Variable and Feature Selection. *Journal of Machine Learning Research*, 3:1157–1182, 2003.

[47] T. Hastie, R. Tibshirani, and J. Friedman. *The Elements of Statistical Learning: Data Mining, Inference, and Prediction*. Springer, 2001.

[48] R. Huang, H. Casanova, and A. A. Chien. Using Virtual Grids to Simplify Application Scheduling. In *Proceedings of the 20th International Parallel and Distributed Processing Symposium*, Rhodes Island, Greece, 2006. IEEE.

[49] R. Jain. *The Art of Computer Systems Performance Analysis.* John Wiley and Sons, Inc, 1991.

[50] G. M. Jenkins and D. G. Watts. *Spectral Analysis and Its Applications.* Holden-Day, 1968.

[51] X. Jinfei and Y. Wei-Yong. A Qualitative Feature Extraction Method for Time Series Analysis. In Yan Wei-Yong, editor, *Control Conference, 2006. CCC 2006. Chinese*, pages 2220–2225, 2006.

[52] A. Jones and S. Li. Temporal Signatures for Intrusion Detection. In *17th Annual Computer Security Applications Conference*, New Orleans, Louisiana, 2001.

[53] M. V. Joshi. On Evaluating Performance of Classifiers for Rare Classes. In *IEEE International Conference on Data Mining*, pages 641–644, 2002.

[54] G. Kandaswamy, A. Mandal, and D. A. Reed. Fault Tolerance and Recovery of Scientific Workflows on Computational Grids. In *Workshop on Resiliency in High-Performance Computing in conjunction with CCGrid08*, 2008.

[55] E. Kandogan. Star Coordinates: A Multi-Dimensional Visualization Technique with Uniform Treatment of Dimensions. *IEEE Symposium on Information Visualization*, 2000.

[56] D. S. Katz, G. B. Berriman, E. Deelman, J. Good, C. Kesselman, A. C. Laity, T. A. Prince, G. Singh, and M.-H. Su. A Comparison of Two Methods for Building Astronomical Image Mosaics on a Grid. In *7th Workshop on High Performance Scientific and Engineering Computing (HPSEC-05)*, 2005.

[57] Y.-S. Kee, D. Nurmi, G. Singh, A. Mutz, C. Kesselman, and R. Wolski. VGES: The Next Generation of Virtualized Grid Resource Provisioning. In *1st IEEE/IFIP International Workshop on End-to-end Virtualization and Grid Management (EVGM 2007)*, 2007.

[58] A. Khan, T. Adye, C. A. J. Brew, F. Wilson, B. Bense, R. D. Cowles, D. A. Smith, D. Andreotti, C. Bozzi, E. Luppi, P. Veronesi, R. Barlow, M. P. Kelly, J. C. Werner, A. Forti, G. Grosdidier, E. Feltresi, A. Petzold, H. Lacker, and J. E. Sundermann. Grid Applications for High Energy Physics Experiments. In *The 6th IEEE/ACM International Workshop on Grid Computing*, page 4, 2005.

[59] B. Kuipers. Introduction to Qualitative Reasoning. In *Qualitative Reasoning: Modeling and Simulation with Incomplete Knowledge*, pages 1–16. The MIT Press, Cambridge, 1994.

[60] A. C. Laity, N. Anagnostou, B. G. Berriman, J. C. Good, J. Jacob, D. Katz, and T. Prince. Montage: An Astronomical Image Mosaic Service for the NVO. In *Astronomical Data Analysis Software and Systems XIV, ASP Conference Series*, volume XXX, 2005.

[61] The Lead Portal: Linked Environments for Atmospheric Discovery. `https://portal.leadproject.org/gridsphere/gridsphere`, 2007.

[62] I. C. Legrand, H. B. Newman, R. Voicu, C. Cirstoiu, C. Grigoras, M. Toarta, and C. Dobre. Monalisa: An Agent Based, Dynamic Service System to Monitor, Control and Optimize Grid Based Applications, September 2004.

[63] R. Levich and R. Rizzo. Alternative Tests for Time Series Dependence Based on Autocorrelation Coefficients. Technical report, Stern School of Business, New York University, 1998.

[64] J. Lin, E. Keogh, P. Patel, and S. Lonardi. Finding Motifs in Time Series. In *2nd Workshop on Temporal Data Mining*, Edmonton, Alberta, Canada, 2002.

[65] S. Lohr. Google and I.B.M. Join in Cloud Computing Research. `http://www.nytimes.com/2007/10/08/technology/08cloud.html`, 8th October 2007.

[66] C.-d. Lu and D. A. Reed. Compact Application Signatures for Parallel and Distributed Scientific Codes. In *Proceedings of Supercomputing*, 2002.

[67] S. Lu, Z. Li, F. Qin, L. Tan, P. Zhou, and Y. Zhou. Bugbench: Benchmarks for Evaluating Bug Detection Tools. In *PLDI Workshop on the Evaluation of Software Defect Detection Tools*, 2005.

[68] J. Markoff. Software Via the Internet: Microsoft in 'Cloud' Computing. `http://www.nytimes.com/2007/09/03/technology/03cloud.html`, 3rd September 2007.

[69] M. L. Massie, B. Chun, and D. Culler. The Ganglia Distributed Monitoring System: Design, Implementation, and Experience. *Parallel Computing*, 30(7), 2004.

[70] Matlab: Statistics Toolbox. `http://www.mathworks.com/products/statistics/demos.html?file=/products/demos/shipping/stats/mvplotdemo.html`, 2007.

[71] H. Meuer, E. Strohmaier, J. Dongara, and H. Simon. Top 500 Supercomputer Sites. `http://www.top500.org/stats/list/30/archtype`, 2007.

[72] J. Michalakes. Development of a Next-Generation Regional Weather Research and Forecast Model. In *Proceedings of the 9th ECMWF Workshop on the Use of Parallel Processors in Meteorology*, 2000.

[73] J. Michalakes, J. Dudhia, D. Gill, T. Henderson, J. Klemp, W. Skamarock, and W. Wang. The Weather Research and Forecast Model: Software Architecture and Performance. `http://wrf-model.org/wrfadmin/docs/ecmwf_2004.pdf`, 2004.

[74] I. Mierswa. Automatic Feature Extraction from Large Time Series. `http://citeseer.ist.psu.edu/736218.html`, 2004.

[75] I. Mierswa and K. Morik. Automatic Feature Extraction for Classifying Audio Data. *Machine Learning*, 58(2):127–149, 2005.

[76] E. L. Miller and R. H. Katz. Input/Output Behavior of Supercomputing Applications. In *Proceedings of the ACM/IEEE Conference on Supercomputing*, pages 567–576, Albuquerque, New Mexico, 1991.

[77] A. Mirgorodskiy, N. Maruyama, and B. P. Miller. Problem Diagnosis in Large-Scale Computing Environments. In *Proceedings of the 2006 ACM/IEEE conference on Supercomputing*, Tampa, FL, USA, 2006.

[78] High Energy Particle Physics Experiments Description. `http://www.griphyn.org/projinfo/physics/highenergy.php`, 2006.

[79] IBM Grid Computing. `http://www-1.ibm.com/grid/about_grid/index.shtml`, 2006.

[80] Integrated Data Radar Services. `https://www.radarservices.org/technical.php#Network`, 2006.

[81] The Montage Project: An Astronomical Image Mosaic Engine. `http://montage.ipac.caltech.edu/`, 2007.

[82] J. Moore. Gamut: Generic Application EMULaTOR. `http://issg.cs.duke.edu/cod/`, 2004.

[83] A. Natrajan, M. Crowley, N. Wilkins-Diehr, M. A. Humphrey, A. D. Fox, A. S. Grimshaw, and C. L. I. Brooks. Studying Protein Folding on the Grid: Experiences Using CHaRMM on NPaCI Resources under LEgion. In *10th IEEE International Symposium on High Performance Distributed Computing*, pages 14–21, 2001.

[84] F. Nerieri, R. Prodan, T. Fahringer, and H.-L. Truong. Overhead Analysis of Grid Workflow Applications. In *7th IEEE/ACM International Conference on Grid Computing*, pages 17–24, 2006.

[85] O. Nickolayev, P. C. Roth, and D. Reed. Real-Time Statistical Clustering for Event Trace Reduction. In *Proceedings of the Third Workshop on Environments and Tools for Parallel Scientific Computing*, Lyon, France, 1997.

[86] P. Nurmi and P. Floreen. Online Feature Selection for Contextual Time Series Data (Extended Abstract). In *Subspace, Latent Structure and Feature Selection techniques: Statistical and Optimisation perspectives Workshop*, 2005.

[87] R. T. Olszewski. *Generalized Feature Extraction for Structural Pattern Recognition in Time-Series Data*. PhD thesis, Carnegie Mellon Univeristy, 2001.

[88] Particle Physics Data Grid. `http://www.ppdg.net/`, 2008.

[89] B. K. Pasquale and G. C. Polyzos. A Static Analysis of I/O Characteristics of Scientific Applications in a Production Workload. In *Proceedings of the 1993 ACM/IEEE conference on Supercomputing*, pages 388–397, Portland, Oregon, United States, 1993.

[90] J. Pearl. *Causality: Models, Reasoning, and Inference* . Cambridge University Press, 2000.

[91] R. A. Pielke and R. Carbone. Weather Impacts, Forecasts, and Policy. *Bulletin of the American Meteorological Society*, 83:393–403, 2002.

[92] R. Plante and J. Annis. Relationship of Galaxy Morphology to the Intra-Cluster Medium: An NVO Demonsration. Technical report, US National Virtual Observatory, 2002.

[93] R. Prodan and T. Fahringer. Dynamic Scheduling of Scientific Workflow Applications on the Grid: A Case Study. In *20th Symposium of Applied Computing*, pages 687–694, Santa Fe, New Mexico, USA, 2005. ACM Press.

[94] R. Prodan and T. Fahringer. Overhead Analysis of Scientific Workflows in Grid Environments. *IEEE Transactions on Parallel and Distributed Systems*, 19(3):378–393, 2008.

[95] C. A. Ratanamahatana, E. Keogh, A. Bagnall, and S. Lonardi. A Novel Bit Level Time Series Representation with Implications for Similarity Search and Clustering. *Data Mining and Knowledge Discovery*, 2005.

[96] D. Reed and C. Mendes. Intelligent Monitoring for Adaptation in Grid Applications. *Proceedings of the IEEE*, 93(2), 2005.

[97] M. Reed and C. Quammen. Health Application Programming Interface (HaPI). `http://www.renci.org/software/hapi/`, 2005.

[98] P. C. Roth and B. P. Miller. On-Line Automated Performance Diagnosis on Thousands of Processes. In *Proceedings of 2006 ACM SIGPLAN Symposium on Principles and Practices of Parallel Programming*, New York, 2006.

[99] J. D. Salas, J. W. Delleur, V. Yevjevich, and W. L. Lane. *Applied Modeling of Hydrologic Time Series*. Water Resources Publications, 1980.

[100] M. Schneider. Improved Storm Forecast Capability Demonstrated. `http://www.teragrid.org/news/news05/0705.html`, July 2005.

[101] P. Shivam, S. Babu, and J. Chase. Active and Accelerated Learning of Cost Models for Optimizing Scientific Applications. In *Conference on Very Large Data Bases (VLDB)*, 2006.

[102] M. Siddiqui and T. Fahringer. GridaRM: Askalons Grid Resource Management System. In *Advances in Grid Computing - Egc 2005*, volume Volume 3470/2005 of *Lecture Notes in Computer Science*. Springer Berlin / Heidelberg, 2005.

[103] V. Taylor, W. Xingfu, and R. Stevens. Prophesy: An Infrastructure for Performance Analysis and Modeling of Parallel and Grid Applications. *Performance Evaluation Review*, 30(4):13, 2003.

[104] Terashake: Simulating a Big Shake in Southern California Basins. `http://www.teragrid.org/news/news05/terashake.html`, 2005.

[105] N. Tran and D. A. Reed. Automatic Arima Time Series Modeling for Adaptive I/O Prefetching. *IEEE Transactions on Parallel and Distributed Systems*, 15(4):362, 2004.

[106] H.-L. Truong, P. Brunner, T. Fahringer, F. Nerieri, R. Samborski, B. Balis, M. Bubak, and K. Rozkwitalski. K-Wfgrid Distributed Monitoring and Performance Analysis Services for Workflows in the Grid. In *e-Science and Grid Computing (e-Science '06)*, Amsterdam, The Netherlands, 2006.

[107] H.-L. Truong, P. Brunner, V. Nae, and T. Fahringer. Dipas: A Distributed Performance Analysis Service for Grid-Based Workflows. Technical report, Vienna University of Technology, June 2007.

[108] H. L. Truong and T. Fahringer. Scalea-G: A Unified Monitoring and Performance Analysis System for the Grid. In *Second European AcrossGrids Conference, AxGrids 2004*, volume 3165 of *Grid Computing. Second European AcrossGrids Conference, AxGrids 2004. Revised Papers (Lecture Notes in Computer Science)*, pages 202–211, Nicosia, Cyprus, 2004. Springer-Verlag.

[109] F. Vraalsen, R. A. Aydt, C. L. Mendes, and D. A. Reed. Performance Contracts: Predicting and Monitoring Grid Application Behavior. In *Grid Computing - GRID 2001: Proceedings of the 2nd International Workshop on Grid Computing*, 2001.

[110] F. Wang, Q. Xin, B. Hong, S. Brandt, E. Miller, D. Long, and T. McLarty. File System Workload Analysis for Large Scale Scientific Computing Applications. In *In Proceedings of the 21st IEEE / 12th NASA Goddard*, College Park, MD, 2004.

[111] W. Wang, D. Barker, C. Bruyre, J. Dudhia, D. Gill, and J. Michalakes. User's Guide for Weather Research and Forecast Modeling System Version 2.0. `http://www.mmm.ucar.edu/wrf/users/docs/user_guide/`, 2004.

[112] A. Ward, P. Glynn, and K. Richardson. Internet Service Performance Failure Detection. *ACM SIGMETRICS Performance Evaluation Review*, 26(3):38–43, 1998.

[113] When the Earth Shakes. `http://www.teragrid.org/news/sci-high07/shakes.html`, 2007.

[114] R. Williams. Grids and the Virtual Observatory. In Fran berman, Geoffrey Fox, and Tony Hey, editors, *Grid Computing: Making the Global Infrastructure a Reality*, Wiley Series in Communications Networking & Distributed Systems, pages 837–858. John Wiley & Sons, Ltd, 2003.

[115] R. Wolski, N. T. Spring, and J. Hayes. Network Weather Service: A Distributed Resource Performance Forecasting Service for Metacomputing. *Future Generation Computer Systems*, 15(5):757, 1999.

[116] WRF Benchmark Data. `http://box.mmm.ucar.edu/wrf/bench/`, 2004.

[117] C. Yuan, N. Lao, J.-R. Wen, J. Li, Z. Zhang, Y.-M. Wang, and W.-Y. Ma. Automated Known Problem Diagnosis with Event Traces. Technical report, Microsoft Research, June 2005.

Biography

Emilia Sorana Buneci was born in Bucharest, Romania on February 14^{th}, 1979. During 1997-2001, she attended Christian Brothers University in Memphis, TN, USA, where she graduated as a valedictorian with B. S. degrees in Computer Science and Mathematics. She was awarded the Alumni Academic Award, and the Dominic Dunn Award - given to the most outstanding science graduate in 2001. In 2003, she has earned a M. S. from Duke University, Durham, NC, USA, for which she has received the Best Master Thesis Award from the Department of Computer Science. She earned a Ph.D. degree in Computer Science from Duke University, Durham, NC, USA in May 2008.

Her scientific publications are listed below:

1. Emma Buneci and Daniel Reed. Analysis of Application Heartbeats: Learning Structural and Temporal Features in Time Series Data for Identification of Performance Problems *Submitted*, 2008.

2. Emma Buneci, Kenneth Roberts, Rachael Brady, Allen Song, Xiaobai Sun, and Marty Woldorff. Component-wise models of the BOLD response in the human primary visual cortex. In *Proceedings of the 10th Annual Meeting of the Organization for Human Brain Mapping*, Budapest, Hungary, June 2003.

3. Emma Buneci. Zope - Making Dynamic Web Applications with an Open-Source Framework, chapter Using DTML Tags. *Software & Support Verlag* GmhH, June 2001.

Academic honors received since obtaining her bachelor's degrees are listed below:

- Doctoral Showcase Presentation at the Supercomputing '07 Conference in Reno, Nevada, USA. November, 2007.

- Best Poster Award at the Teragrid '07 Conference, Student Research Competition, Madison, Wisconsin, USA. June, 2007.

- Best Master Thesis Award, Department of Computer Science, Duke University, Durham, NC, USA. October, 2004.

- Graduate Teaching Assistant Award, Department of Computer Science, Duke University, Durham, NC, USA. October, 2002.

- Graduate School Fellowship, Department of Computer Science, Duke University, Durham, NC, USA. 2001-2002.

She has been a member of professional organizations such as ACM, IEEE and USENIX, and a member of the Women in Science and Engineering, and of the Graduate and Professional Student Council at Duke University.